CARLETON UNIVERSITY

MASTER'S THESIS

Simulation of an Organic Memristor

Author:
Cem Bonfil

Supervisor:
Dr. Tom Smy
Dr. Steven P. McGarry

A thesis submitted in fulfilment of the requirements
for the degree of Master's of Science in Electrical and Computer Engineering

in the

Carleton University

November 2013

Carleton
UNIVERSITY

"Quote"

Cem Bonfil

CARLETON UNIVERSITY

Abstract

Faculty of Engineering

Department of Electronics

Master's of Science in Electrical and Computer Engineering

Simulation of an Organic Memristor

by Cem BONFIL

The Thesis Abstract is written here (and usually kept to just this page). The page is kept centered vertically so can expand into the blank space above the title too...

Acknowledgements

The acknowledgements and the people to thank go here, don't forget to include your project advisor...

Contents

List of Figures

List of Tables

Abbreviations

BTE	Boltzmann Transport Equations
CFL	Courant-Friedrichs-Lewy
ClO_4^-	Perchlorate
DD	Drift Diffusion
FD	Finite Difference
Li^+	Lithium
PEDOT	Poly(3,4-ethylenedioxythiophene)
PSS	Poly(styrenesulfonate)
SG	Scharfatter-Gummel

Physical Constants

Boltzmann Constant	k	$=$	$8.6173324 \ 10^{-5}$ eV/K
Elementary Charge	q	$=$	$1.6021765 \ 10^{-19}$ C
Vacuum Permittivity	ϵ_0	$=$	$8.8541878 \ 10^{-12}$ F/m

Symbols

D	Diffusivity	m^2/s
E	Electric Field	V/m
h	Unit Distance	m
I	Current	A
J	Current Density	A/m^2
L_D	Debye Length	m
l_f	Mean Free Path	m
M	Memristance	Ω
n	Electron Density	m^{-3}
N_A	Acceptor Density	m^{-3}
N_D	Donor Density	m^{-3}
n_i	Intrinsic Carrier Density	m^{-3}
T	Temperature	K
t	Time	s
t_{dr}	Dielectric Relaxation Time	s
U	Generation Recombination Rate	$m^{-3}s^{-1}$
V	Potential	V
V_{th}	Thermal Voltage	V
Δ	Unit Distance	m
ε_r	Relative Permittivity	unitless
μ	Mobility	$m^2/(Vs)$
φ	Flux Linkage	Wb
ρ	Charge Density	C/m^3
υ	Drift Speed	m/s

For/Dedicated to/To my. . .

Chapter 1

Introduction

The purpose of this thesis is to create a numerical model to simulate a device called "Memristor". In order to achieve this goal we will be using an approximate version of Boltzmann Transport Equations (BTE) called drift diffusion equations and a numerical method called finite difference (FD).

The term memristor was first used by Chua in 1971 in his paper called "Memristor The Missing Circuit Element" [1]. He theorized that there is a fourth passive circuit element yet to be discovered in addition to resistor,capacitor and inductor. He said that we already know and use five out of six possible combinations that can be made out of four fundamental circuit variables, current I, voltage V, charge q and flux linkage φ. Chua claimed that we were missing a circuit element which produces a relationship between flux linkage(time integral of the potential) and charge. He introduced a new variable named memristance which has units of resistance and it is a function of charge. The relationship between the current and the potential of a memristor is calculated by replacing the resistance by memristance in ohms law [1] [2] [3] [4] [5] [6] [7] [8] [9].

$$v(t) = M(q(t))i(t) \tag{1.1}$$

Theoretically memristor retains its resistance in the absence of any power source. When a potential is applied the resistance can be influenced by the direction and the magnitude of the current. If the current flows in one dirfection resistance increases and if it flows in the other direction resistance decreases. This produces an I-V response which looks like a pinched hysteresis curve. This response is the main characteristic of a memristor.

This new element remained mostly a theory and did not get much academic attention until a group of researches in Hewlett Packard claimed to have found the Chua's missing

memristor in 2008. They have successfully fabricated a nano scale memristor using TiO_2 (titanium dioxide). After the discovery in HP labs there was an increase of interest in memristors due to its potential applications for data storage and addition of learning capabilities into passive circuits.

The memristor we are going to be looking at is in millimeter rather then nano meter scale and uses a conductor made out of a polymer called PEDOT:PSS. It is made of two polymer chains attached together and conducts electricity via hole transport. Unfortunately this conduction mechanism is not perfectly understood and needs further research due to the complexity of the material.

Unlike a semiconductors like silicon, the structure of a polymer is quite irregular. Polymers have individual molecules with different chain lengths and changing amounts of defects. Additionally, they can be amorphous or partially crystalline and further differences occur through aging. The conduction and electronic properties depend the orientation of polymer chains which can change in x,y and z directions. These irregularities in the structure makes these conducting polymers resemble amorphous inorganic semiconductors. Following the concept of charge transport in amorphous inorganic semiconductors, the conduction mechanism of conducting polymers is commonly explained by variable range hopping. This mechanism was first introduced by Mott in 1968. He proposed a model for charge transport in systems that are randomly disordered. In variable range hopping charge transport occurs via jumps between available sites. Every charge carrier has a probability of jumping between two sites depending on its energy and the distance to the next available site. Temperature has a big impact on conductivity since it changes the structure of the molecules and increases the energy of charge carriers.

Apart from temperature there are other ways to change the conductivity of PEDOT. It is possible to affect conductivity by either doping or counter doping. Depending on the method used, doping can be reversible or permanent. When reversible doping is employed, resulting device behaves like a memristor since its resistance is now dependent on charge.

There are few approximate analytic solutions for inorganic memristors similar to the one produced in HP labs. These solutions are mostly based on parameter fitting and some basic physics. Studies on organic memristors are even more sparse than studies on inorganic ones. The physics behind the conduction mechanism and the changes in conductivity due to doping requires further research and development of a computer model can help in various ways. First of all it is very difficult to get experimental data on the movement of ions and holes inside PEDOT due its disordered structure and its geometry. Since experimental data is hard to get it is also hard to come up with theories

that explain the movement of charged particles and their interactions with each other. A simulation can be a useful tool in testing various theories without having to set up and perform complicated experiments. Also once a solid understanding of the conduction mechanism has been achieved, simulations can be very useful to test different device structures and optimize them before fabrication.

In this thesis we will try to develop a simple method to simulate a memristor using PEDOT:PSS as a conductor and lithium as a reversible counter doping agent. First we will be examining drift diffusion equations and its solutions in order to create some test cases for our simulation scheme. Then, we will be using a method called finite difference in order to create a numerical solution to drift diffusion equations. After we developed a method to solve drift diffusion equations we will be using analytic solutions as well as a commercially available simulator called COMSOL Multiphysics in order to test the accuracy and reliability of our simulation method. Finally once we have a reliable way to solve drift diffusion problems we will be simulating a memristor based on physical structure, experimental data and observations.

Chapter 2

Theory

2.1 Carrier Transport Equations

We will be solving drift-diffusion equations, which are based on BTE, in order to model the complex behaviour of the memristor. Drift-diffusion equations can be obtained by simplifying BTE equation via approximations. These simplifications dictate the limits of the drift-diffusion model. The approximations also serve as guidelines for where this model can and can not be used, therefore they need to be well understood.

Derivation of Boltzmann transport equation starts by stating that charged particles can be defined by their position in space **r** and momentum **k** at time **t** using a probability distribution function f(k,r,t). We get the most general form of Boltzmann transport equation. [8]

$$\frac{d}{dt} f(k, r, t) = 0 \tag{2.1}$$

This general form of BTE needs to be expanded and relevant physical equations need to be plugged in to get an appropriate equation describing specific a problem or device. Many different device simulators use some sort of approximation to BTE. In a semiconductor device we are usually interested in the movement and the density distribution of charge carriers, holes (p) and electrons (n).

After this brief introduction to BTE, rather than going through the tedious mathematical derivation of the drift diffusion model we can directly discuss the approximations that are made along the process of derivation in order to get a better insight on the model. As a particle travels in a solid state device it collides with other particles as well as the atoms in the device. For drift-diffusion equations individual lattice scattering events or

collisions are averaged and the particles have an average constant velocity under the effects of an electric field. This means that all the particles respond instantaneously to the changes in the electric field. The movement of the particles due to electric field is called the drift current. The relationship between drift velocity and the electric field is given by the following equation:

$$v = \mu E \tag{2.2}$$

μ is called mobility constant and it determines the speed at which the particles are going to move when subject to an electric field. Based on drift velocity we can get a term for drift current density.

$$J_E = qn\mu E = qnv \tag{2.3}$$

Where q is the elementary charge and n is the electron density. In addition to the previous assumptions, we assume that the lattice is perfectly uniform, has a uniform temperature distribution and all the particles are close to the temperature of the lattice. Based on this assumption we can say that all the particles that move due to thermal effects has the same thermal velocity (v_{th}) and mean free path (l_f). These quantities can be combined into one single coefficient called diffusion constant.

$$D = v_{th} \, l_f \tag{2.4}$$

Drift and diffusion coefficients are related to each other via Einstein relationship:

$$D = \frac{\mu kT}{q} \tag{2.5}$$

Where k is the Boltzmann constant and T is the lattice temperature. Now we have a second term which contributes to carrier movement which is called the diffusion current density.

$$J_D = qD\frac{dn}{dx} \tag{2.6}$$

Unlike the drift current density, which is directly related to the carrier density, diffusion current density is related to the carrier density's first order derivative in space.

Combining these two terms we get the current density equation for electrons in one dimension.

$$\vec{J_n^x} = q\mu_n n\vec{E_x} + qD_n\frac{dn}{dx} \tag{2.7}$$

This equation can be easily extended to more dimensions by simply using the appropriate terms.

$$\vec{J_n^y} = q\mu_n n\vec{E_x} + qD_n\frac{dn}{dy} \tag{2.8}$$

At this point we can also note that anisotropic drift and diffusion coefficients can also be handled with ease by using different coefficients for different directions. Current density equation works equivalently well for positively or negatively charged particles.

$$\vec{J_p^x} = q\mu_p p\vec{E_x} - qD_p\frac{dp}{dx} \tag{2.9}$$

Current density equations by themselves are not enough to solve a time dependent problem. For this we need to account the movement of charge over time which is captured in the continuity equation. It is basically a statement of conservation of particle density over time. The change in the amount of carriers over time in a particular area must be equal to the difference in current density over the same area. Additionally the amount of charge can change due to generation-recombination of charged particles.

$$\frac{\partial n}{\partial t} = \frac{1}{q}\nabla \cdot \vec{J_n} + U_n \tag{2.10}$$

$$\frac{\partial p}{\partial t} = -\frac{1}{q}\nabla \cdot \vec{J_p} + U_p \tag{2.11}$$

U_n and U_p are net generation recombination rates.

We must keep in mind that electric field in an area can be generated in two different ways. One is through the distribution of net charge over the area and the other one is an externally applied field. It is possible calculate the potential distribution over an area by using Poisson's equation. Once the potential is known the electric field can be obtained by just calculating the negative gradient of the electric potential.

$$\nabla \cdot (\varepsilon\nabla V) = -\rho = -q(p - n + N_D^+ - N_A^-) \tag{2.12}$$

$$\vec{E} = -\nabla V \tag{2.13}$$

We can split the electric field into two components $\vec{E_x}$ and $\vec{E_y}$.

$$\vec{E_x} = -\frac{\partial V}{\partial x} \tag{2.14}$$

$$\vec{E_y} = -\frac{\partial V}{\partial y} \tag{2.15}$$

It is possible to see that through the electric field and net charge distribution, Poisson's equation and drift-diffusion equations are coupled and non linear. The strength of the non linearity depends on the size of the device and charge density which determines the total amount of charge over an area.

Usually we are particularly interested in finding the amount of current in a device. This can be easily calculated by integrating the current density over an area.

$$I = \int_s \vec{J_{tot}} \cdot ds = \int_s (J_n + J_p + \varepsilon \frac{\partial E}{\partial t}) ds \tag{2.16}$$

Overall the main equations for the drift-diffusion model can be compactly written as:

$$\nabla \cdot (\varepsilon \nabla V) = -q(p - n + N_D^+ - N_A^-) \tag{2.17}$$

$$\vec{J_n} = q\mu_n n\vec{E} + qD_n\nabla n \tag{2.18}$$

$$\vec{J_p} = q\mu_p p\vec{E} - qD_p\nabla p \tag{2.19}$$

$$\frac{\partial n}{\partial t} = \frac{1}{q}\nabla \cdot \vec{J_n} + U_n \tag{2.20}$$

$$\frac{\partial p}{\partial t} = -\frac{1}{q}\nabla \cdot \vec{J_p} + U_p \tag{2.21}$$

Unfortunately even after so many approximations and simplifications to BTE, drif diffusion equations have analytical solutions for only few isolated cases. The simplicity of these analytical solutions makes them a good candidate for testing any numerical methods that is created to solve drift diffusion equations.

2.2 Analytic Solutions

2.2.1 Steady State Solution Over a Finite Domain

The simplest problem we can solve using drift diffusion model is charge enclosed over a finite area. Basically there is no flow in or out of the area we are solving for. There is a finite amount of charge and a uniform electric field which does not get affected by the enclosed charge. Now to get an analytic solution we assume that everything is at steady state and all the transients have died. In this case the total current density in the device must be zero. It is important to note here that the initial distribution of the charge density does not matter in this problem since everything will be redistributed in steady state. We only need to know the total amount of charge over the entire area.

$$J_p(x) = q\mu_p p E - q D_p \frac{dp}{dx} = 0 \tag{2.22}$$

Total current density will only be zero when the drift current density generated by the electric field is completely balanced by the diffusion current density.

$$q\mu_p p E = q D_p \frac{dp}{dx} \tag{2.23}$$

$$\frac{\mu_p E}{D_p} p = \frac{dp}{dx} \tag{2.24}$$

Here we have a very simple differential equation that can be solved by assuming that it has the following form:

$$p(x) = Ce^{ax} \tag{2.25}$$

C and **a** are arbitrary constants. Now we can plug equation (2.25) into (2.24)

$$\frac{\mu_p E}{D_p} Ce^{ax} = aCe^{ax} \tag{2.26}$$

$$a = \frac{\mu_p E}{D_p} \tag{2.27}$$

Plugging **a** back to equation (2.25) we get a general form for the solution.

$$p(x) = Ce^{\frac{\mu_p E}{D_p}x} \tag{2.28}$$

It is possible to solve for **C** by observing that the total number of charges at steady state must be equal to the initial number of charges. So the integral of charge density at time zero must be equal to the integral of charge density at steady state.

$$\int_0^L Ce^{\frac{\mu_p E}{D_p}x}dx = \int_0^L p(t=0,x)dx$$

$$C = \frac{\int_0^L p(t=0,x)dx}{\int_0^L e^{\frac{\mu_p E}{D_p}x}dx}$$

$$C = \frac{\int_0^L p(t=0,x)dx}{\frac{D_p}{\mu_p E}[e^{\frac{\mu_p E}{D}L}-1]} \tag{2.29}$$

So the full solution takes the following form:

$$p(x) = \frac{\int_0^L p(t=0,x)dx}{\frac{D_p}{\mu_p E}[e^{\frac{\mu_p E}{D}L}-1]}e^{\frac{\mu_p E}{D_p}x} \tag{2.30}$$

By examining the solution we can tell that increasing electric field will concentrate the charge density at the edge of the area. Physically this makes perfect sense since the force that is pushing the particles is getting greater and it is making the charges accumulate more in one side.

Since this solution does not have any time dependence it is not suitable for testing a numerical methods transient response but it is quite good for testing the accuracy of a steay-state solution as well as the conservation of mass over time.

2.2.2   Transient Solution Over an Infinite Domain

This time, in order to find a transient solution, we need to use the continuity equation (2.10). The problem we are going to solve consists of an initial particle density distribution subject to a uniform electric field over an infinitely long conductor. Same as the steady state problem we solved earlier, the particle density's effect on the electric field is negligible therefore we do not need to solve for Poisson's equation at the same time.

We start our solution by plugging (2.7) into (2.10) and assuming that generation/recombination rate is zero, so $U_n = 0$.

$$\frac{\partial n}{\partial t} = \frac{1}{q} \nabla \cdot (\vec{J_n}) \tag{2.31}$$

$$\frac{\partial n}{\partial t} = \frac{1}{q} \nabla \cdot (q\mu_n n \vec{E} + qD_n \frac{dn}{dx}) \tag{2.32}$$

For 1-D above equation can be simplified to:

$$\frac{\partial n}{\partial t} = \mu_n E \frac{dn}{dx} + D_n \frac{d^2 n}{dx^2} \tag{2.33}$$

Here we make use of separation of variables which assumes that the solution can be separated into a time and space dependent functions.

$$n(t,x) = n(t)n(x) = n_t n_x \tag{2.34}$$

Plugging equation (2.34) into (2.33) and dividing by n(t,x),

$$\frac{1}{n_t} \frac{dn_t}{dt} = \mu_n E \frac{1}{n_x} \frac{dn_x}{dx} + D \frac{1}{n_x} \frac{d^2 n_x}{dx^2} \tag{2.35}$$

Assuming both sides of the equation are equal to a constant -k, time dependent part of the problem becomes a simple first order differential equation.

$$\frac{1}{n_t} \frac{dn_t}{dlt} = -k$$

$$\frac{dn_t}{dt} = -kn_t$$

Based on the above differential equation we can get a general form for n_t:

$$n_t = C_1 e^{-kt} \tag{2.36}$$

Now for n_x assume a solution in the following form,

$$n_x = C_2 e^{-j\omega x} \tag{2.37}$$

Plug (2.37) into (2.35)

$$\omega^2 D C_2 e^{-j\omega x} - j\omega\mu_n E C_2 e^{-j\omega x} + k C_2 e^{-j\omega x} = 0 \tag{2.38}$$

Simplifying equation (2.38) and solving for k gives,

$$k = \omega^2 D + j\omega\mu_n E \tag{2.39}$$

Combining equation (2.36), (2.37) and (2.39) to get the initial form of the solution. $(C = C_1 C_2)$

$$n = n_t n_x = C e^{(-\omega^2 D + j\omega\mu_n E)t} e^{-j\omega x} \tag{2.40}$$

Using superposition principle we get,

$$n = n_t n_x = \int_{-\infty}^{\infty} C(\omega) e^{(-\omega^2 D + j\omega\mu_n E)t} e^{-j\omega x} d\omega \tag{2.41}$$

The distribution of n_x is known at t=0.

$$n(x, t = 0) = \int_{-\infty}^{\infty} C(\omega) e^{-j\omega x} d\omega \tag{2.42}$$

$C(\omega)$ is just the inverse fourier transform of $n(x, 0)$.

$$C(\omega) = \int_{-\infty}^{\infty} n(x, 0) e^{-j\omega x} dx \tag{2.43}$$

Plugging equation (2.43) into (2.41) we get the final form of the solution,

$$n = \int\limits_{-\infty}^{\infty} \int\limits_{-\infty}^{\infty} n(z,0)e^{j\omega z}dz e^{(\omega^2 D - j\omega\mu_n E)t}e^{-j\omega x}d\omega \tag{2.44}$$

Rearranging equation (2.44),

$$n = \int\limits_{-\infty}^{\infty} \int\limits_{-\infty}^{\infty} n(z,0)e^{(\omega^2 D - j\omega\mu_n E)t}e^{-j\omega x}e^{j\omega z}dz d\omega \tag{2.45}$$

If the initial distribution is a gaussian distribution then we get,

$$n(x,0) = e^{-(\frac{x-x_o}{\sigma})^2} \tag{2.46}$$

$$n(x,t) = \frac{1}{\sqrt{4D_n\sigma^{-2}t+1}}e^{-\frac{(t\mu_n E - x + x_o)}{4D_n t + \sigma^2}} \tag{2.47}$$

If the initial distribution is a rectangular distribution then we get,

$$n(x,0) = \prod(w(x)) \tag{2.48}$$

$$n(x,t) = \frac{1}{2}erf(\frac{w + 2t\mu_n E - 2x}{4\sqrt{D_n t}}) - \frac{1}{2}erf(\frac{-w + 2t\mu_n E - 2x}{4\sqrt{D_n t}}) \tag{2.49}$$

2.2.3   PN Junction

Previous analytical solutions involved the solution of Poisson's equation and continuity equation which were not coupled. Now we can look at an example where these equations are tightly coupled. There are usually no direct analytical solution for coupled equation but it is possible to get a closed form solution by making use of certain approximations. One simple example of this situation is an abrupt p-n junction. An abrupt p-n junction is created when two materials of uniform opposite doping,p type and n type, are brought together. A p type material has an excess number of acceptors N_A and an n type material has an excess number of donors N_D. The junction is defined at the interface where $N_A = N_D$.
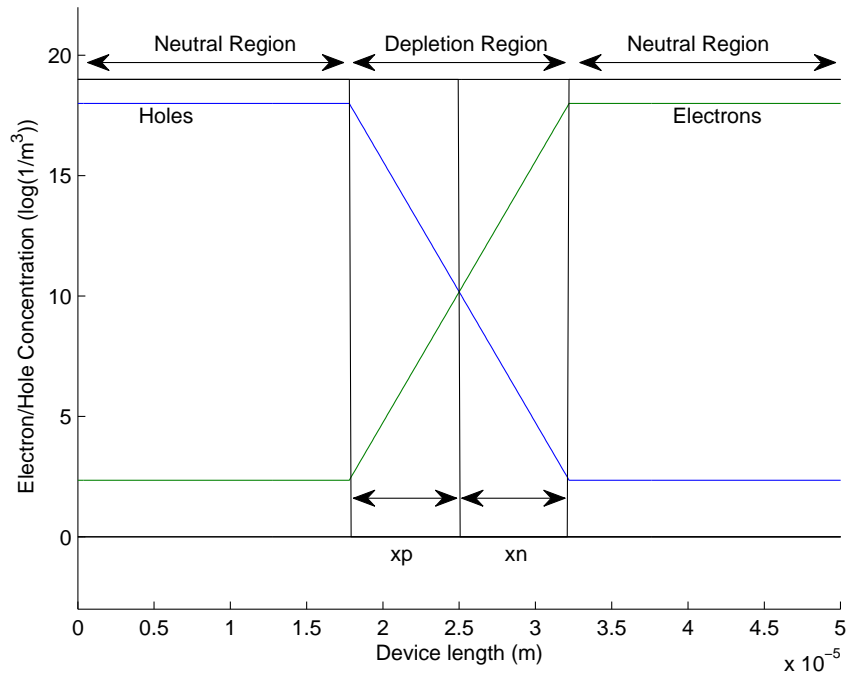
FIGURE 2.1: PN junction electron/hole density

In this example we will be deriving an analytical solution for an abrupt p-n junction. In order to get a solution for this problem we can make use of the depletion region approximation. This approximation starts by assuming that the charges are fully depleted around the junction. All the electric field is confined in the depletion region and regions far away from the junction are neutral. Based on this the net charge density over the entire region is:

$$\frac{d\vec{E}}{dx} = \frac{\rho}{\varepsilon} = \frac{q}{\varepsilon}(-N_A + N_D) \tag{2.50}$$

$$\rho = \begin{cases} 0 & \text{for } x < -x_p \\ -qN_A & \text{for } -x_p \leq x \leq 0 \\ qN_D & \text{for } 0 \leq x \leq < x_n \\ 0 & \text{for } x > x_n \end{cases} \tag{2.51}$$

The electric field over the entire region can be calculated by integrating ρ.

$$E = \begin{cases} \int \frac{-qN_A}{\varepsilon} dx + C_1 & \text{for } -x_p \leq x \leq 0 \\ \int \frac{qN_D}{\varepsilon} dx + C_2 & \text{for } 0 \leq x \leq x_n \end{cases} \tag{2.52}$$

We can solve for C_1 and C_2 since electric field must go to zero at x_p and x_n.

$$E(x = -x_p) = 0 \quad \Rightarrow \quad C_1 = \frac{-qN_A}{\varepsilon} x_p \tag{2.53}$$

$$E(x = x_n) = 0 \quad \Rightarrow \quad C_1 = \frac{qN_D}{\varepsilon} x_n \tag{2.54}$$

Then E(x) becomes:

$$E(x) = \begin{cases} \frac{-qN_A}{\varepsilon}(x + x_p) & \text{for } -x_p \leq x \leq 0 \\ \frac{qN_D}{\varepsilon}(x - x_n) & \text{for } 0 \leq x \leq x_n \end{cases} \tag{2.55}$$

Additionally, we know that the electric field must be continuous across the interface therefore the electric field in the p-type side and the n-type side must equal each other at the interface or when x = 0.

$$\frac{-qN_A}{\varepsilon}(x_p) = \frac{qN_D}{\varepsilon}(-x_n) \tag{2.56}$$

$$N_A x_p = N_D x_n \tag{2.57}$$

This equation makes physical sense since it states that the total charge on one side of the junction must be the same as the total charge on the other. In other words, the net charge on each side keeps the electric field confined to the depletion region.

To find the voltage as a function of distance, we can make use of equation 2.13 and integrate the electric field.

$$V(x) = \begin{cases} \int -E(x)dx = \int \frac{qN_A}{\varepsilon}(x + x_p)dx = \frac{qN_A}{\varepsilon}(\frac{x}{2} + x_p) + C_3 & \text{for } -x_p \leq x \leq 0 \\ \int -E(x)dx = \int \frac{qN_D}{\varepsilon}(x - x_n)dx = \frac{qN_D}{\varepsilon}(-\frac{x}{2} + x_n) + C_4 & \text{for } 0 \leq x \leq x_n \end{cases}$$

$$(2.58)$$

We are usually interested in the potential difference across the junction and can arbitrarily set one side to zero. Here we define the voltage on the p type side as zero, such that at x= x_p, V=0. This gives the constant C3 as:

$$C_3 = \frac{qN_A}{2\varepsilon}x_p^2 \tag{2.59}$$

$$V(x) = \frac{qN_A}{2\varepsilon}(x + x_p)^2 \quad \text{for } -x_p \leq x \leq 0 \tag{2.60}$$

We can find C4 by using the fact that the potential on the n-type side and p-type side are equal at the interface, such that:

$$V_p(x = 0) = \frac{qN_A}{2\varepsilon}x_p^2 = V_n(x = 0) = \frac{qN_A}{2\varepsilon}(x_n - \frac{x}{2})x + C_4 \tag{2.61}$$

$$C_4 = \frac{qN_A}{2\varepsilon}x_p^2 \tag{2.62}$$

Now we can get an overall expression for V(x).

$$V(x) = \begin{cases} \frac{qN_A}{\varepsilon}(x + x_p)^2 & \text{for } -x_p \leq x \leq 0 \\ \frac{qN_D}{\varepsilon}(-\frac{x}{2} + x_n)x & \text{for } 0 \leq x \leq x_n \end{cases} \tag{2.63}$$

The maximum voltage across the junction is at $x = x_n$, which is:

$$V_{bi} = \frac{q}{2\varepsilon}(N_D x_n^2 + N_A x_p^2) \tag{2.64}$$

Using (2.57) in the above equation and rearranging allows x_p and x_n to be determined. They are:

$$x_n = \sqrt{\frac{2\varepsilon V_{bi}}{q}\frac{N_A}{N_D(N_D + N_A)}} \tag{2.65}$$

$$x_p = \sqrt{\frac{2\varepsilon V_{bi}}{q} \frac{N_D}{N_A(N_D + N_A)}} \tag{2.66}$$

The value of the built in potential can also be calculated using fermi levels of p and n doped materials.

$$E_{FN} - E_i = kT \ ln(\frac{N_D}{n_i}) \tag{2.67}$$

$$E_i - E_{FP} = kT \ ln(\frac{N_A}{n_i}) \tag{2.68}$$

E_{FN} and E_{FP} are fermi energy levels of electrons and holes respectively. The difference between the fermi levels divided by the single electron charge gives us the built in potential of the pn junction.

$$E_{FN} - E_{FP} = qV_{bi} = kT \ ln(\frac{N_D}{n_i}) + kT \ ln(\frac{N_A}{n_i}) = kT \ ln(\frac{N_A N_D}{n_i^2}) \tag{2.69}$$

$$V_{bi} = \frac{kT}{q} \ ln(\frac{N_A N_D}{n_i^2}) \tag{2.70}$$

With the calculation of the built in potential we have all the information we need for the analytical solution of the pn junction without any external bias. Following graphs shows the plots of approximate solutions for net charge, electric field and the junction potential.
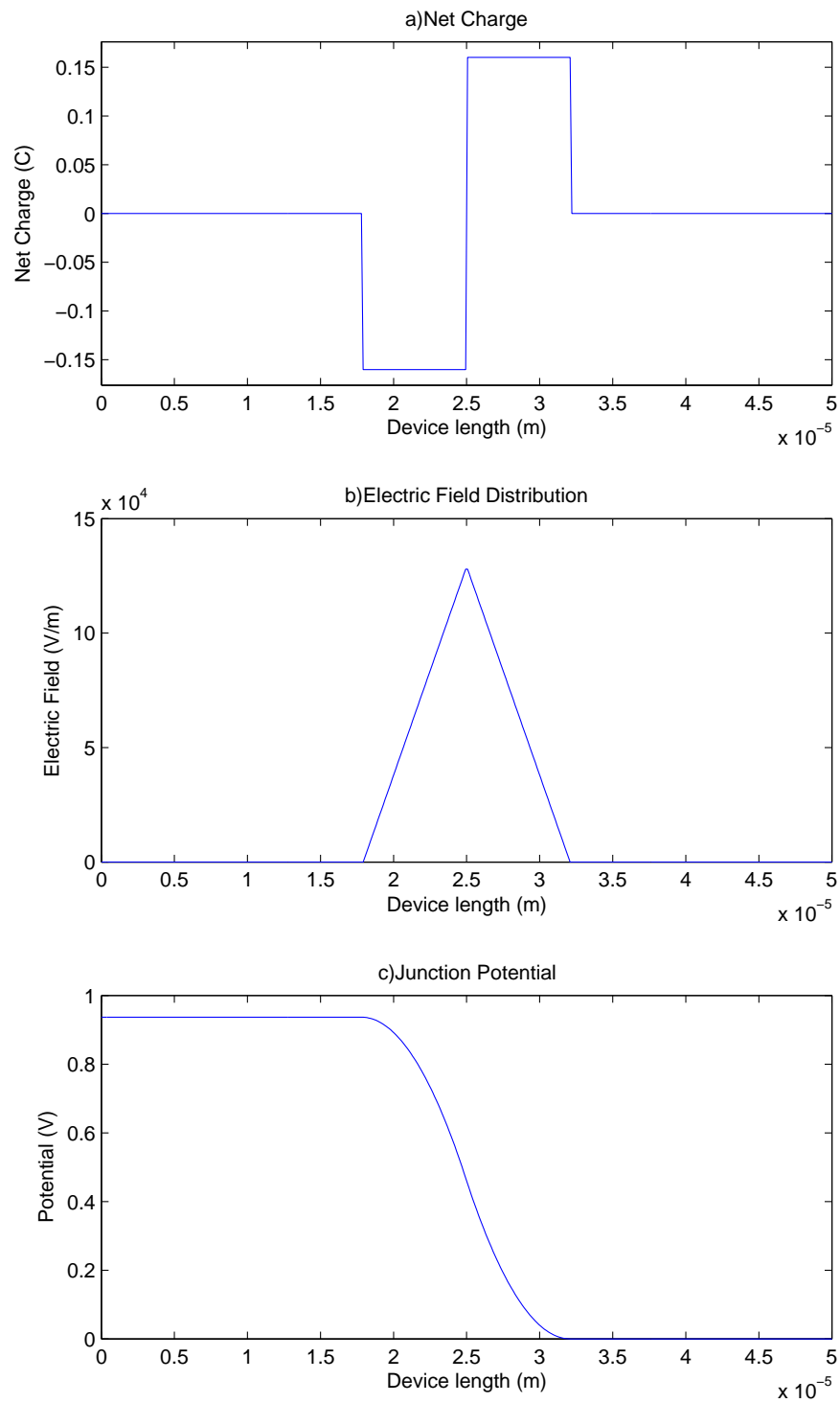
FIGURE 2.2: Approximate Solution of a PN Junction

Chapter 3

Numerical Solution of Drift-Diffusion Equation

3.1 Finite Difference Method

There are many different methods that can be used to solve drift diffusion equations such as finite elements, finite difference or meshless methods. We will be using finite difference method which uses an approximation for the derivative of a function based on the mathematical definition of the derivative.

$$\frac{df}{dx} = \lim_{h \to 0} \frac{f(x+h) - f(x)}{h} \tag{3.1}$$

We can get a numerical approximation for the first derivative by dropping the limit and assuming that h is small enough to get a value for the derivative reasonably close to the actual value. Of course as h gets smaller the approximation becomes more and more accurate. The difference between the calculated value and the real value is called the truncation error and it is captured using $O(h^n)$ notation. n signifies the order of h which determines how fast the approximation is approaching the real solution as h decreases.

$$\frac{df}{dx} = \frac{f(x+h) - f(x)}{h} + O(h) \tag{3.2}$$

It is possible to uniformly discretise the entire region over which a function is defined in order to calculate its derivative. We start by dividing the region over which the function is defined into *n-1* segments therefore there will be n number of points. Then we can find the length of each segment using the following relationship:

$$h = \frac{L}{n} \tag{3.3}$$

The function we are interested in is defined on the edge of every segment. We can label each point consecutively, $x_0, x_1, x_2 \dots x_{n-1}$ where $x_i = ih$. Our function is discretely defined on $f_i = f(x_i)$ where $i=0,1,2..n-1$. It is possible to use equation 3.2 to discretely calculate the first derivative of the function with respect to x.

$$\frac{df(x_i)}{dx} = \frac{f(x_{i+1}) - f(x_i)}{h} + O(h) \tag{3.4}$$

Above equation is called forward difference because the derivative for point x_i was calculated using the point that is coming right after it, x_{i+1}.

$$f_i' = \frac{f_{i+1} - f_i}{h} + O(h) \tag{3.5}$$

Forward difference is not the only way to calculate a discrete derivative. Here are a few more ways calculate the same derivative by making use of different points.

$$f_i' = \frac{f_i - f_{i-1}}{h} + O(h) \tag{3.6}$$

$$f_{i+\frac{1}{2}}' = \frac{f_{i+1} - f_i}{h} + O(h^2) \tag{3.7}$$

Equation 3.6 is called backward difference and equation 3.7 is called central difference. One important thing to note here is that in the central difference formula the derivative falls exactly in the middle of two points. It also gives more accurate results using the same number of points as forward and backward difference.

Using finite difference formulas it is possible to construct higher derivatives. Lets look at how to get a formula for a second order derivative at point x_i using central difference. First step is to calculate the first order derivative on $x_{i-\frac{1}{2}}$, x_i and $x_{i+\frac{1}{2}}$

$$f_{i+\frac{1}{2}}' = \frac{f_{i+1} - f_i}{h} \tag{3.8}$$

$$f_{i-\frac{1}{2}}' = \frac{f_i - f_{i-1}}{h} \tag{3.9}$$

$$f'_i = \frac{f_{i+\frac{1}{2}} - f_{i-\frac{1}{2}}}{h} \tag{3.10}$$

We can take the second derivative of the last function and plug in the first two.

$$f''_i = \frac{f'_{i+\frac{1}{2}} - f'_{i-\frac{1}{2}}}{h}$$

$$f''_i = \frac{\frac{f_{i+1}-f_i}{h} - \frac{f_i-f_{i-1}}{h}}{h}$$

$$f''_i = \frac{f_{i+1} - f_i - f_i + f_{i-1}}{h^2}$$

After some algebra we get the final form of the second derivative.

$$f''_i = \frac{f_{i+1} - 2f_i + f_{i-1}}{h^2} + O(h^2) \tag{3.11}$$

Overall these finite difference equations are enough to solve drift diffusion equations. Even though all the derivations were done in 1-D it is trivial to extend them to higher dimensions. Now we can use finite difference method to solve Poisson's equation and drift diffusion equations.

3.2   Solving Drift-Diffusion Equations

3.2.1   Poisson Solver

Since we are dealing with electronic devices there is usually going to be an electric field in the system generated by an external source or generated within the device through charged particles. Either way we need to solve Poisson's equation in order find the potential distribution as well as the electric field inside the device. We can start by simplifying the equation through assumptions and then we can employ finite difference to solve this simplified equation. The first step of simplification is assuming that the permittivity is isotropic, then we can get:

$$\nabla \cdot (\varepsilon \nabla V) = -\rho \tag{3.12}$$

$$\nabla \cdot (\varepsilon \nabla V) = \varepsilon \nabla^2 V \tag{3.13}$$

We can also move the permittivity to the right hand side and get,

$$\nabla^2 V = -\frac{\rho}{\varepsilon} \tag{3.14}$$

Expanding the left hand side,

$$\nabla^2 V = \frac{\partial^2 V}{\partial^2 x} + \frac{\partial^2 V}{\partial^2 y} \tag{3.15}$$

After discretizing electric potential over a 2-D uniform grid and using the second order central finite difference formula (3.11) we get the following equation,

$$\nabla^2 V_{i,j} = \frac{V_{i+1,j} - 2V_{i,j} + V_{i-1,j}}{\Delta x^2} + \frac{V_{i,j+1} - 2V_{i,j} + V_{i,j-1}}{\Delta y^2} \tag{3.16}$$

Since the grid is uniform we can use the same value for the distance between the nodes in each direction.

$$\Delta = \Delta x = \Delta y \tag{3.17}$$

Of course the net charge density and the permittivity is also discretized over the same uniform mesh. Putting all this information together we have generated a numerical approximation for Poisson's equation.

$$\nabla^2 V_{i,j} = \frac{V_{i-1,j} + V_{i,j-1} - 4V_{i,j} + V_{i+1,j} + V_{i,j+1}}{\Delta^2} = -\frac{\rho_{i,j}}{\varepsilon_{i,j}} \tag{3.18}$$

If we rearrange this equation by keeping all the known values on the right hand side and all the unknown values on the left hand side we get the following equation.

$$\varepsilon_{i,j}(V_{i-1,j} + V_{i,j-1} - 4V_{i,j} + V_{i+1,j} + V_{i,j+1}) = -\Delta^2 \rho_{i,j} \tag{3.19}$$

Above equation is valid for almost all the nodes in the system except two cases, boundary nodes and interface nodes. We can have two different types of boundary conditions which determine how the boundaries are going to be handled. The first one is Dirichlet boundary condition which forces a particular value for the potential at the boundary.

$$V_{i,j} = V_b \tag{3.20}$$

Where V_b is the value of the potential at the boundary. The other possible boundary condition is called Neumann boundary condition which states that the derivative of the potential at the boundary is zero. This gives us the following equation:

$$\frac{\partial V}{\partial x} = \frac{V_{i+1,j} - V_{i,j}}{\Delta} = 0 \tag{3.21}$$

So for a boundary over y axis we get:

$$V_{i+1,j} = V_{i,j} \tag{3.22}$$

Following the same procedure we can get Neumann boundary condition over x axis:

$$V_{i,j+1} = V_{i,j} \tag{3.23}$$

After we have handled all the boundary conditions we have to figure out how to handle interfaces. These interfaces occur when two materials with different permittivities come into contact. So when we have a node at the interface the permittivity of that node is ambiguously defined. We need a special way to solve this ambiguity. It is possible to derive a finite difference equation that handles dielectric interfaces properly starting

from Gauss's Law.

$$\oint \varepsilon \vec{E} \cdot \vec{ds} = Q \tag{3.24}$$

After piecewise integration around the boundary we can get an equation for a horizontal interface and a vertical interface respectively:

$$(\varepsilon_1 + \varepsilon_2)V_{i-1,j} + (\varepsilon_1 + \varepsilon_2)V_{i+1,j} - 4(\varepsilon_1 + \varepsilon_2)V_{i,j} + 2\varepsilon_1 V_{i,j+1} + 2\varepsilon_2 V_{i,j-1} = Q_{i,j} = \Delta^2 \rho_{i,j} \tag{3.25}$$

$$(\varepsilon_1 + \varepsilon_2)V_{i,j-1} + (\varepsilon_1 + \varepsilon_2)V_{i,j+1} - 4(\varepsilon_1 + \varepsilon_2)V_{i,j} + 2\varepsilon_1 V_{i+1,j} + 2\varepsilon_2 V_{i-1,j} = Q_{i,j} = \Delta^2 \rho_{i,j} \tag{3.26}$$

Now that we have all the equations we need for all the nodes over the simulation domain it is possible to combine them ((3.19),(3.20),(3.25), (3.26)) into a matrix and turn Poisson's equation, which is a second order differential equation, into a linear equation.

$$D_2\vec{V} = -\Delta^2 \vec{\rho} - \vec{V_b} \tag{3.27}$$

One can easily get the potential distribution by simply solving the matrix equation obtained. Due to the nature of the problem the matrix we end up with is quite sparse and using a sparse LU decomposition dramatically increases the computational efficiency.

$$\vec{V} = D_2^{-1}(-\Delta^2 \vec{\rho_{i,j}} - \vec{V_b}) \tag{3.28}$$

After solving for the potential distribution it is easy to calculate the electric field distribution discretely using the relationship between electric field and electric potential (2.13) and central difference equation (3.7).

$$\vec{E_{i,j}^x} = -\frac{V_{i+1,j} - V_{i-1,j}}{2\Delta} \tag{3.29}$$

$$\vec{E_{i,j}^x} = -\frac{V_{i,j+1} - V_{i,j-1}}{2\Delta} \tag{3.30}$$

3.2.2   Current Density Equations

After we have calculated the electric field distribution over the entire region we can now figure out how the particles move. Both drift and diffusion currents can be calculated over the entire grid. There are few different methods that can be used to calculate the current density. The accuracy of the methods we will look at change based on the physics of the device.

3.2.2.1   Finite Difference Method

The first method involves simply applying finite difference to calculate drift and diffusion currents. Drift current is quite simple since it does not involve any differentials and the diffusion current can be calculated using first order central difference. The current density is calculated in such a way that it falls between two points which simplifies the application of the boundary conditions.

$$J^x_{i+\frac{1}{2},j,k} = q\mu_n n_{i+\frac{1}{2},j,k} E^x_{i+\frac{1}{2},j,k} + D_n \frac{n_{i+1,j,k} - n_{i,j,k}}{\Delta} \tag{3.31}$$

The electric field was calculated exactly on the nodes but we can use linear interpolation in order to get a value between the nodes. Same argument is also valid for particle densities p and n. They were defined on the nodes but can be linearly interpolated.

$$n_{i+\frac{1}{2},j,k} = \frac{n_{i+1,j,k} + n_{i,j,k}}{2}$$

$$E^x_{i+\frac{1}{2},j,k} = \frac{E^y_{i+1,j,k} + E^y_{i,j,k}}{2}$$

We can follow the same method in order to calculate the current density in y direction:

$$J^y_{i,j+\frac{1}{2},k} = q\mu_n n_{i,j+\frac{1}{2},k} E^y_{i,j+\frac{1}{2},k} + D_n \frac{n_{i,j+1,k} - n_{i,j,k}}{\Delta} \tag{3.32}$$

$$n_{i,j+\frac{1}{2},k} = \frac{n_{i,j+1,k} + n_{i,j,k}}{2}$$

$$E^y_{i,j+\frac{1}{2},k} = \frac{E^y_{i,j+1,k} + E^y_{i,j,k}}{2}$$

Same current density equations can be used for positively charged particles by replacing n by p and changing the sign of the diffusion term.

3.2.2.2   Scharfatter-Gummel Method

This method assumes that $J_n, \mu E$ and D are constant over the interval $[x_i, x_{i+1}]$. What is not constant is the density n, but we assume that we do know the boundary values of n. We thus have a boundary value problem for the equation:

$$J_n = \mu_n nE + D_n \frac{\partial n}{\partial x} \tag{3.33}$$

Now, we know that any first-order equation can be integrated with the proper integrating factor. In this case it is an exponential, and we can write:

$$J_n e^{\frac{\mu E(x-x_i)}{D_n}} = (\mu_n nE + D_n \frac{\partial n}{\partial x})e^{\frac{\mu_n E(x-x_i)}{D_n}} \tag{3.34}$$

$$J_n e^{\frac{\mu_n E(x-x_i)}{D_n}} = D_n \frac{\partial}{\partial x}(ne^{\frac{\mu_n E(x-x_i)}{D_n}}) \tag{3.35}$$

Integrating both sides of this equation we get:

$$\int_{x_i}^{x_i+h} J_n e^{\frac{\mu_n E(x-x_i)}{D_n}} dx = \int_{x_i}^{x_i+h} D_n \frac{\partial}{\partial x}(ne^{\frac{\mu_n E(x-x_i)}{D_n}})dx$$

$$J_n \int_{0}^{h} e^{\frac{\mu_n E(x-x_i)}{D_n}} dx = D_n(ne^{\frac{\mu_n E(x-x_i)}{D_n}})|_{x_i}^{x_i+h}$$

$$J_n \frac{D}{\mu_n E}(e^{\frac{\mu_n Eh}{D_n}} - 1) = D_n(n_{i+1}e^{\frac{\mu_n Eh}{D_n}} - n_i)$$

After some algebra we get the final form of the equation. Same as the previous method, current density falls between two points.

$$J_n = \mu_n E \frac{(n_{i+1}e^{\frac{\mu_n Eh}{D_n}} - n_i)}{e^{\frac{\mu_n Eh}{D_n}} - 1} \tag{3.36}$$

Even though the derivation was made for negatively charged particles it can be extended to positively charged by changing the sign of the exponential terms.

$$J_p = \mu_p E \frac{(p_{i+1} e^{\frac{-\mu_p E h}{D_p}} - p_i)}{e^{\frac{-\mu_p E h}{D_p}} - 1} \tag{3.37}$$

We can double check that this equation gives the right formula for drift and diffusion separately. Lets start by pure diffusion and assume that drift term goes to zero.

$$\lim_{\mu_n E \to 0} J_n = \lim_{\mu_n E \to 0} \mu_n E \frac{(n_{i+1} e^{\frac{\mu_n E h}{D_n}} - n_i)}{e^{\frac{\mu_n E h}{D_n}} - 1} \tag{3.38}$$

We can use Taylor expansion on the exponential and keep first two terms.

$$\lim_{\mu_n E \to 0} J_n = \lim_{\mu_n E \to 0} \mu_n E \frac{(n_{i+1}(1 + \frac{\mu_n E h}{D_n}) - n_i)}{(1 + \frac{\mu_n E h}{D_n}) - 1} \tag{3.39}$$

Since $\mu_n E$ is going to zero we can assume that the term multiplying n_{i+1} is just 1.

$$\lim_{\mu_n E \to 0} J_n = \lim_{\mu_n E \to 0} \mu_n E \frac{(n_{i+1} - n_i)}{\frac{\mu_n E h}{D_n}} \tag{3.40}$$

So the final form of the pure diffusion is the same as the central difference formula.

$$\lim_{\mu_n E \to 0} J_n = D_n \frac{n_{i+1} - n_i}{h} \tag{3.41}$$

For pure drift we assume that $\mu|E| >> D$ instead of setting using $D = 0$ since it physically does not make sense. Particles will always have random movements due to thermal energy. We have two different cases for pure drift because the electric field can have positive and negative values based on its direction. For the positive case the exponential term gets fairly large so we can assume n_i is insignificant compared to n_{i+1}. Same argument is also valid for the denominator.

$$J_n = \mu_n E \frac{(n_{i+1} e^{\frac{\mu_n E h}{D_n}})}{e^{\frac{\mu_n E h}{D_n}}} \tag{3.42}$$

$$J_n = \mu E n_{i+1} \tag{3.43}$$

For negative electric field values exponential terms go to zero. This means that any value multiplied by the exponential term goes to zero as well.

$$J_n = \mu_n E \frac{(-n_i)}{-1} \tag{3.44}$$

$$J_n = \mu_n E n_i \tag{3.45}$$

So overall we have:

$$J_n = \begin{cases} \mu E n_i & \text{for } E < 0 \\ \mu E n_{i+1} & \text{for } E > 0 \end{cases} \tag{3.46}$$

This equation works the same way as an upwind scheme which is a method used to simulate pure drift processes. The equation we get for almost pure drift is quite different than what we get from directly applying finite difference and averaging the electric field and particle density. They are both valid solutions but their accuracy depends on the physics of the problem.

3.2.2.3 Boundary Conditions

For a drift diffusion problem there are two different possibilities for boundary conditions. The first one is when the particles cannot go past through a certain boundary, no flow boundary condition. This can be achieved by using Dirichlet bounday condition and setting the flow at the boundary to zero.

$$J = 0 \tag{3.47}$$

This boundary condition can also be used conditionally. A straightforward example is when there is a particle density limit over an area. This condition can be used to cut the flow of particles into an area when a certain particle concentration is reached.

Dirichlet boundary condition can also be used in cases where there is a flow through the boundary. A good example is a metal contact. It is assumed that metal contact has infinite amount of charge and the boundary is always charge neutral. For example if we have holes, electrons, positive and negative doping we can assume that at the boundary positive charge concentration will be equal to the negative charge concentration.

$$N_D + p = N_A + n \tag{3.48}$$

If we are dealing with a semiconductor the amount of holes and electrons has to obey mass action law at equilibrium.

$$np = n_i^2 \tag{3.49}$$

n_i here is the concentration of the semiconductor at equilibrium before getting doped. Solving (3.49) and (3.48) together we get,

$$n = \frac{1}{2}(N_D - N_A + \sqrt{(N_D - N_A)^2 + 4n_i^2}) \tag{3.50}$$

We can calculate the hole concentration using mass action law.

$$p = \frac{n_i^2}{n} \tag{3.51}$$

So we have a Dirichlet condition for electrons and hole which are given by 3.50 and 3.51 respectively.

3.2.3 Continuity Equation

Continuity equation is needed to calculate a transient solution for drift diffusion equations. The equation is simple to discretize using finite difference method. There are two terms that need to be discretized, a first order derivative in time and space. We can first start by evaluating the divergence term in equation (2.10).

$$\nabla \cdot J = \frac{\partial J}{\partial x} + \frac{\partial J}{\partial y} = \frac{dJ_x}{dx} + \frac{dJ_y}{dy} \tag{3.52}$$

It is possible to replace the derivative with central finite difference terms.

$$\frac{dJ_x}{dx} = \frac{J^x_{i+\frac{1}{2},j,k} - J^x_{i-\frac{1}{2},j,k}}{h} \tag{3.53}$$

$$\frac{dJ_y}{dy} = \frac{J^y_{i,j+\frac{1}{2},k} - J^y_{i,j-\frac{1}{2},k}}{h} \tag{3.54}$$

$$\nabla \cdot J_{i,j,k} = \frac{J^x_{i+\frac{1}{2},j,k} - J^x_{i-\frac{1}{2},j,k}}{h} + \frac{J^y_{i,j+\frac{1}{2},k} - J^y_{i,j-\frac{1}{2},k}}{h} \tag{3.55}$$

This is the general form of the divergence of the current density. We can plug in the current density equations from either finite difference or Scharfatter-Gummel approach. Collecting everything in a matrix gives rise to the following equation:

$$\nabla \cdot J_k = B \tag{3.56}$$

The time derivative can also be replaced by a forward or backward finite difference terms respectively.

$$\frac{\partial \vec{n}_k}{\partial t} = \frac{\vec{n}_{k+1} - \vec{n}_k}{\Delta t} \tag{3.57}$$

$$\frac{\partial \vec{n}_k}{\partial t} = \frac{\vec{n}_k - \vec{n}_{k-1}}{\Delta t} \tag{3.58}$$

It is possible to find a numerical transient solution for the drift-diffusion problem by combining finite difference form of the time derivative ((3.57) or (3.58)) and the divergence of the current density equations (3.56).

Using forward difference approximation we get,

$$\frac{\vec{n}_{k+1} - \vec{n}_k}{\Delta t} = B$$

$$\vec{n}_{k+1} = \vec{n}_k + \Delta t B \tag{3.59}$$

Both forward and backward difference formulas work sequentially in order to generate a transient solution. In order to calculate the next time step we need the solution of the previous time step. Forward difference gives us an explicit solution which has few advantages. This solution can be implemented without forming any matrices, just by directly calculating the divergence of the current density for each node and then marching through time using equation 3.59. Additionally, unlike backward difference, there are no equations to be solved for every time step. These two properties ease the computational load of the problem and speed up the solution process. Unfortunately this scheme has very strict stability conditions which has to be met in order to get a reasonable solution.

Using backward difference approximation we get,

$$\frac{\vec{n}_k - \vec{n}_{k-1}}{\Delta t} = \frac{1}{q}(qB)$$

$$\vec{n}_k - \Delta t B = \vec{n}_{k-1}$$

Since all the equations in B matrix are linear we can pull n out $(B = Cn)$ and rearrange the equation.

$$\vec{n}_k - \Delta t C \vec{n}_{k-1} = \vec{n}_{k-1}$$

$$\vec{n}_k = (I - \Delta t C)^{-1} \vec{n}_{k-1} \tag{3.60}$$

Now we have an implicit solution which seem quite similar to the previous solution but in fact they are quite different. This solution needs a matrix inversion every time step but it is unconditionally stable. The decision to use implicit or explicit solution is not very simple and it will be discussed in detail the next section.

3.2.4 Stability and Computational Efficiency

Before we go into numerical limitations of solving drift diffusion equation via finite difference we should look into physical limitations of the problem. These limitations persist no matter what kind of numerical scheme is employed to solve drift diffusion equations.

3.2.4.1 Physical Limitations

Debye length is the length over which mobile charge carriers screen out an external electric field. It determines how steeply charges will accumulate over a certain distance when subject to an electric field.

$$L_D = \sqrt{\frac{\varepsilon V_{th}}{qn}} \tag{3.61}$$

Debye length limits how coarse the grid can be since we need to be able to accurately capture the distribution of charge density. As it can bee seen from the formula above the higher the charge density is the steeper the charge will accumulate. This can become a major problem for device sizes in millimetre range or higher and high charge concentrations since the mesh density needs to be extremely high.

The amount if time it takes for charge fluctuations to disappear is called Dielectric relaxation time. It limits the maximum time step of a simulation since the fluctuations that are not properly resolved over time will make the simulation unstable.

$$t_{dr} = \frac{\varepsilon}{qn\mu} \tag{3.62}$$

Dielectric relaxation time is only important when electric potential is highly affected by redistribution of charge over time. Otherwise it has minimal impact on the stability of the problem.

3.2.4.2 Numerical Limitations

There are also numerical limits which can affect convergence and stability of a solution when using an explicit scheme. These are called Courant-Friedrichs-Lewy (CFL)conditions. We can look at CFL conditions for pure diffusion and pure drift.

$$\frac{\Delta^2}{2D_n} > \Delta t \tag{3.63}$$

Above condition is for pure diffusion and it restricts the maximum time step. Following condition is for drift dominated systems:

$$\frac{2\Delta}{\mu E} > \Delta t \tag{3.64}$$

This is the second numerical restriction on our simulation. Interestingly the condition for drift depends on the electric field therefore it needs to be satisfied as the electric field changes over time during simulation.

Now we have all the conditions we need to ensure the stability of the simulation. Both physical and numerical constraints have to be evaluated and mesh density and time step need to be selected in order to satisfy all these conditions discussed above. Particularly mesh density have a very strong effect on the accuracy, stability and computational efficiency of the simulation. Increasing mesh density increases the computational time needed to calculate every time step since we have more points. Additionally because of the CFL condition for diffusion time step is related to the square of the mesh size. This means that maximum allowed step size decreases much quicker than the mesh density. Also, increasing charge density can decrease the maximum mesh size to a very small value. This can be somewhat fixed by using a non uniform mesh which can dramatically decrease the amount points needed for the simulation. Unfortunately this is usually not very straightforward to implement in a finite difference scheme.

3.2.4.3 Explicit vs. Implicit Solution

Overall explicit and implicit solutions have their advantages and disadvantages. Choosing one over the other requires careful analysis of the problem. Implicit solution by itself is unconditionally stable therefore it can support very large time steps without any stability issues. However with increased time step, the accuracy of the transient solution decreases but the steady state solution does not get affected. So for steady state solutions it is better to use an implicit method which can reach steady state very quickly. This advantage disappears when particle densities are high enough to affect the electic field and Poisson's equation needs to be solved for every time step. In this scenario the maximum step size is determined by dielectric relaxation time which tends to be around the same order as CFL conditions. Now since the time step is going to be around the same order for both implicit and explicit methods it makes sense to use the explicit one because it is computationally less expensive.

We can sum this brief analysis by stating that implicit solution is preferable when there is no coupling between Poisson's equation and drift diffusion equations and the transient

response is not very important. Explicit solution have an edge over the implicit solution due to its lower computational resource requirement when the equations are coupled and the time steps for both schemes are restricted to fairly small values.

3.2.5 Simulation Procedure

Over the past section we have gone through different equations and schemes that are used to solve drift diffusion and Poisson's equation. Using all this information we can create a general strategy to solve a drift diffusion problem.

First of all we need to define the geometry and physical properties of the problem as well as all initial and boundary conditions. Initialization sets up the first time step of the problem at $t = 0$. Once this first step is done we can generate required vectors and matrices and solve the problem for the next time steps, $t = t_i$.

The solution process starts by solving Poisson's equation using the charge distribution at current time step. Once it is solved we can calculate the electric field distribution and use it in drift diffusion equations to calculate current density distribution. One important choice to make here is to either use finite difference method or Scharfatter-Gummel method in order to calculate current density. The conditions that favor one or the other are not simple to determine and will be discussed in detail in the next chapter. The next decision to be made is either to use an implicit or explicit solution which will determine if we can directly calculate the next step or need to solve a matrix. Finally once we have the carrier distribution for the next step we can check for a stopping criterion. If this criterion is not met then the whole process will start all over again with a small difference. If the charge concentration is so small that the equations are decoupled then we can skip solving Poisson's equation again. This can significantly speed up the simulation since we only need to solve for the continuity equation after this point.

There are two different criteria that can be used to decide weather to finish the simulation or not. We can stop if we intend to solve for a certain time frame and we reached the final time. This is quite simple since we look at the current time and if it is equal or greater than the required simulation time we can just stop the simulation. We could also be interested in reaching a steady state solution. This can be determined by comparing the current carrier distributions with distribution at the previous time step. If the difference is very small then we can conclude that the simulation has reached steady state and it is time stop the solution process. This makes physical sense since it makes sure that the time derivative of the carrier densities are close to zero. The flowchart in figure 3.1 summarizes the solution procedure.
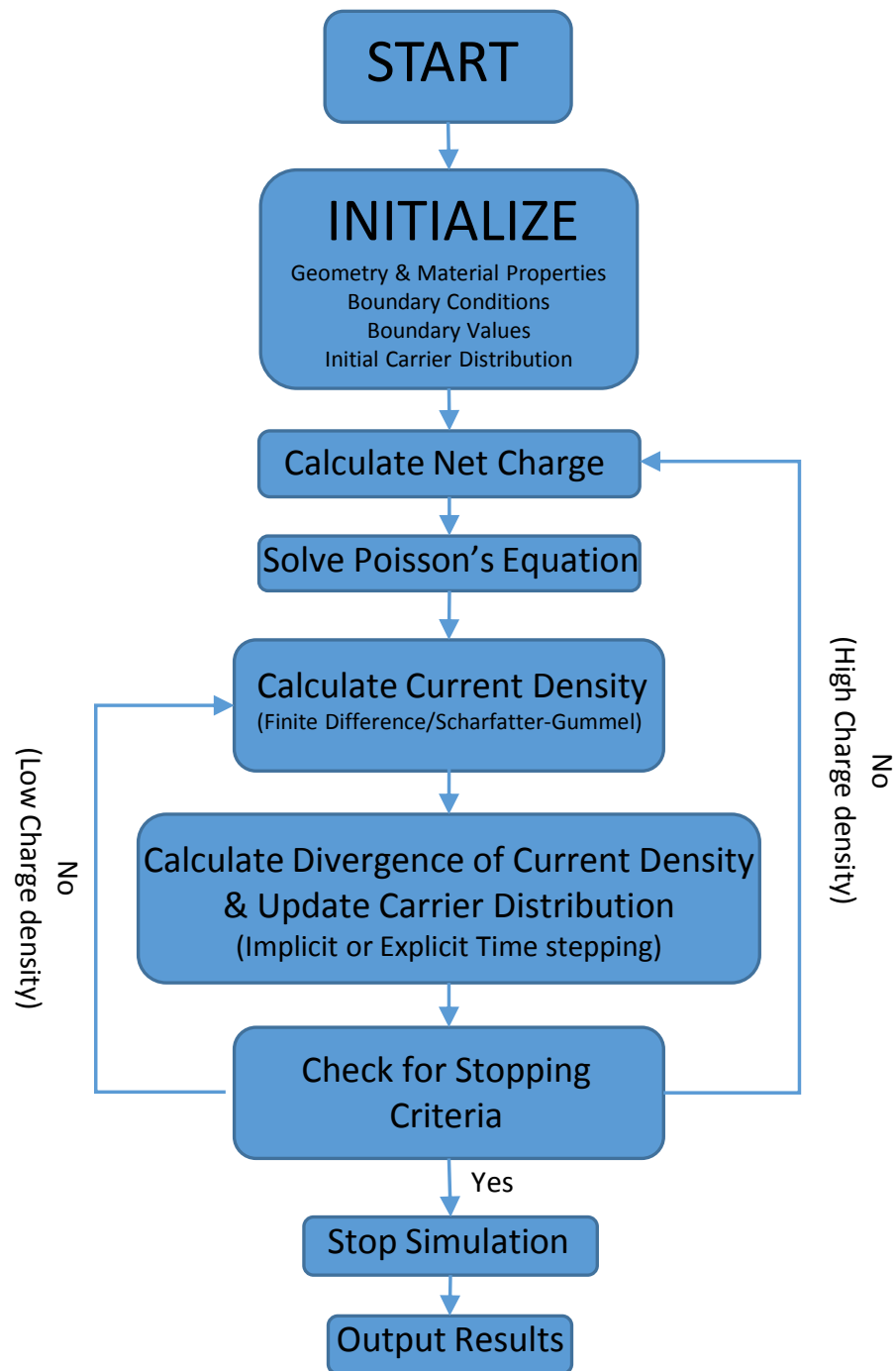
FIGURE 3.1: Finite Difference Drift-Diffusion Scheme Flowchart

Chapter 4

Test Cases: Analytic vs. Numerical Solutions

In the past chapter we have gone through the details of how to solve drift-diffusion and Poisson's equation using finite difference method. Now we can do steady state and transient analysis and compare the results with analytical solutions as well as a commercially available simulator called 'COMSOL Multiphysics' which uses finite element method instead of finite difference. Following test cases were made to ensure that the key parts of the finite difference scheme runs properly and does not produce unexpected results.

4.1 Solution for Closed Boundary

In this test case we will examine the accuracy of the finite difference solution in steady state. In order to do this we can use a simple 1-D problem where we have a finite number of negatively charged particles over a certain distance subject to constant electric field. This is the same problem we have solved analytically in section 3.3.1. We also assume that the charge density is very low and does not affect the electric field. Both ends of the simulation domain have no flow boundary conditions for charged particles. The solution process requires an initial distribution for charge density over the area. For this problem the density of the negative particles was initialized to be uniform over the entire area. Since our differential equations are uncoupled solving Poisson's equation only once is sufficient to determine the electric field over the course of the entire simulation. Figures 4.2 and 4.1 show the potential and the electric field distribution over the entire simulation area calculated from Poisson's equation using finite difference.
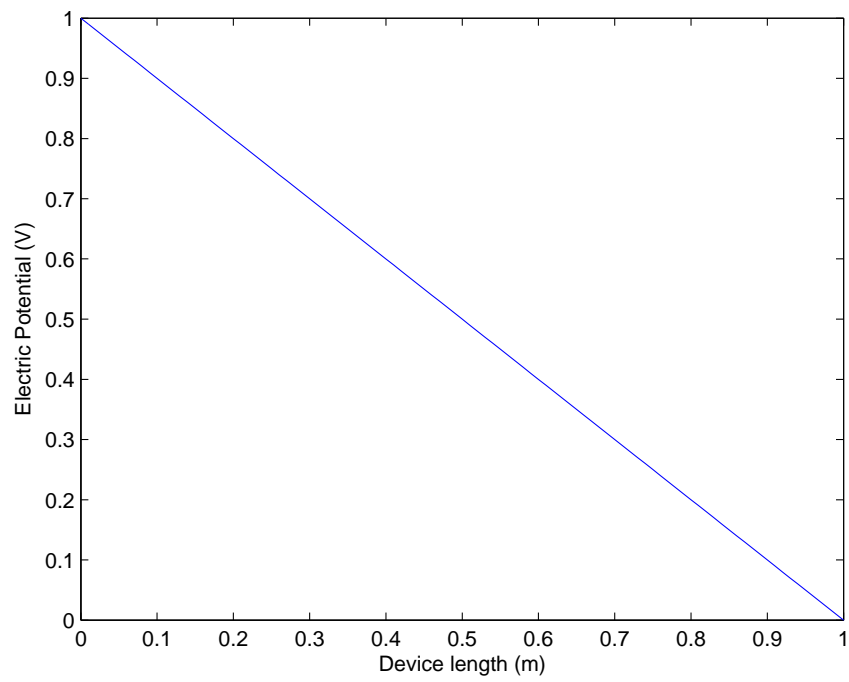
FIGURE 4.1: Potential Distribution
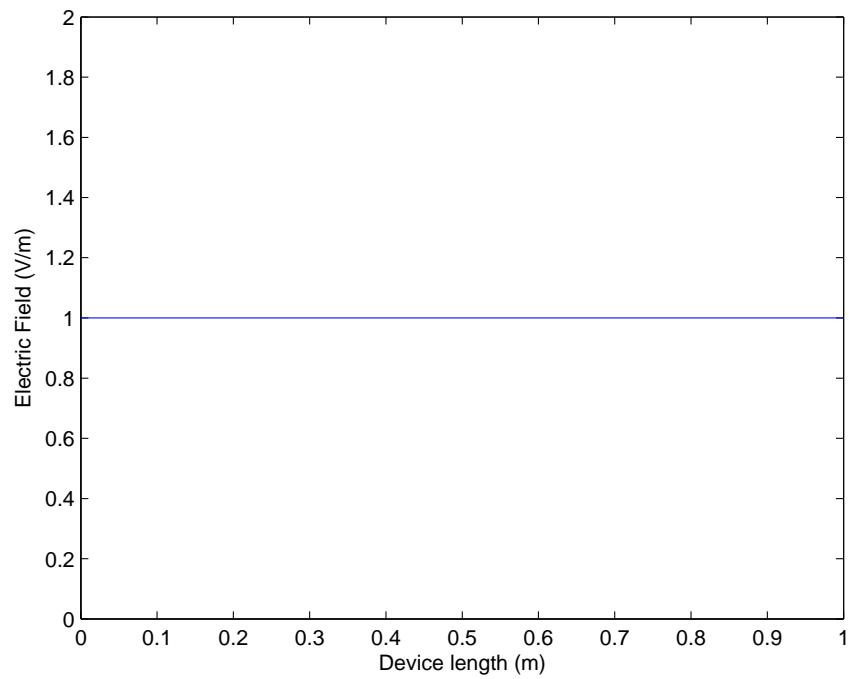
FIGURE 4.2: Electric Field Distribution
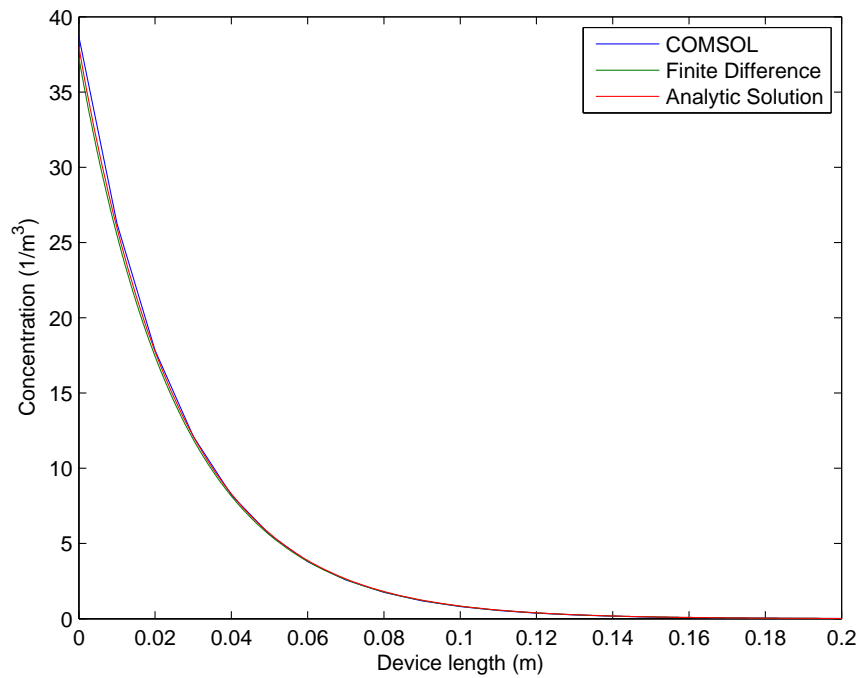
FIGURE 4.3: Steady State Negative Charge Density

Figure 4.3 has two simulation results as well as the exact solution of this problem. The green line represents the result given by the finite difference method once the transient response reaches steady state. It can be seen from the graph that the steady state solution generated by both COMSOL and finite difference matched the analytical solution.
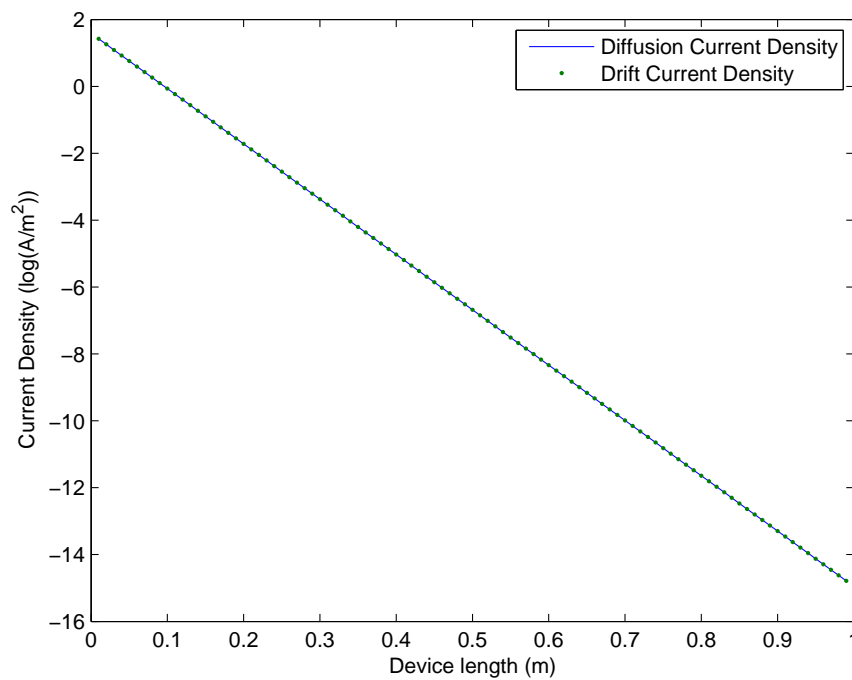
FIGURE 4.4: Finite Difference Drift and Diffusion Current Densities

While deriving an analytical solution for this problem we have assumed that at steady state the drift current density must be equal to the diffusion current density. In figure 4.4 we see drift and diffusion current densities in log scale. Overall both currents match quite tightly.

4.2 Solutions for Open Boundary

Another very important aspect of drift-diffusion simulation is its transient response. Like the previous test case, we can use a closed form solution to test the accuracy of the transient response. In section 3.3.2 we have found two different analytic solutions for a similar drift diffusion problems which involved infinite boundaries and a uniform electric field. The only difference between two cases are their initial carrier distribution. One has a rectangular and the other one has a gaussian initial carrier distribution. Since we have not implemented any way to deal with infinite boundaries we will just simulate these two problems until the carrier distributions gets close to one boundary.
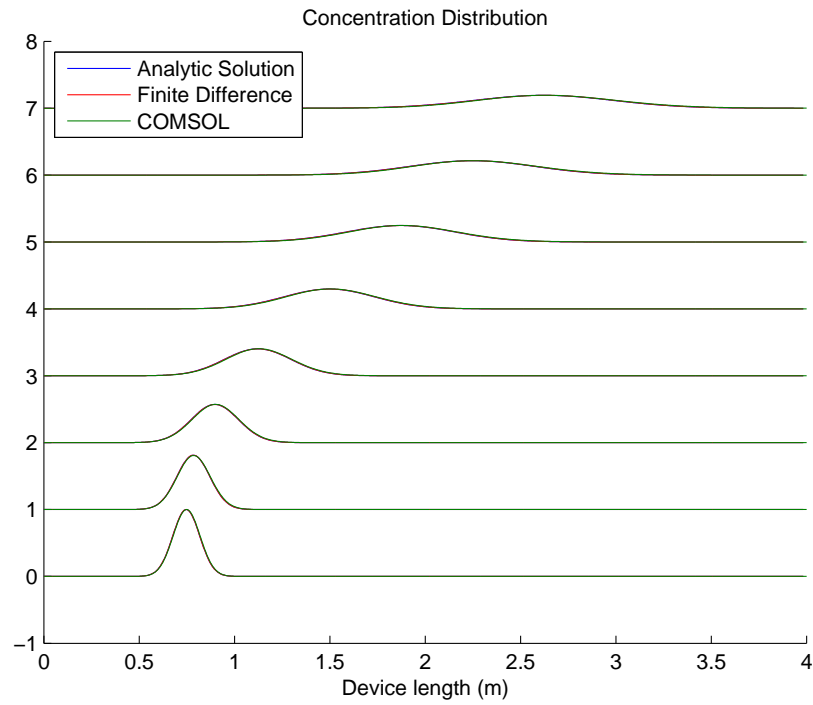
FIGURE 4.5: Gaussian Carrier Distribution Evolving Over time

Figure 4.5 has the transient response from COMSOL, finite difference and analytical solution. Snapshots of the carrier distributions were taken for each method at different time steps and they were superposed on top of each other. Increasing levels on y axis represent a carrier distributions at a different time starting from the bottom and moving forward in time towards the top. Figure 4.5 has a gaussian initial carrier distribution. It can be seen from that the transient solution generated by both COMSOL and finite difference are quite close to the analytical solution.

4.3 Hybrid Method

While developing a method for numerically calculating current density we have seen that Scharfatter-Gummel scheme turns into a first order upwind scheme for drift dominant problems. Most of the time first order upwind schemes has a major drawback which is numerical dispersion. This means that we will see diffusion due to numerical error even though it almost does not exist. In order to investigate this issue and look for possible remedies we will use the previous example ,with a much higher electric field, as a starting point Here in figure 4.6 we see the transient response of a drift dominant problem. Finite difference has no problem producing an accurate transient response but SG has a fair amount of numerical diffusion.
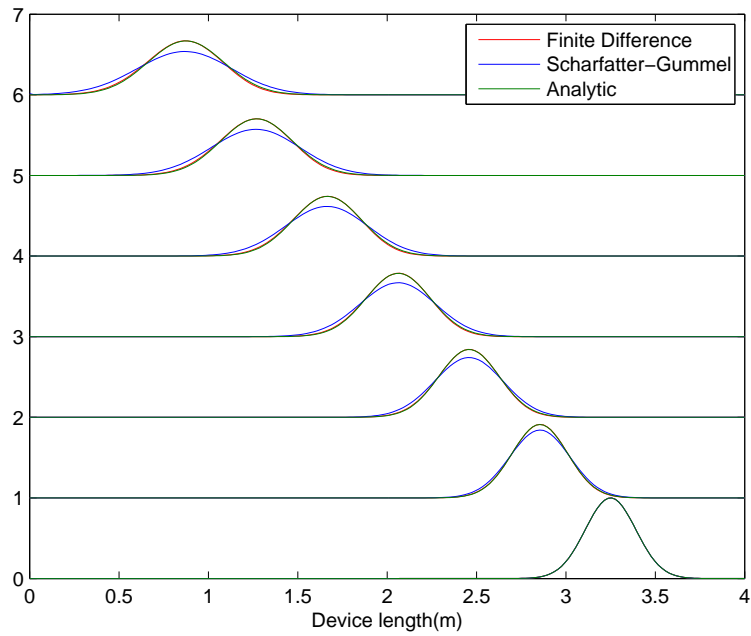
FIGURE 4.6: Gaussian Carrier Distribution Evolving Over time

We can also look at the differences between finite difference and SG in steady state. In this case as it can be seen from figures 4.7 and 4.8 SG produces a solution much closer to the analytical solution. This is not surprising. Both steady state solution and SG scheme has an exponential form. So SG can capture the non-linearity at the boundary much better than finite difference which has linear terms. Also in figure 4.8 we can see finite difference producing negative carrier density distribution which is not physical and it can easily make the simulation unstable.

We can see that both methods have their advantages. It is possible to develop a method where we can switch between two methods to get more accurate results. From the analysis above it seems like in transient cases finite difference method have an advantage
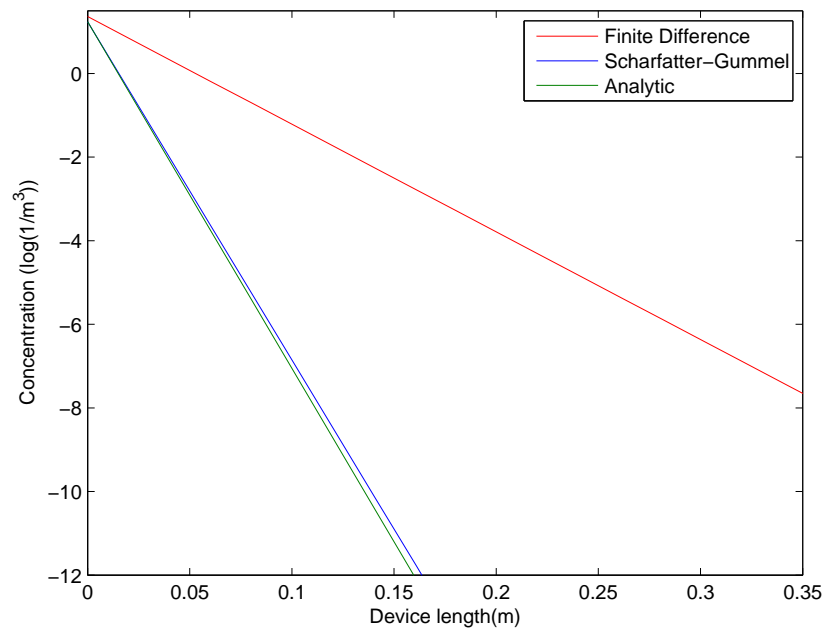
FIGURE 4.7: Steady State Carrier Distribution of a Drift Dominant Problem
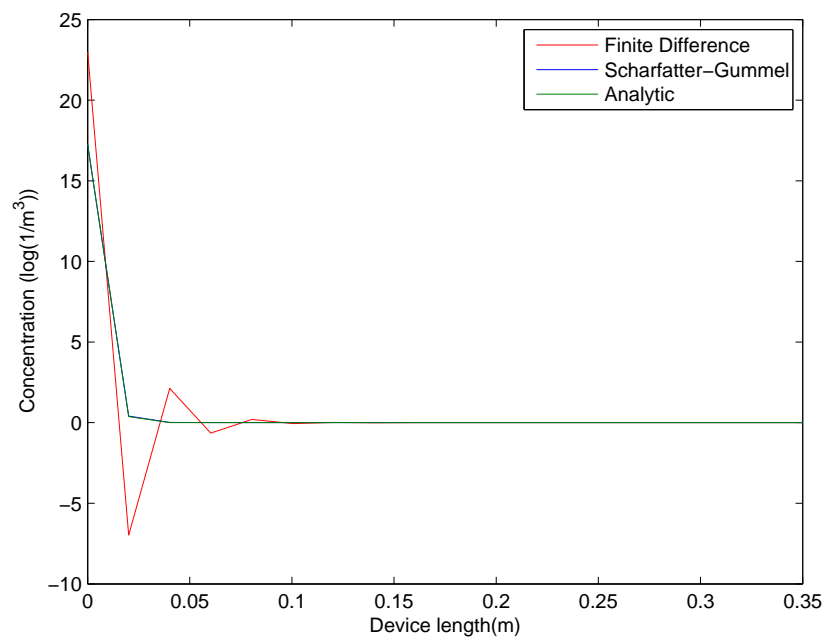
FIGURE 4.8: Steady State Carrier Distribution of a Drift Dominant Problem

and SG is better in steady state where drift and diffusion cancel each other out. We can switch between methods by keeping track of two key properties, closeness to steady state and the non linearity of the final solution. The difference between drift and diffusion currents is a good estimator for closeness to steady state and the ratio of drift velocity to diffusion constant can be used to measure non linearity. We can use following two equations to calculate these parameters.

$$K_1 = |\frac{J_{drift} + J_{diff}}{J_{drift} - J_{diff}}| \tag{4.1}$$

$$K_2 = \frac{\mu E}{D} = \frac{v}{D} \tag{4.2}$$

K_1 will always have a value between 0 and 1 depending on how close drift and diffusion current densities are to each other. When K_1 is close to 1 it means that drift and diffusion do not have equal values and opposite signs therefore the simulation is far away from steady state. On the other hand if K_1 is close to 0 it means that the simulation is in steady state or close to it.

K_2 is a measure of how non linear the solution is going to be since it appears in an exponential. If this value is between 0 and 2 then the final solution is slightly non linear. As K_2 increases further the non linearity becomes stronger.

Now that we have established a way to check closeness to steady state and non linearity of the final solution we can use these to improve the accuracy of our transient and steady state responses. During simulation if K_1 is close to 1 it means that we are not close to steady state therefore it is better to use finite difference. When K_1 is getting close to zero it is time to check if the final solution is going to be very non linear using K_2. If that is the case then we can switch to SG method to calculate the steady state solution. Figure 4.9 shows the evolution of the transient response over time using this hybrid method. The solution is in transient mode so finite difference is used to calculate the current density. As expected numerical diffusion does not occur and the response is quite close to the analytic solution.

Figures 4.10 to 4.13 shows the changes in the concentration over time as the simulation approaches steady state. By looking at the following sequence of figures we can see that finite difference has fluctuation problems and it gets worse over time. At the same time we can see the hybrid method transitioning from finite difference to SG method and not having any fluctuation problems. Finally in steady state plots in figure 4.14 shows the difference in accuracy at steady state between the hybrid method and finite

difference. By mixing two methods we were able to reach higher accuracy without needing to increase the mesh density.
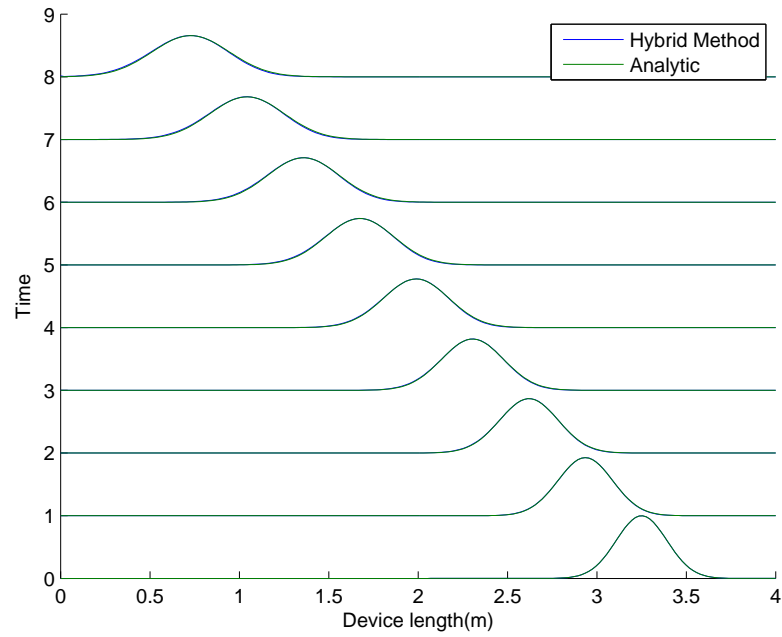
FIGURE 4.9: Gaussian Carrier Distribution Evolving Over time
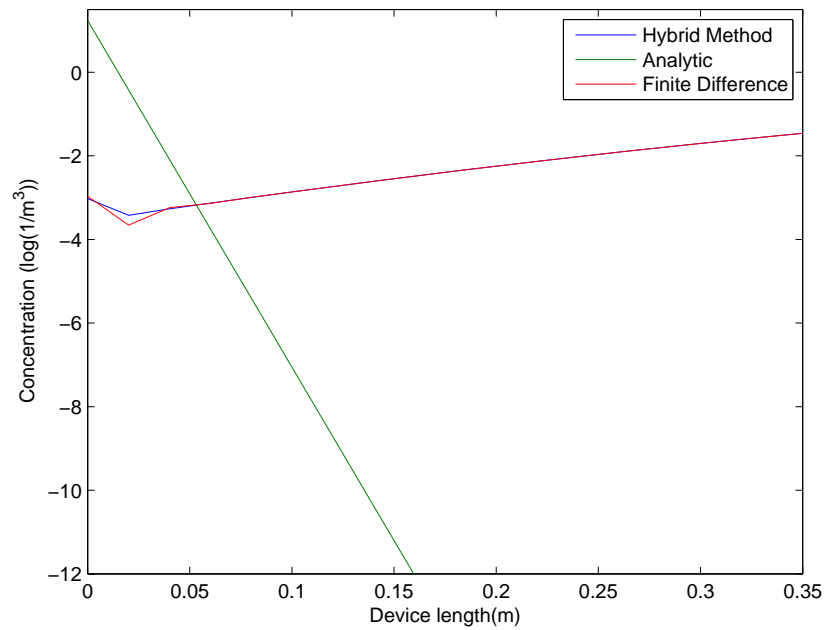
FIGURE 4.10: Transient Solution of a Drift Dominant Problem
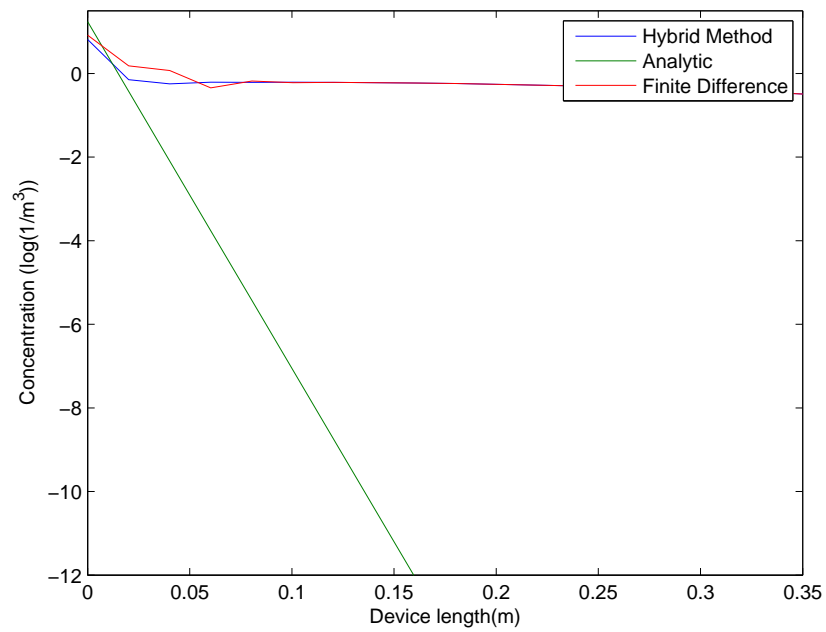
FIGURE 4.11: Transient Solution of a Drift Dominant Problem
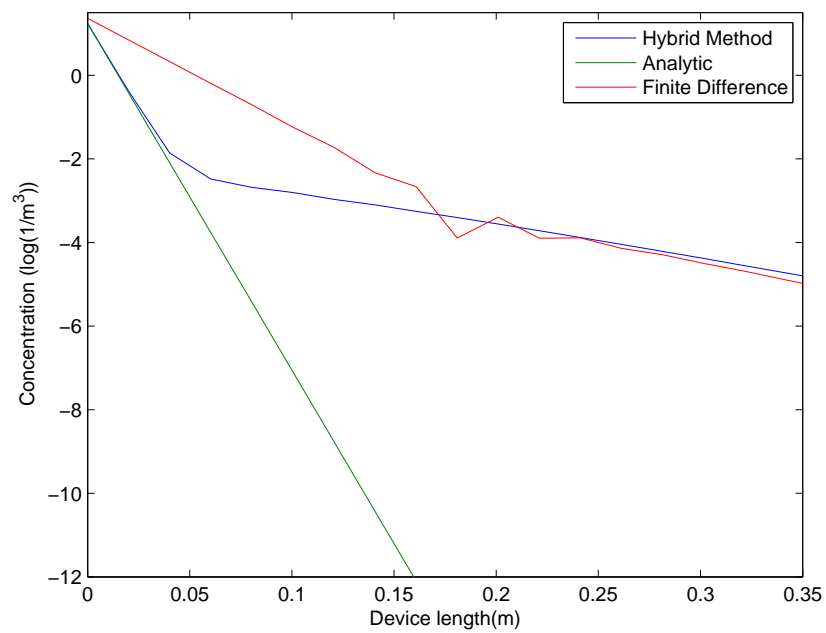
FIGURE 4.12: Transient Solution of a Drift Dominant Problem
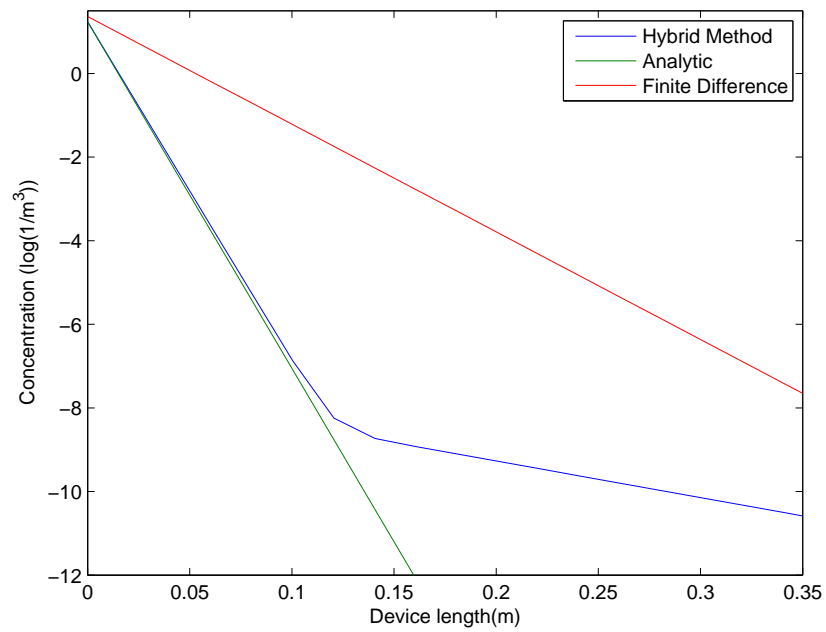
FIGURE 4.13: Transient Solution of a Drift Dominant Problem
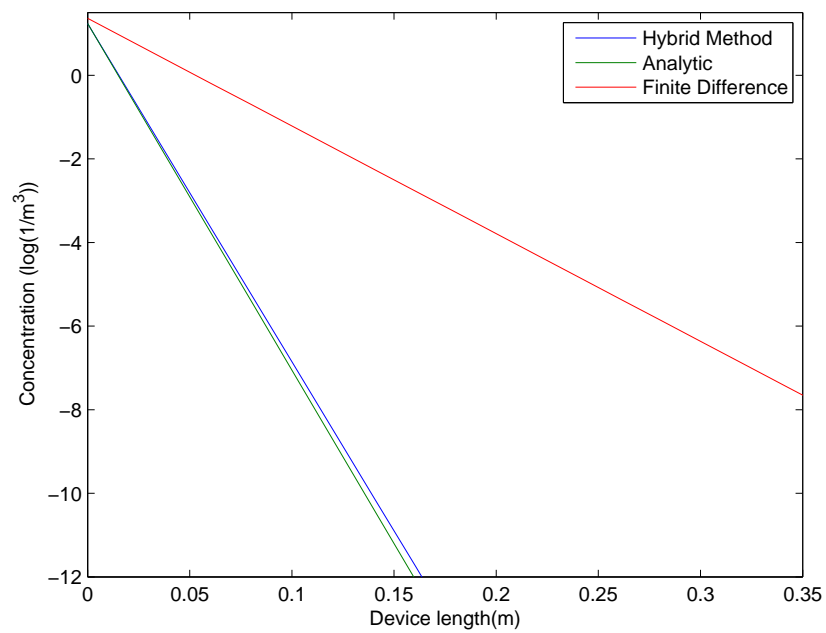
FIGURE 4.14: Steady State Carrier Distribution for a Drift Dominant Problem

4.4 PN Junction

In previous sections of this chapter we have put finite difference drift diffusion model to test. In all the cases we ran before, Poisson's equation was not coupled with drift diffusion equations. In this example we will be testing both drift diffusion and Poisson's equation to see how well they work when they are coupled together. A simple pn junction is quite adequate for this task since it has analytical solutions, under certain assumptions, for electric potential, electric field and net charge.

For the simulation ,the initial hole and electron distributions were determined using mass action law and they were assumed to be constant at the boundaries. Keeping carrier concentrations constant at the boundaries creates a mechanism in which the charge can move in and out of the simulation domain. If the charge density at any time step is higher than the fixed density then the difference will move out of the system. If there is a lack of charge at the boundary then carriers will move in to fill in the gap. Following figure (4.15) shows the final result of bringing p and n type materials together.
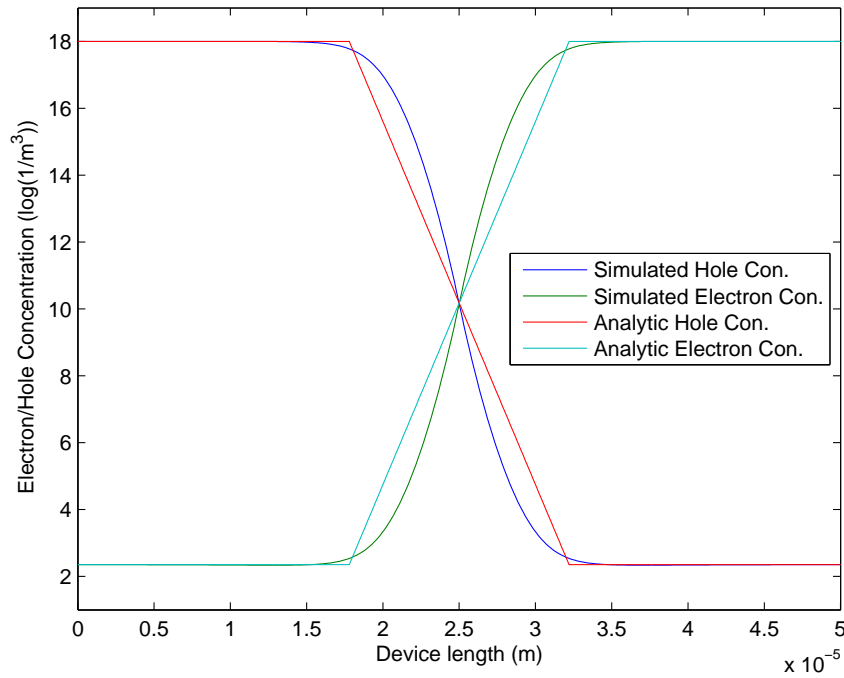
FIGURE 4.15: Electron/hole Concentration of a PN Junction

We can see a little mismatch between simulated and analytic concentration densities. Analytic solution have sharp edges and simulated solution does not. This is due to all the assumptions made in order to find an analytic solution. We will be seeing this little mismatch also for electric field, electric potential and net charge .

Since the purpose of this problem is to test Poisson's equation as well, we can look at the final potential distribution due to pn junction. Figure 4.16 shows the potential distribution for simulated and analytic solution. Close match in electric potential distribution shows that coupled equations can generate fairly accurate solutions.
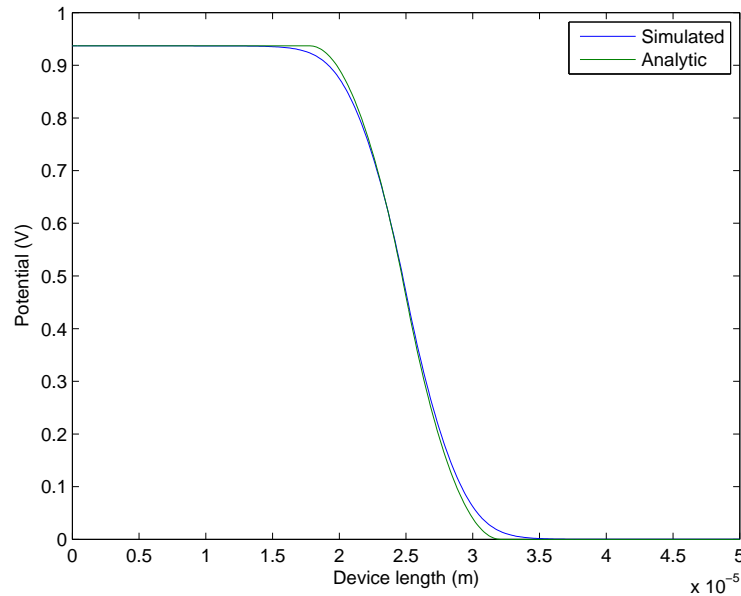
FIGURE 4.16: Potential Distribution of a PN Junction

Calculation of the electric field involves one basic derivative. Since simulated potential is matching the analytic solution quite nicely the electric field should follow a similar pattern. Figure 4.17 shows that this is indeed the case, simulated electric field matches the calculated electric field.

Finally we can look at the total charge distribution at steady state(4.18). Simulated net charge density follows the analytic one except the abrupt changes at two ends.
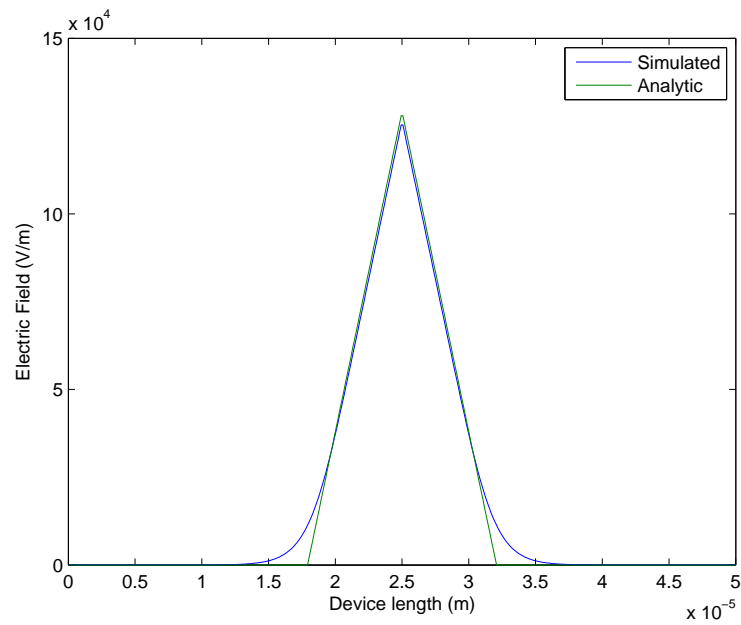
FIGURE 4.17: Electric Field Distribution of a PN Junction
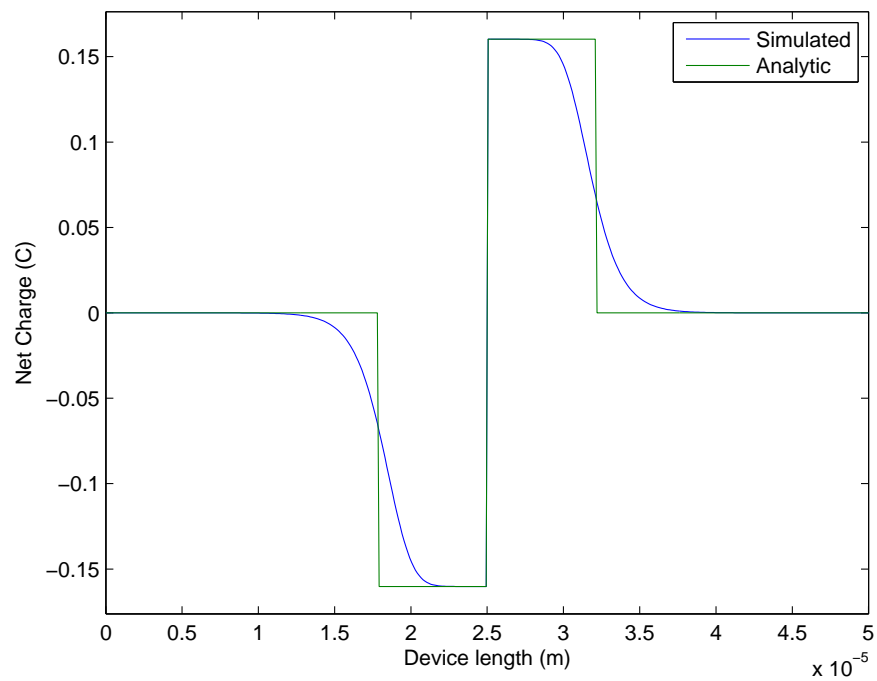
FIGURE 4.18: Total Charge Distribution of a PN Junction

4.5 Region Specific Particle Density Limit

In section 4.2.2.3 we have talked about using a Dirichlet boundary condition (J=0) to stop the particle flow into a node. This can be done by precalculating the particle density of concentration restricted nodes at the next time step, setting any influx to zero if the concentration is going to go over the limit and finally calculating the concentration at the next time step using the updated current densities.

In order to test this method we can use a simple example where we have two particles of the same charge initialized like the figure below (4.19). One set of particles has a concentration limit of $2 \ 10^{10} \ m^{-3}$ on the right side of the simulation area and no limit on the left side. The other set has no restrictions.
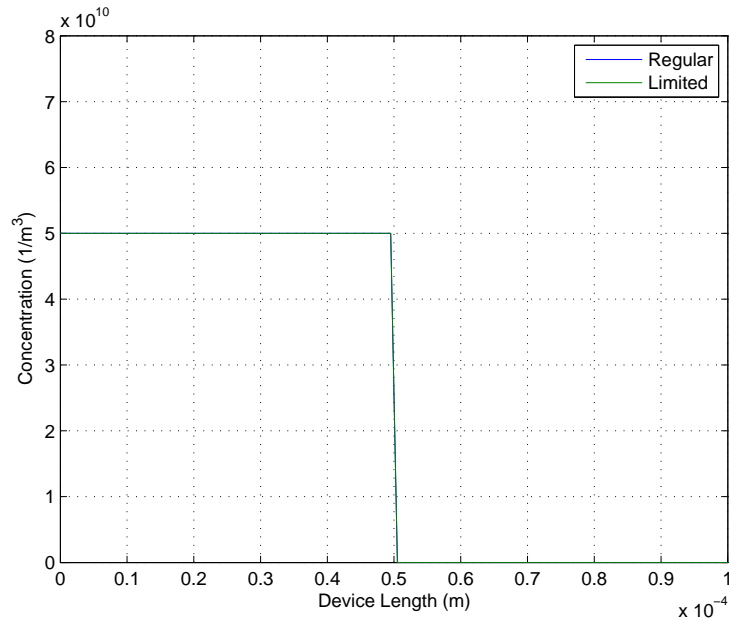
FIGURE 4.19: Initial Particle Density

This transient simulation was done using a potential as a function of time. For the first half of the simulation applied potential was positive and for the second half it was negative. Figure 4.19 shows how two simulations differ when the particles are pushed towards the right wall due to the electric field created by the positive potential. Particles with no limit on the right side move freely and accumulate on the right side. The limit for the other particles is effectively stopping them from going in and accumulating freely. Once the limit is reached at a certain node the concentration cannot increase any further and that node becomes a no flow wall.

When the potential is switched all the particles accumulate freely to the left side of the simulation domain since there are no restrictions on this side (figure 4.21).
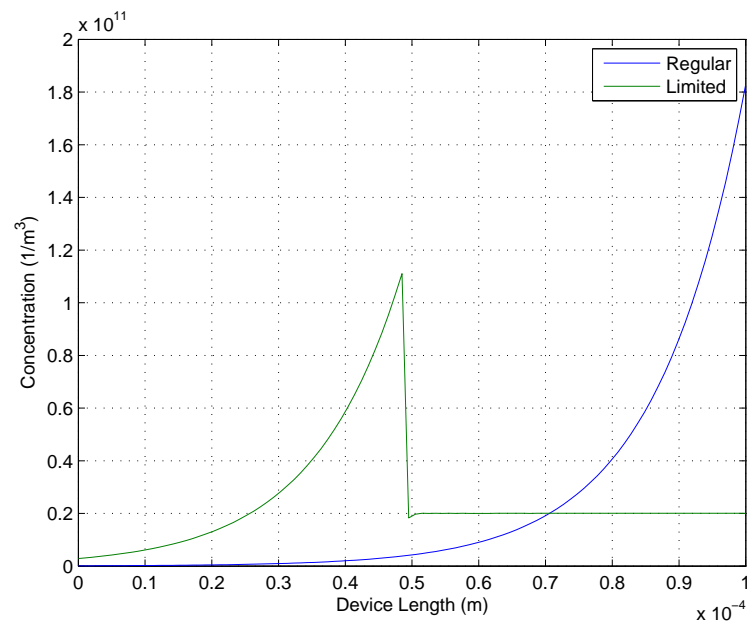
FIGURE 4.20: Limited Concentration Accumulation on the Right Side
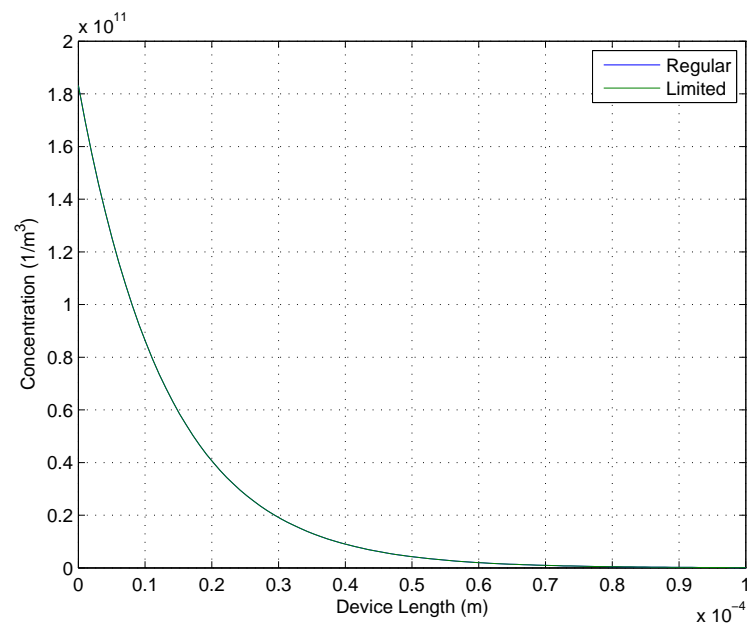
FIGURE 4.21: Limited Concentration Accumulation on the Left Side

This last figure (4.22) shows the transient response over time of a single node on the right side. The potential is positive for the first 1.5 seconds and it is switched to negative for the last 1.5 seconds. The node without limit keeps accepting charge until steady state has been reached but the node with a limit on stops accepting charged particles once the limit is reached. After the potential is switched density limited node has no problem releasing the particles.
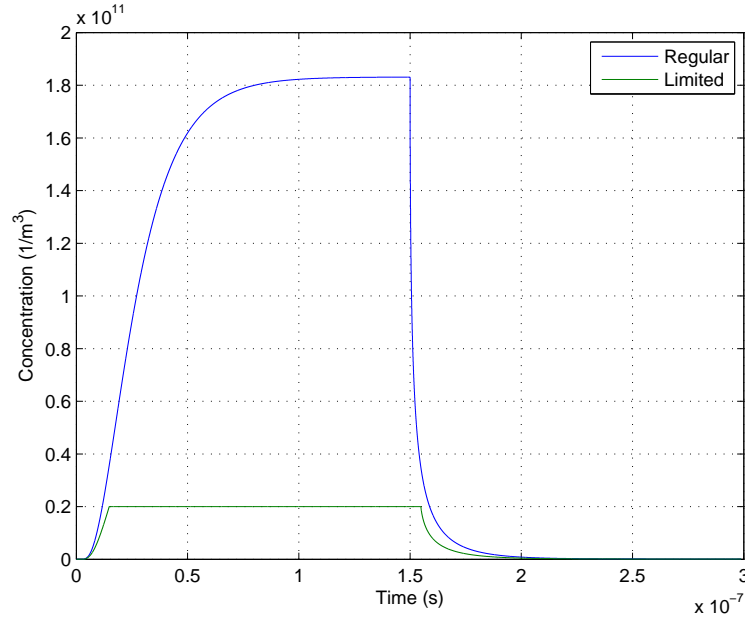
FIGURE 4.22: Accumulation at the right wall over time

Additional to the test we ran using finite difference we can also try to simulate the exact same behaviour in COMSOL.

COMSOL does not have a built in option that allows limiting particle density. One possible solution to this is making particle mobility and diffusivity a function particle density. It is possible to use a sigmoid function which switches from 1 to 0 very quickly when particle density is close to its limit. Here is the equation of the sigmoid function used to limit the particle flow:

$$\mu = \frac{\mu_0}{1 + e^{\sigma(n-n')}} \tag{4.3}$$

μ_0 is the original mobility of the charge carrier. σ controls the sharpness of the switch and n' determines the density at which the switch will be.

Another problem with COMSOL was the definition of mobility and diffusion coefficients over different areas. If these constants are defined as one single value per area it works just fine but if they are defined as a function of concentration it causes convergence

issues. This can be overcome by defining using two more sigmoid functions to distinguish between two areas with different mobilities and diffusion constants. Left sigmoid in figure 4.23 was multiplied by the mobility/diffusivity of the left side of the area and the right sigmoid was multiplied by the mobility/diffusivity of the right side of the area. Both functions were summed to obtain a function which describes the characteristics of the entire area.

$$\mu = \frac{\mu_l}{1 + e^{\sigma_x(x-x')}} + \frac{\mu_r}{1 + e^{-\sigma_x(x-x')}} \tag{4.4}$$

In this problem μ_r is the same as equation 4.3 since the region on the right side has a particle density limit. A sharp switch between right and left side mobility using the function above would be ideal for this simulation but unfortunately it causes convergence issues in COMSOL therefore there is a gradual change between two mobilities.
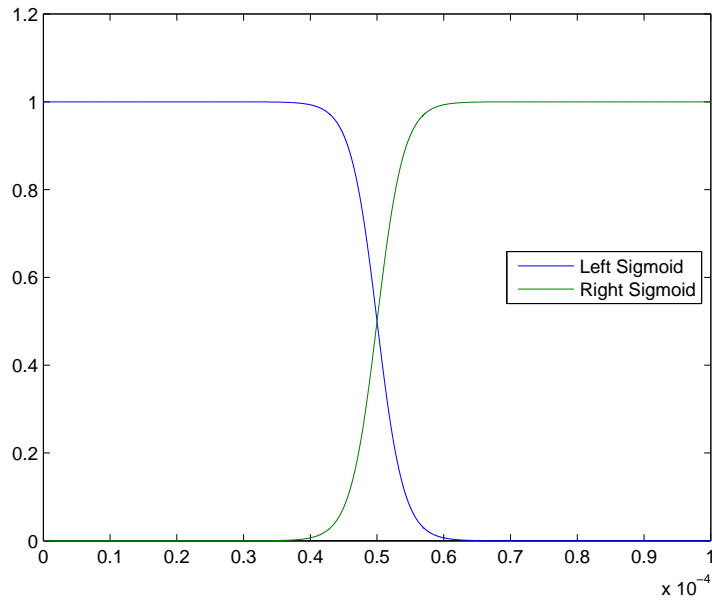
FIGURE 4.23: Mobility change from left to right side

The initial carrier distribution for COMSOL was set to be exactly the same as finite difference simulation. Figures 4.24 and 4.25 show results for both COMSOL and finite difference simulations at steady state before the potential switch. The plot on the left side gives insight on how COMSOL simulation behaves for limited and limitless accumulation on the right wall. Due to the gradual change of mobility and diffusion constants between two areas we end up with concentration on the right side higher than the limit which is $2\ 10^{10}$. Additionally, the particle density goes over its limit near the right wall. In figure 4.25 the difference between COMSOL and finite difference becomes

more visible. In FD simulation the accumulation goes much higher due to higher electric
field and unlike COMSOL it does not penetrate the right half of the simulation domain.
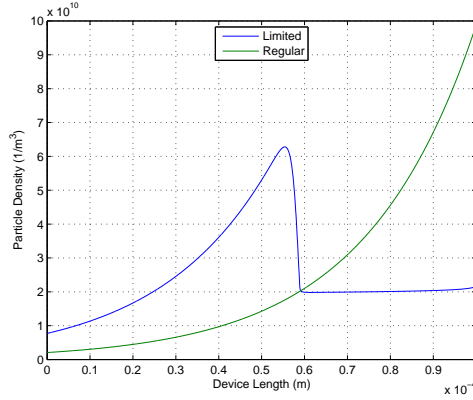
FIGURE 4.24: COMSOL Simula-
tion for Particle Density Limit
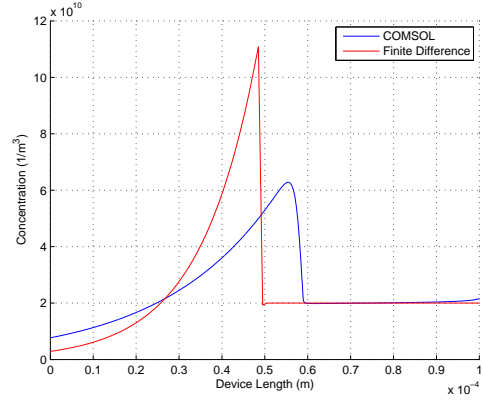
FIGURE 4.25: COMSOL and Fi-
nite Difference Simulation

In figure 4.26 we can see the accumulation of charge near the middle after the potential is
switched. This is due to mobility being a function of distance and concentration. As the
ions move from left to right they go from a low mobility region to a high mobility region
and they slowly accumulate around the area where the change in mobility occurs. Figure
comparing both COMSOL and finite difference shows that the accumulation does not
happen in the case of finite difference due to the way concentration limiting mechanism
was implemented.
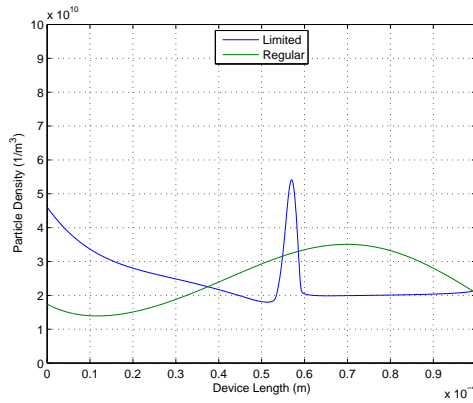
FIGURE 4.26: COMSOL Simula-
tion for Particle Density Limit
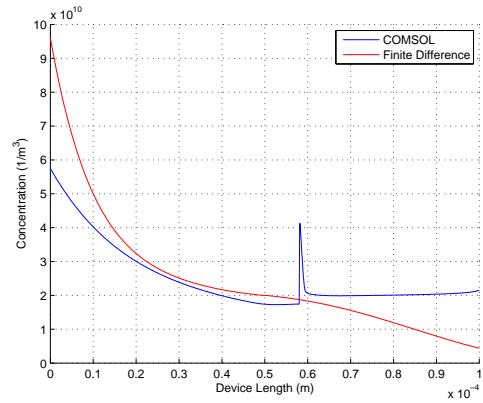
FIGURE 4.27: COMSOL and Fi-
nite Difference Simulation

With the decrease of ion concentration on the limited region the difference between low
and high mobility regions diminish. Once the concentration on the limited side is low
enough the whole system behaves as if there was no limit and ion mobility becomes
equal for all regions and the ions freely accumulate on the left wall (figure 4.28). Aside
from the difference in electric field strength both simulations behave the same way as
they approach steady state. Figure 4.29 shows concentration densities at steady state.

COMSOL simulation has a lower electric field since it has convergence issues with high electric fields.
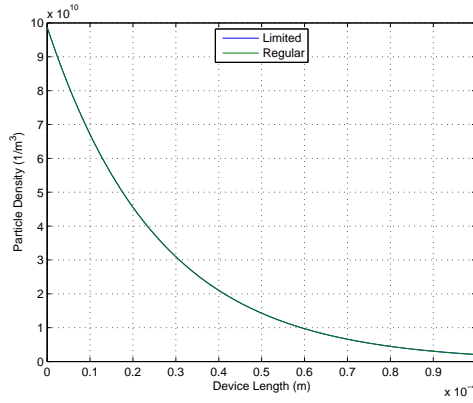
FIGURE 4.28: COMSOL Simulation for Particle Density Limit
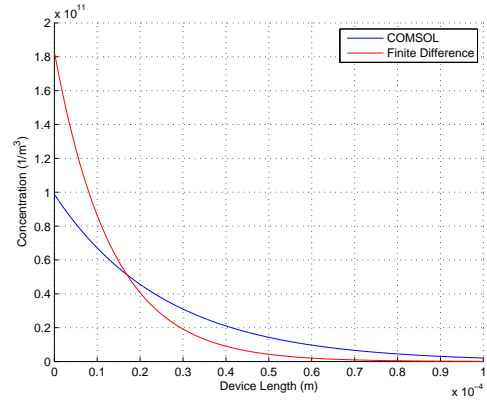
FIGURE 4.29: COMSOL and Finite Difference Simulation

To finish our comparison we can look at the particle density transient response of the rightmost node. For the first half of the simulation everything is the same as the finite difference case except COMSOL goes a little bit over the limit. When the potential is switched node without the limit has no noticeable difference in behaviour. The node with concentration limit has a lag when it comes to releasing the particles. This is due to the sigmoid function used to achieve a limiting behaviour. Once the limit is reached mobility and diffusivity are stuck at a very low value until the particle density starts to go lower than the limit.
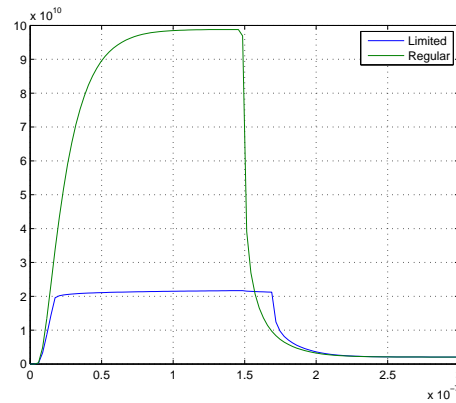
FIGURE 4.30: Density on the right wall over time using COMSOL
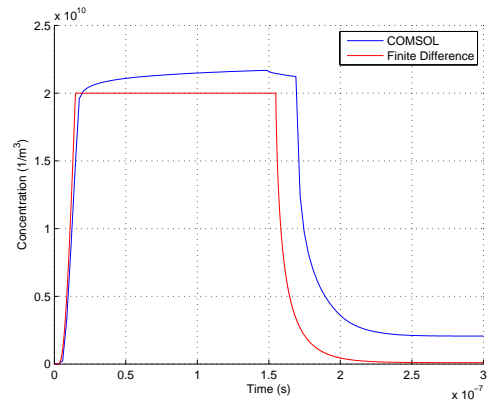
FIGURE 4.31: Density on the right wall over time, COMSOL vs. Finite Difference

In this example we have seen that it is possible to impose a density limit over any area using a simple no flow boundary condition in finite difference. For COMSOL we had to use some workarounds in order to simulate the same behavior but the results were not very satisfying because of convergence issues.

Chapter 5

Chapter Title Here

5.1   Problem Analysis
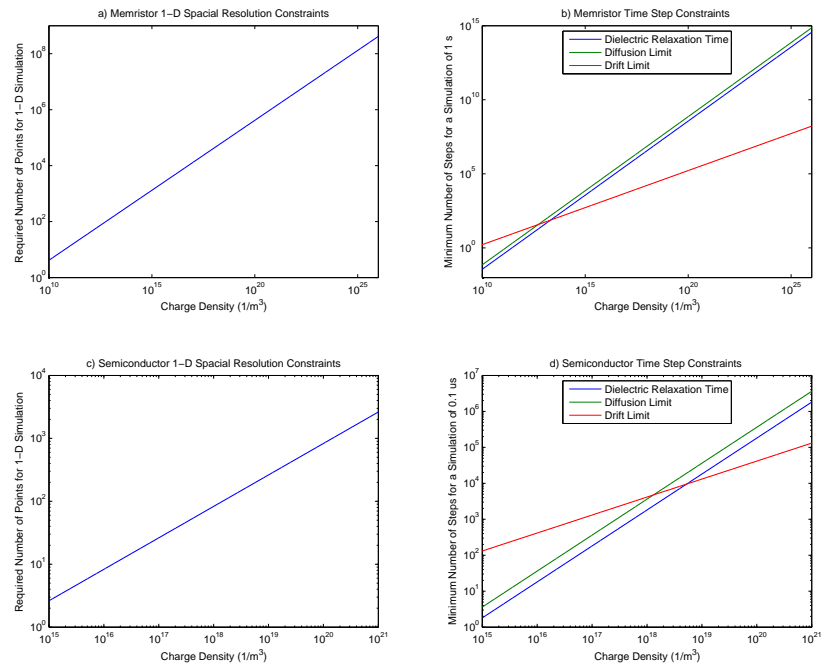
Figure 5.1

5.2 Debye Length and Simulation Validity
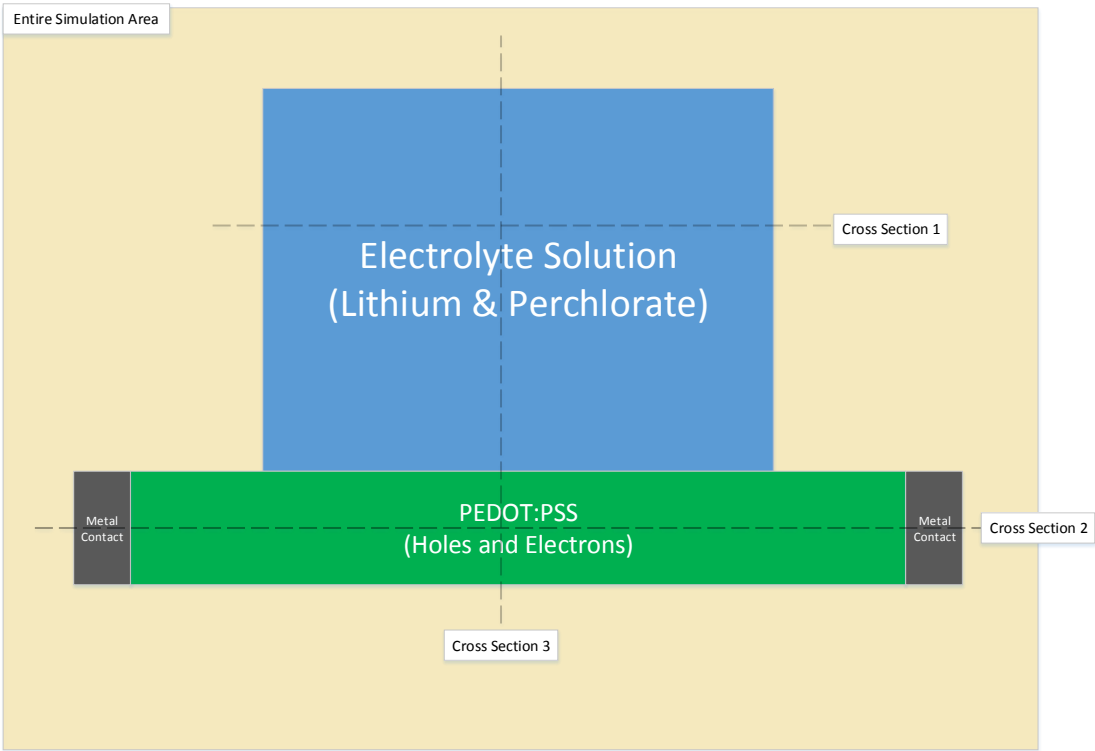
FIGURE 5.2

5.2.1 1-D Horizontal Electrolyte
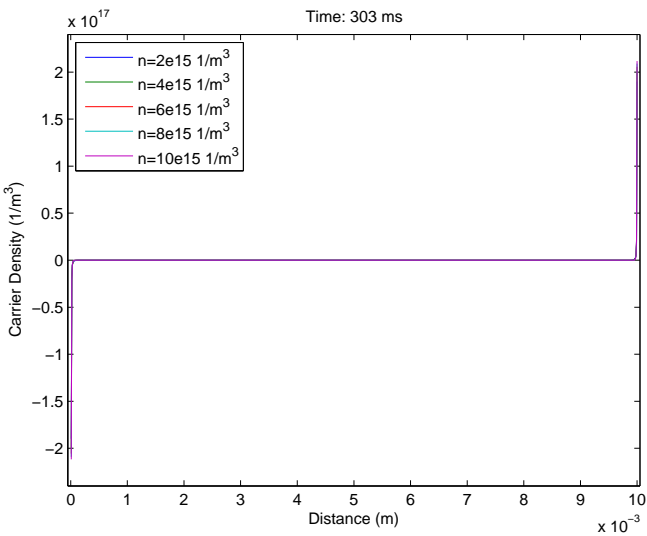
FIGURE 5.3
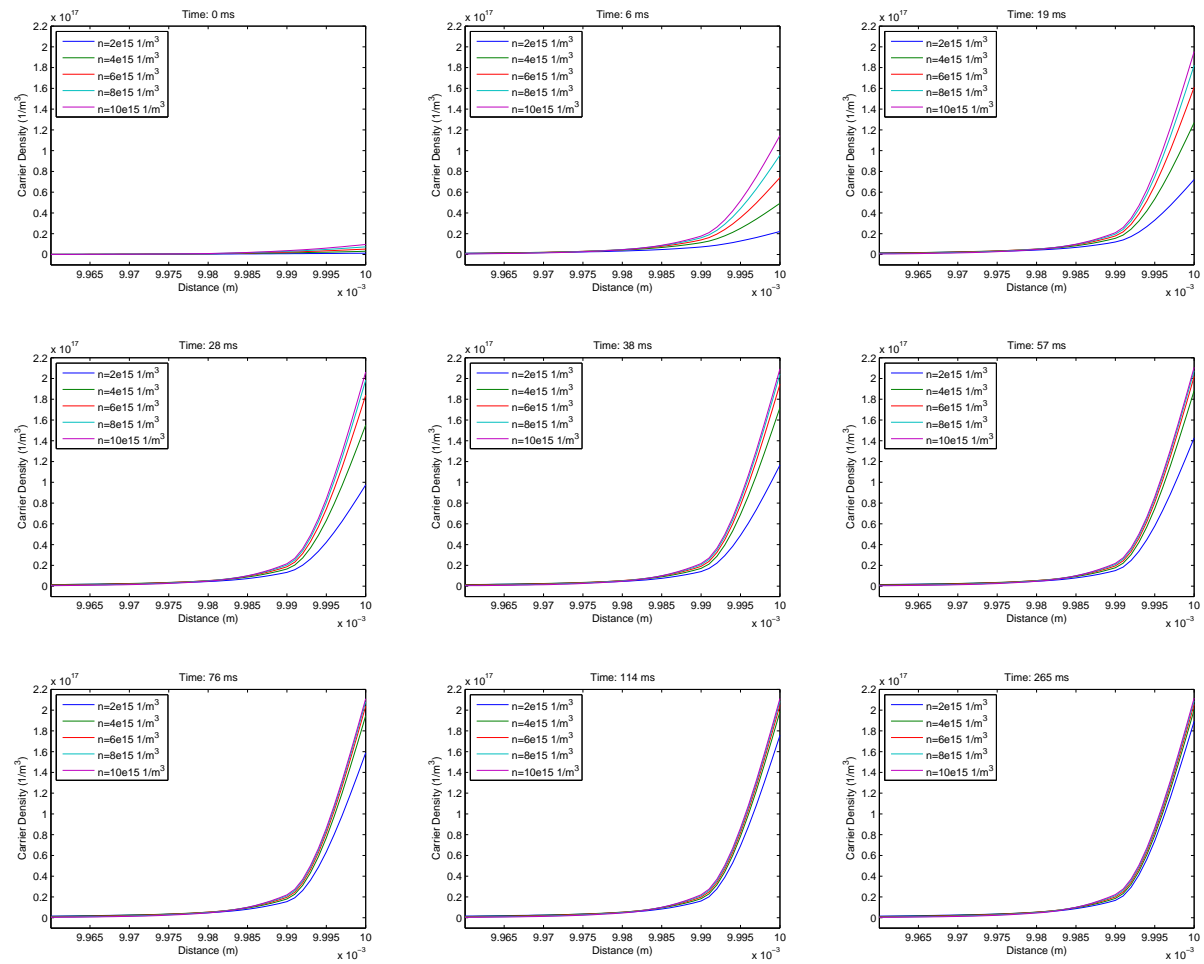
FIGURE 5.4
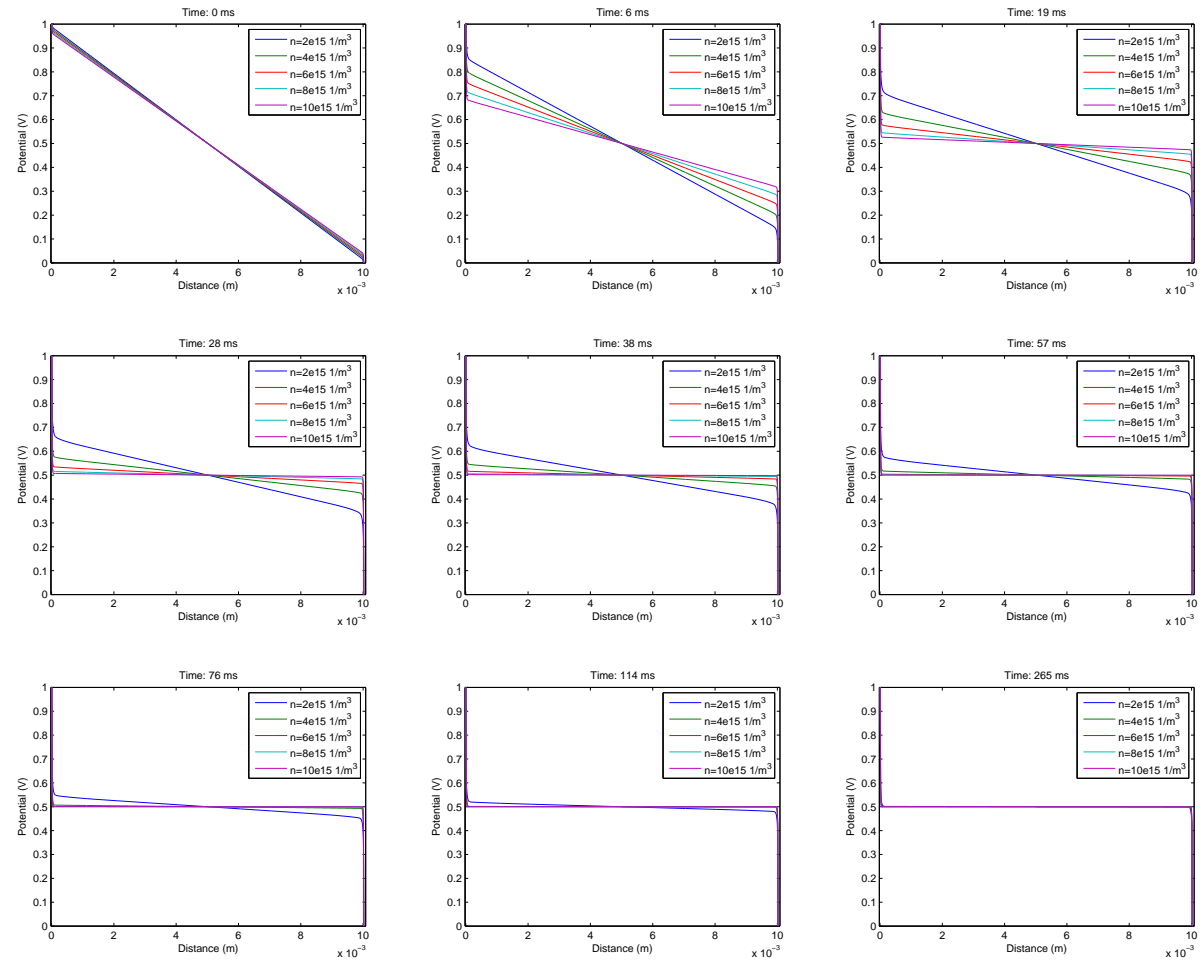
FIGURE 5.5
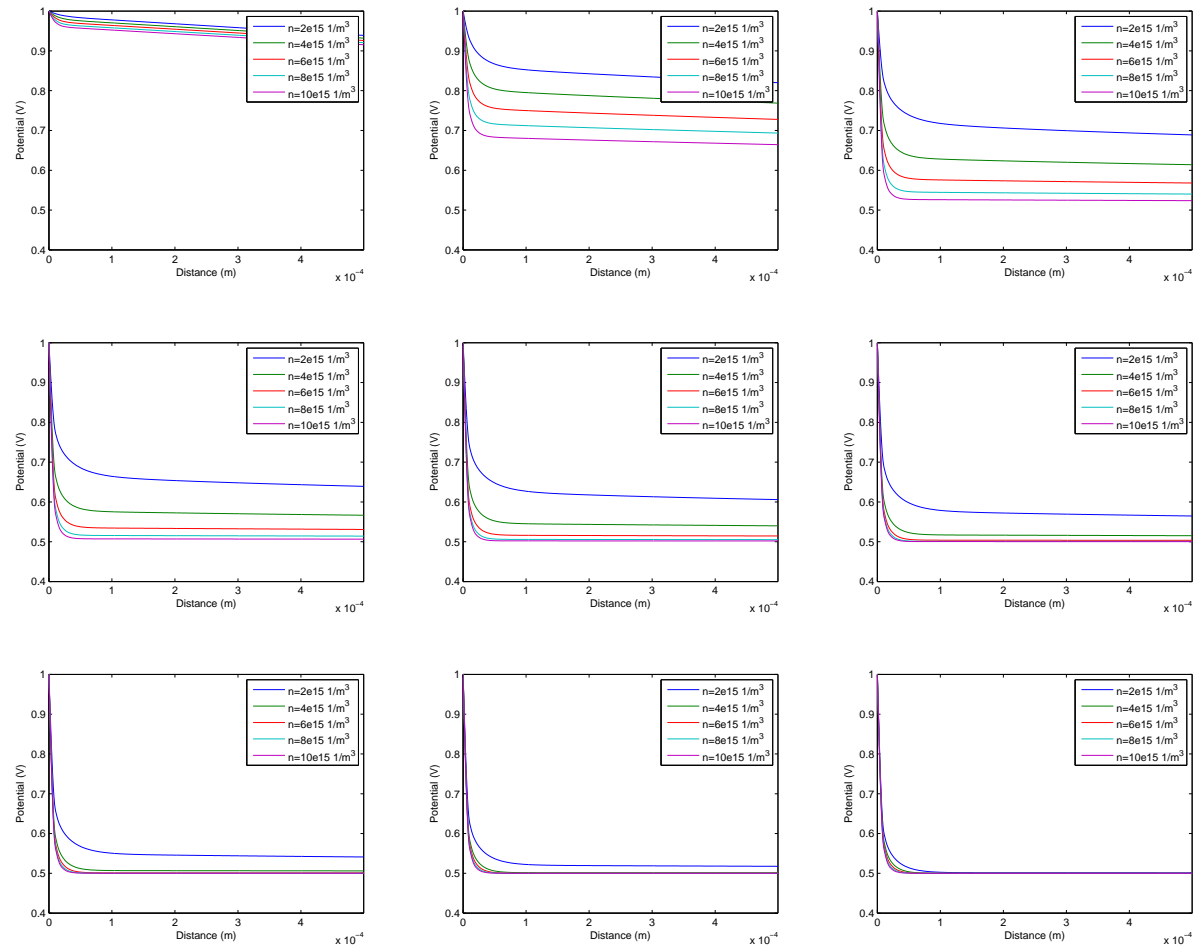
FIGURE 5.6

5.2.2   1-D ?
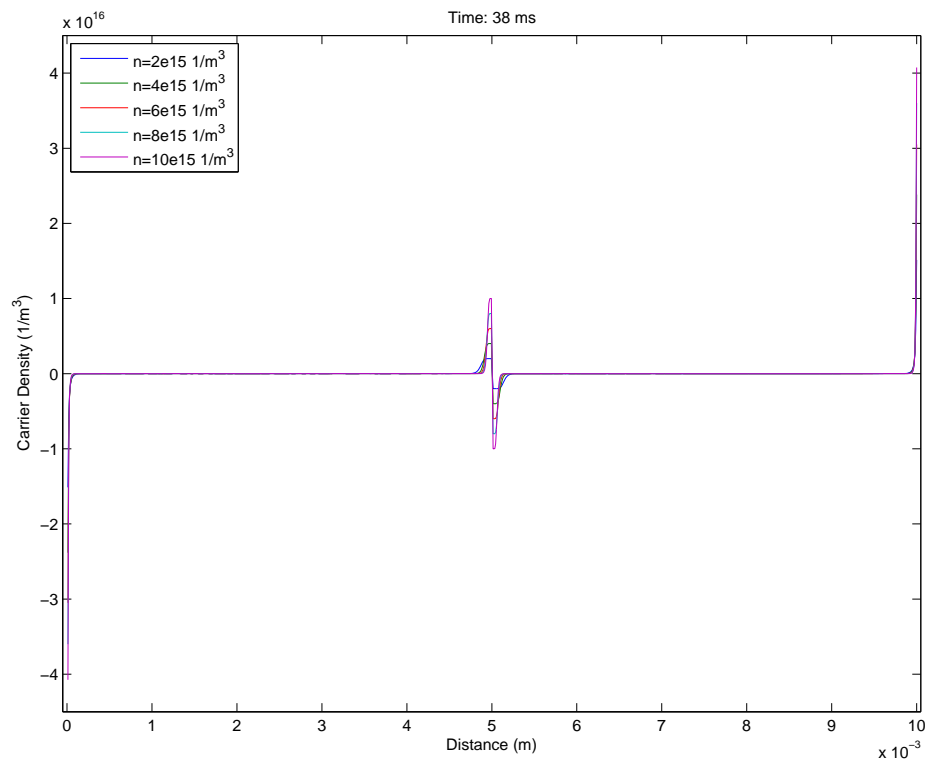
FIGURE 5.7
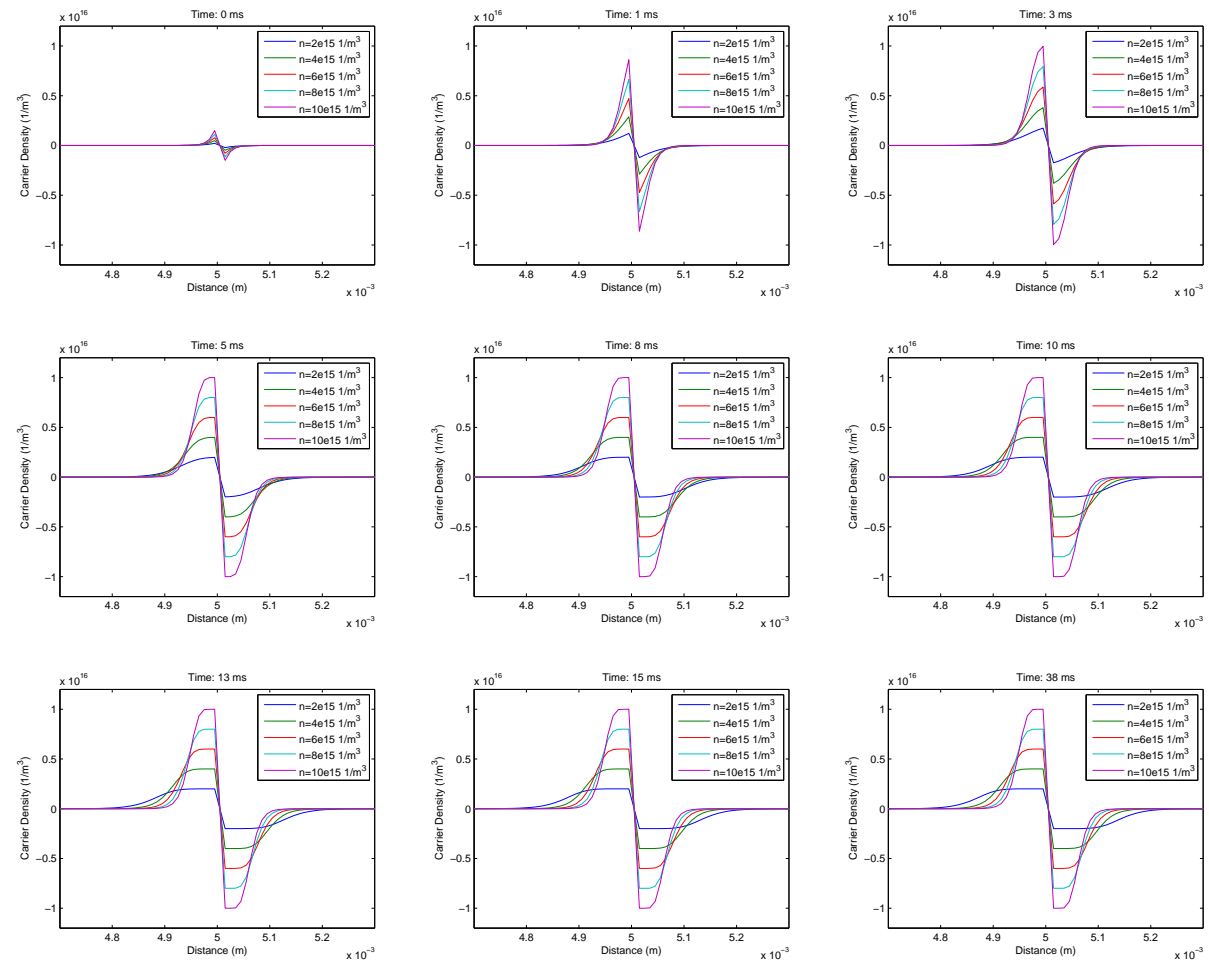
FIGURE 5.8
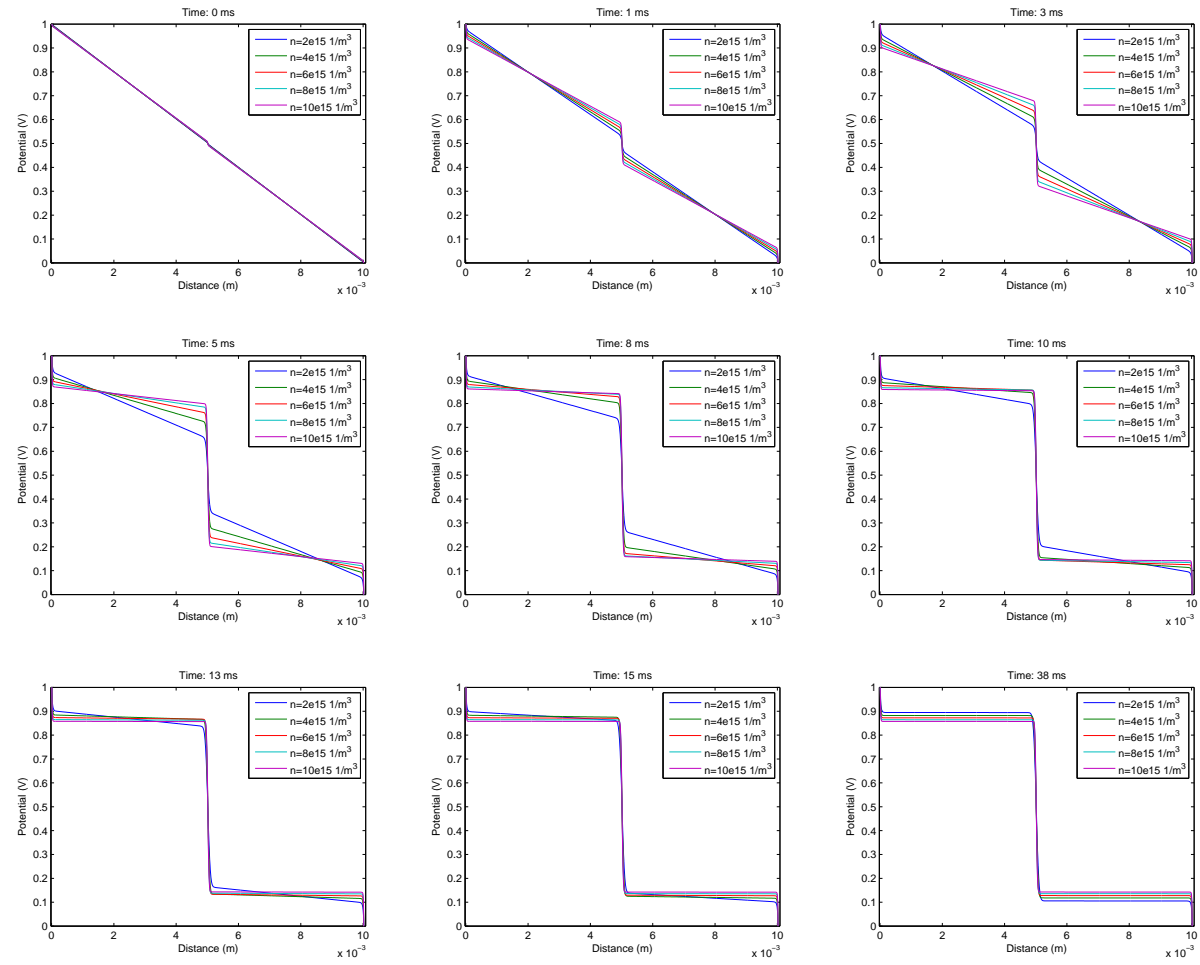
FIGURE 5.9

5.2.3 1-D Horizontal PEDOT:PSS with Notch
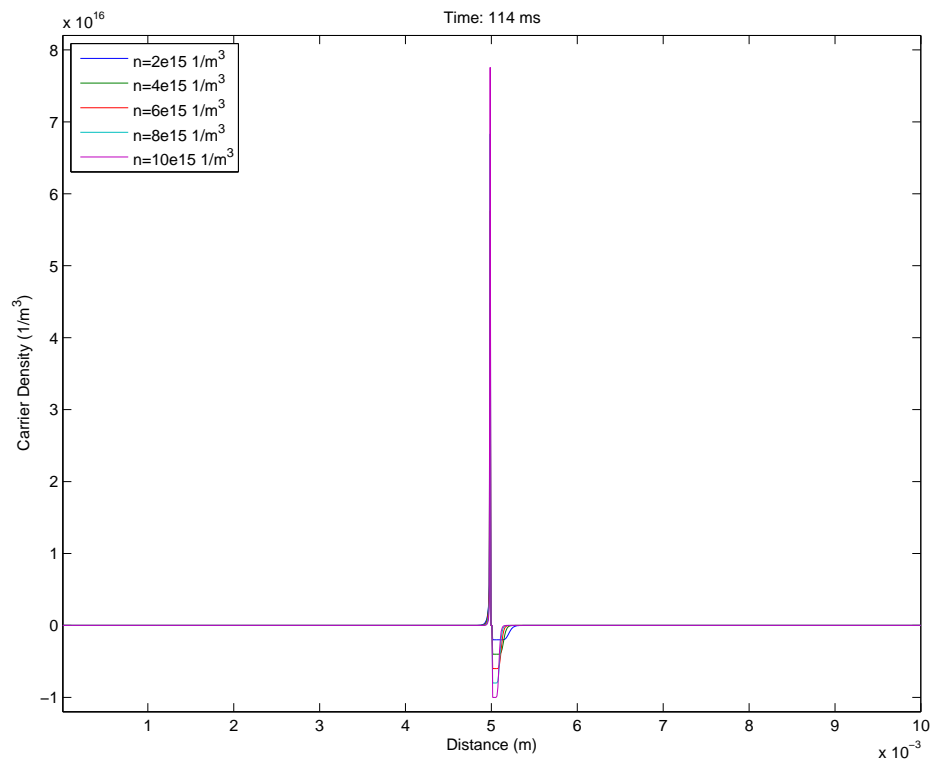
FIGURE 5.10
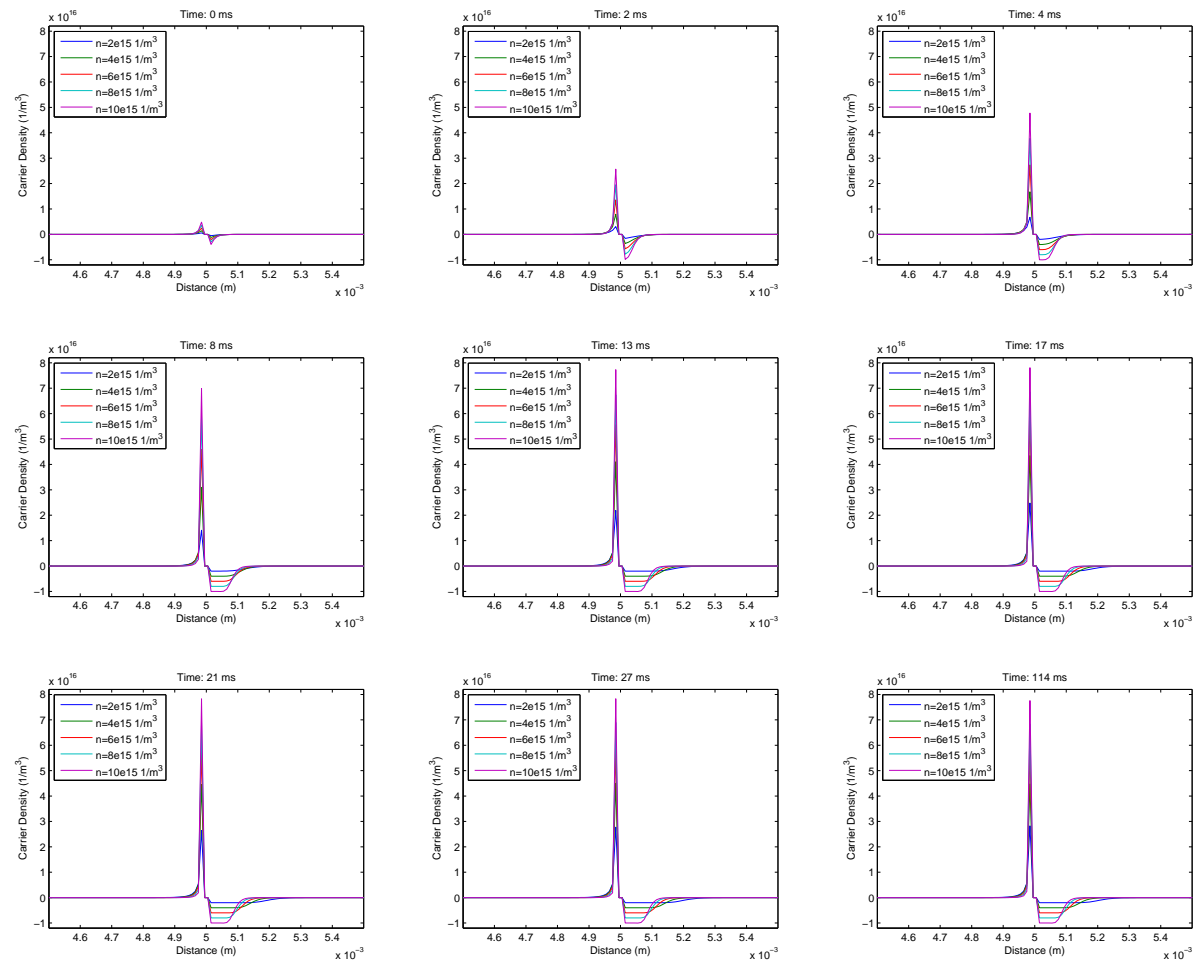
FIGURE 5.11
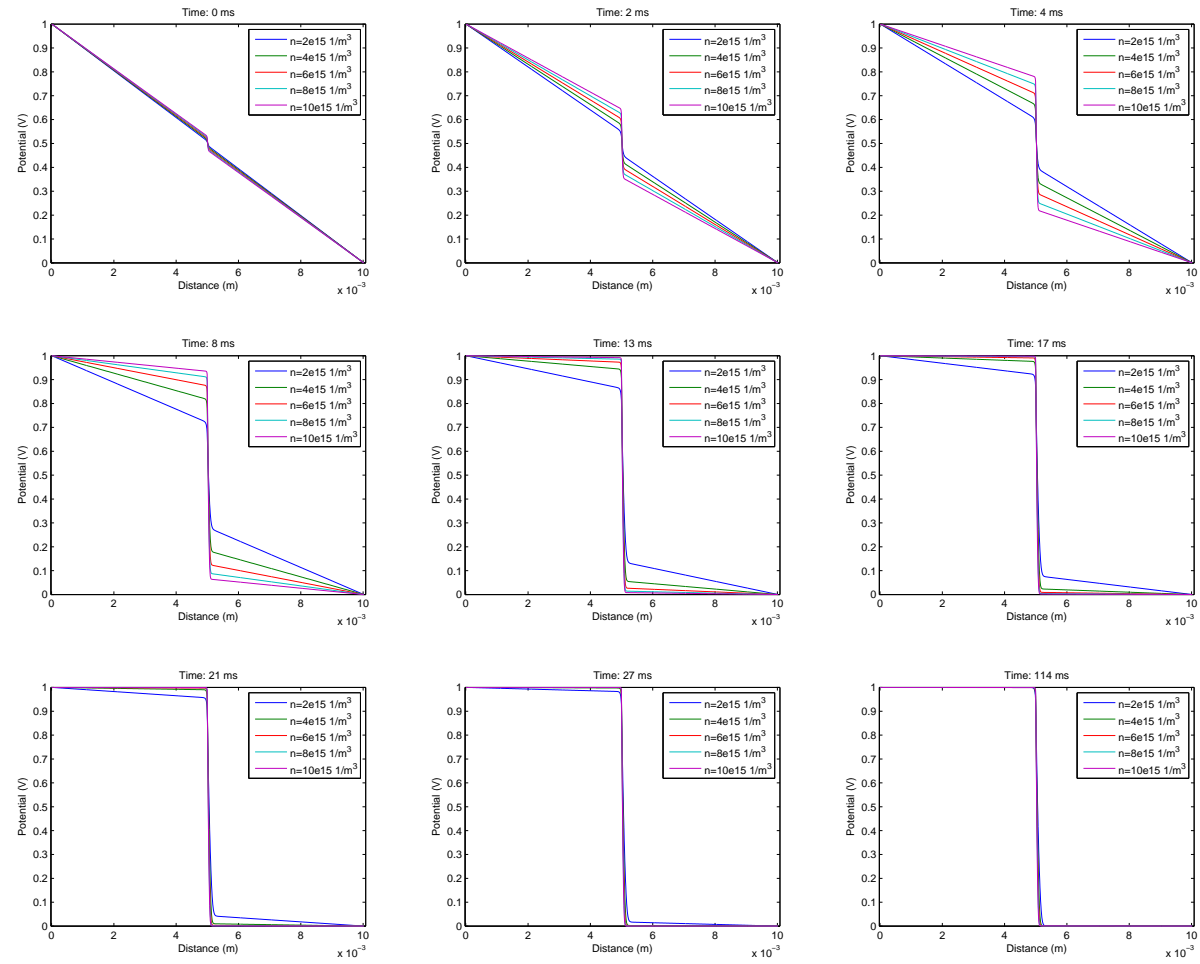
FIGURE 5.12

5.2.4 1-D Vertical Electrolyte/PEDOT Interface
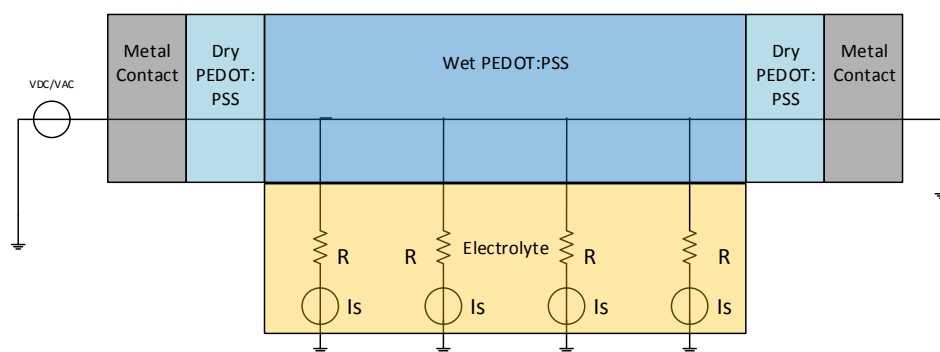
FIGURE 5.13
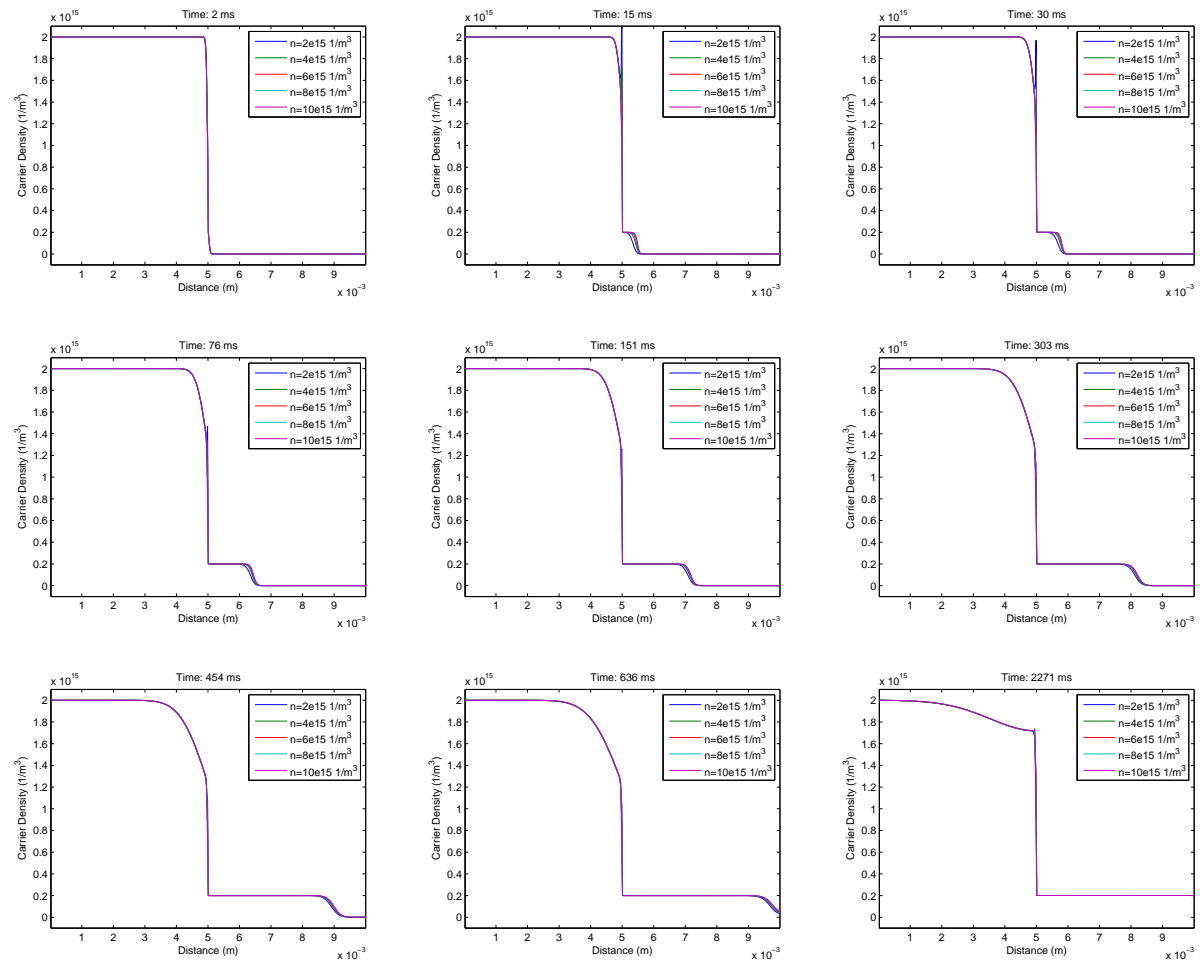
FIGURE 5.14
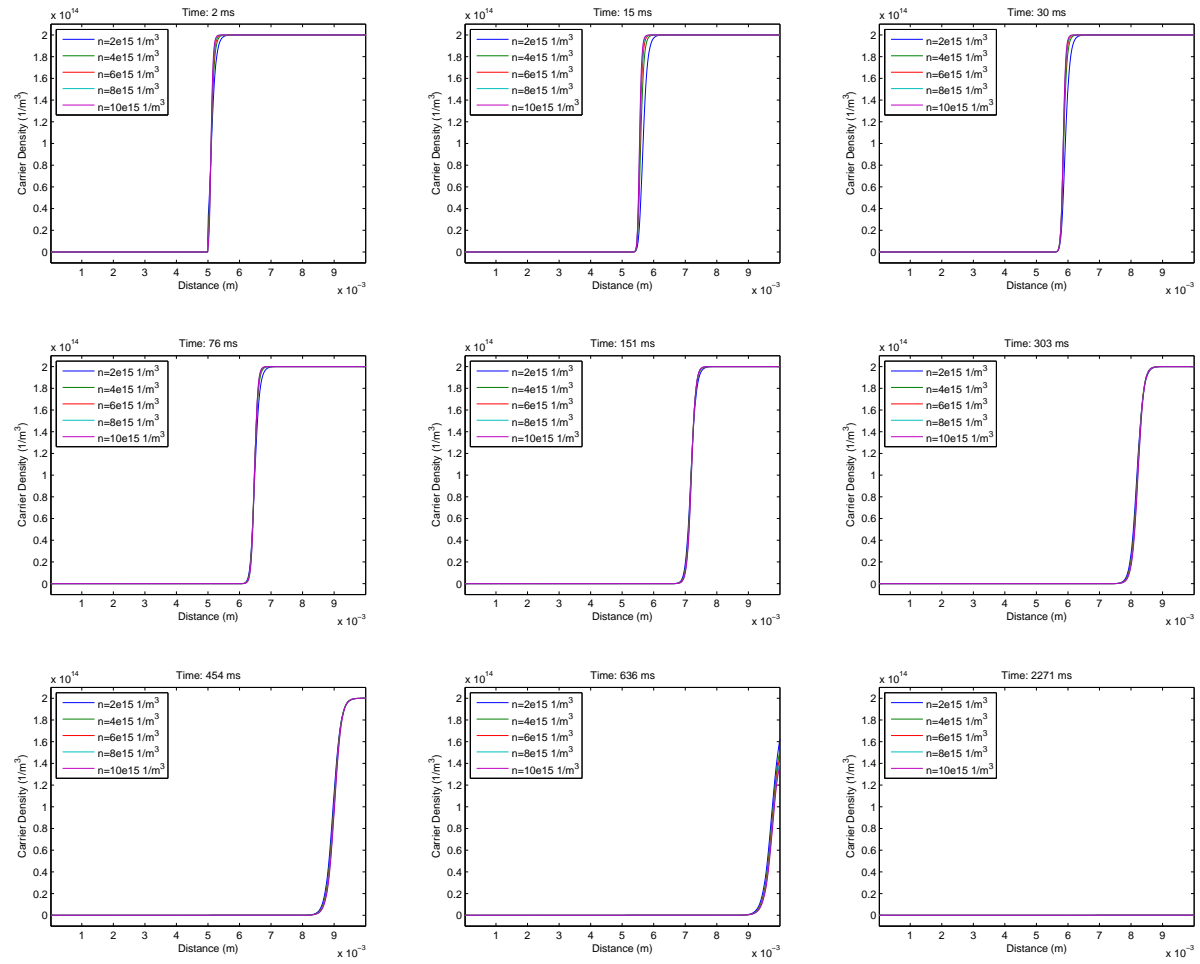
FIGURE 5.15
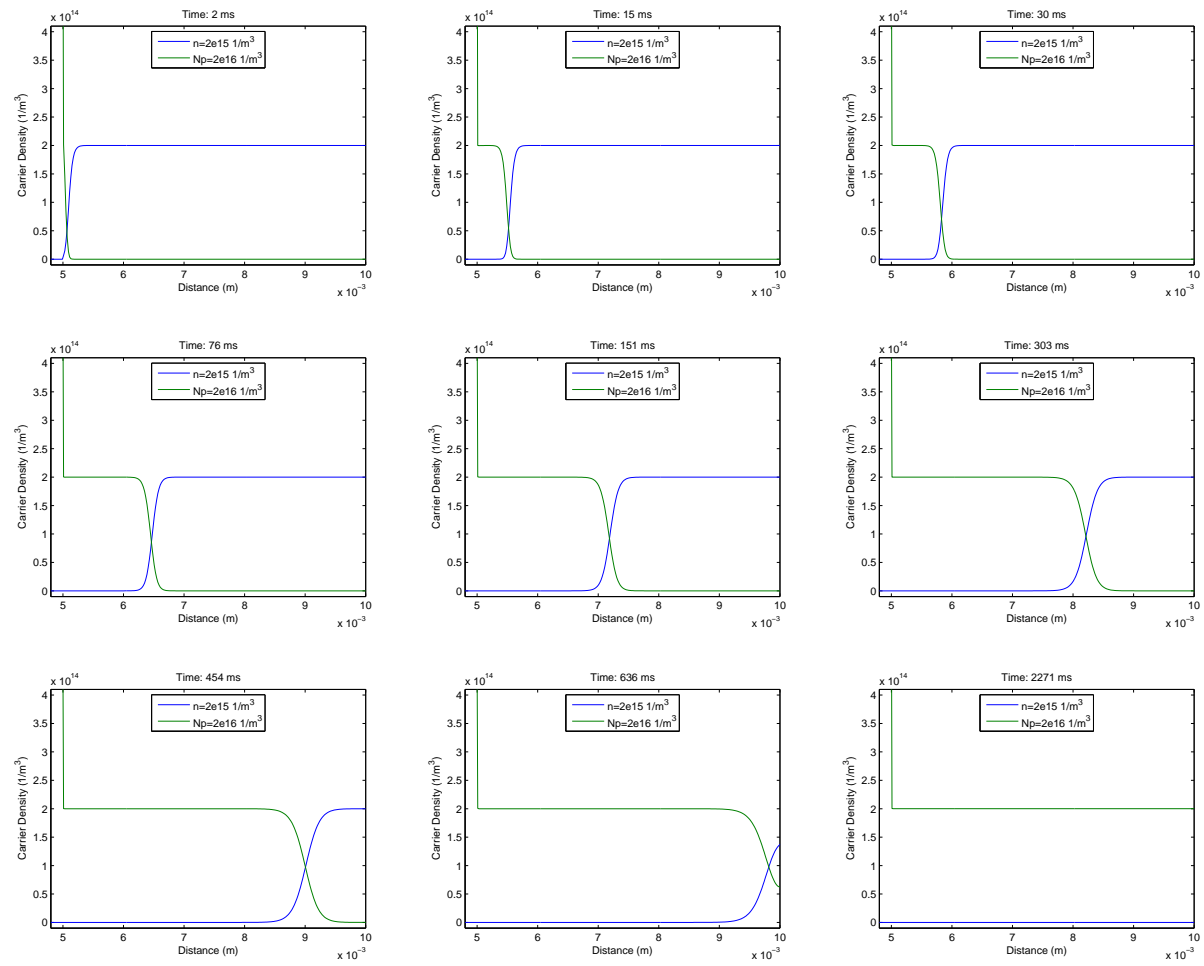
FIGURE 5.16
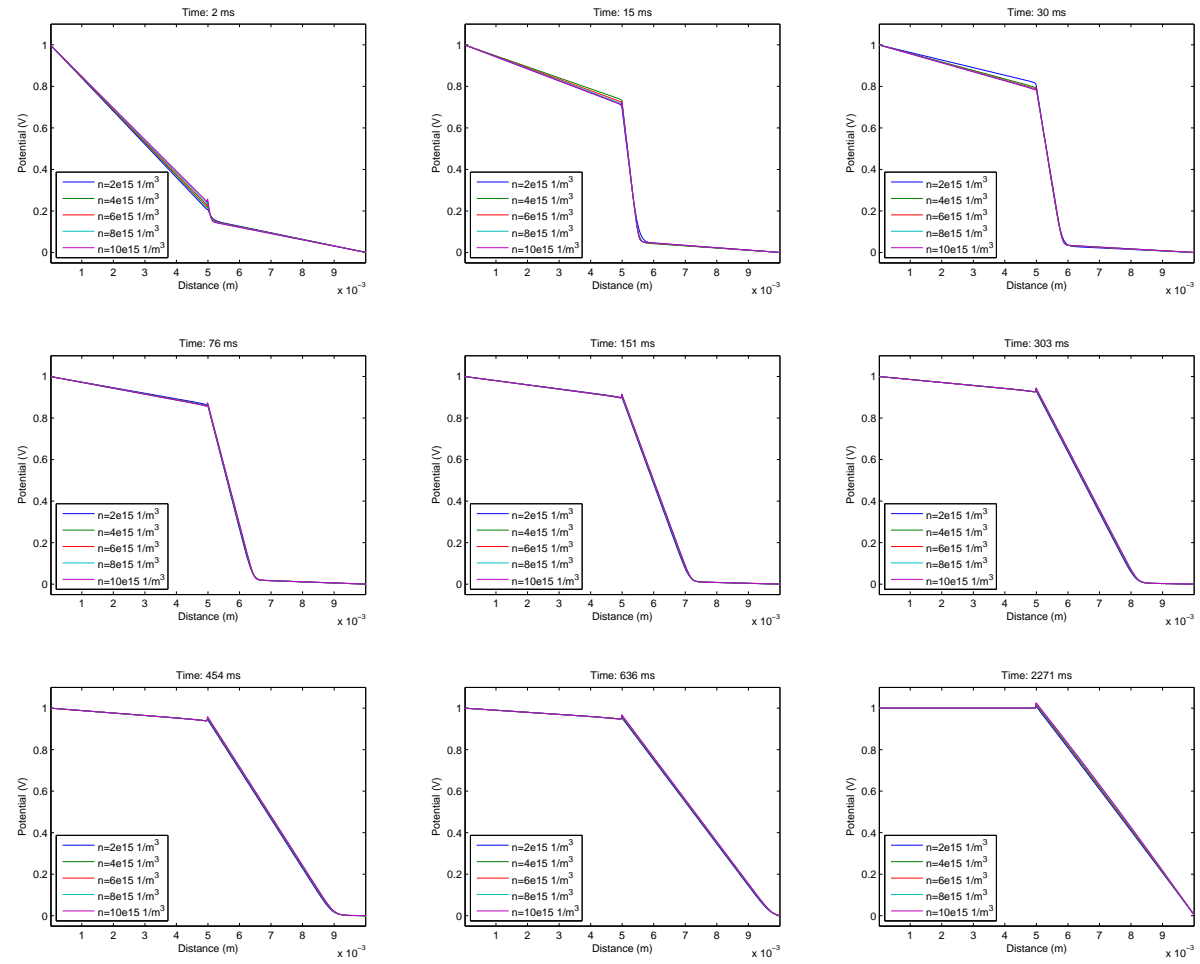
FIGURE 5.17

5.3 Ion movement in a 1-D Memristor
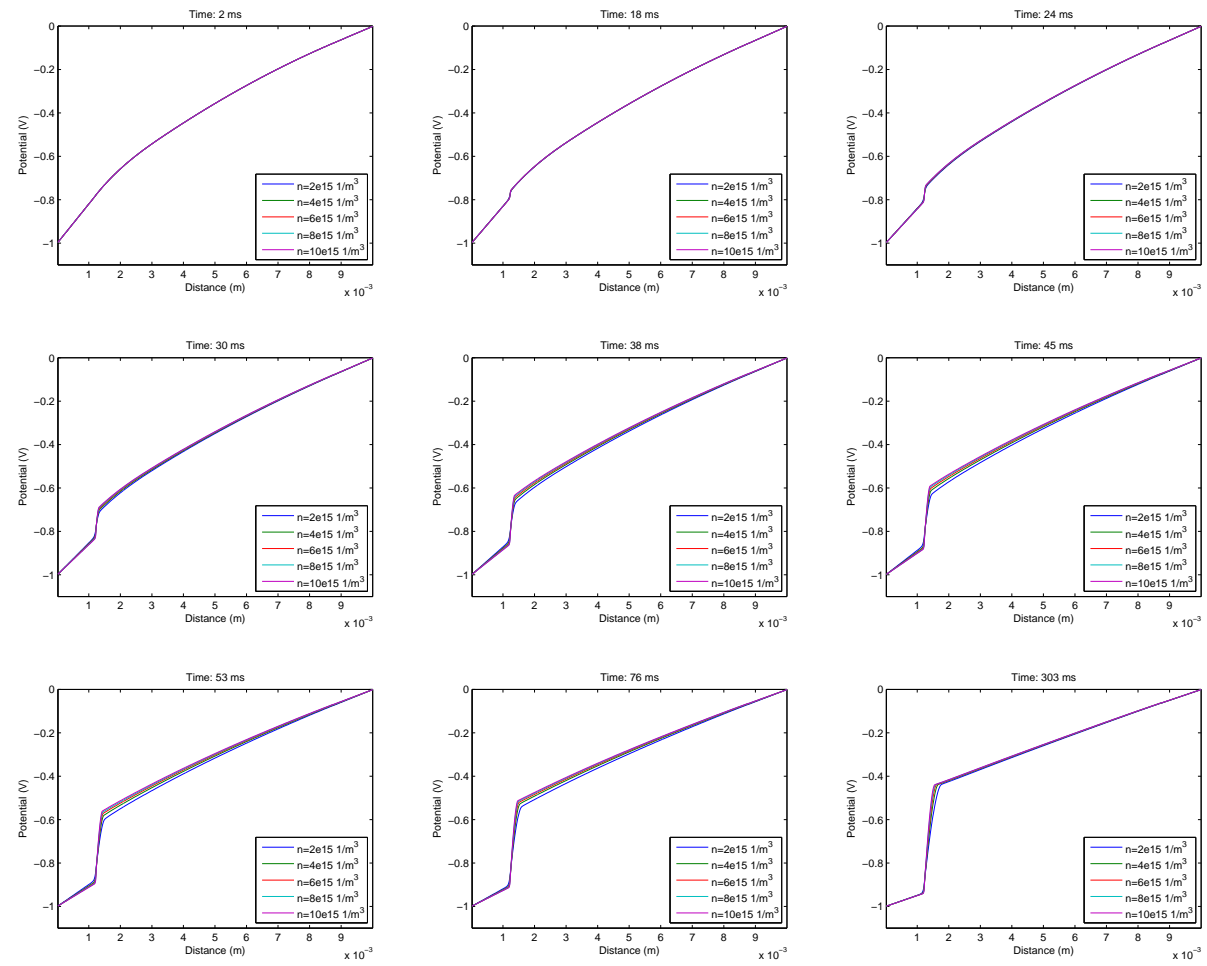
FIGURE 5.18
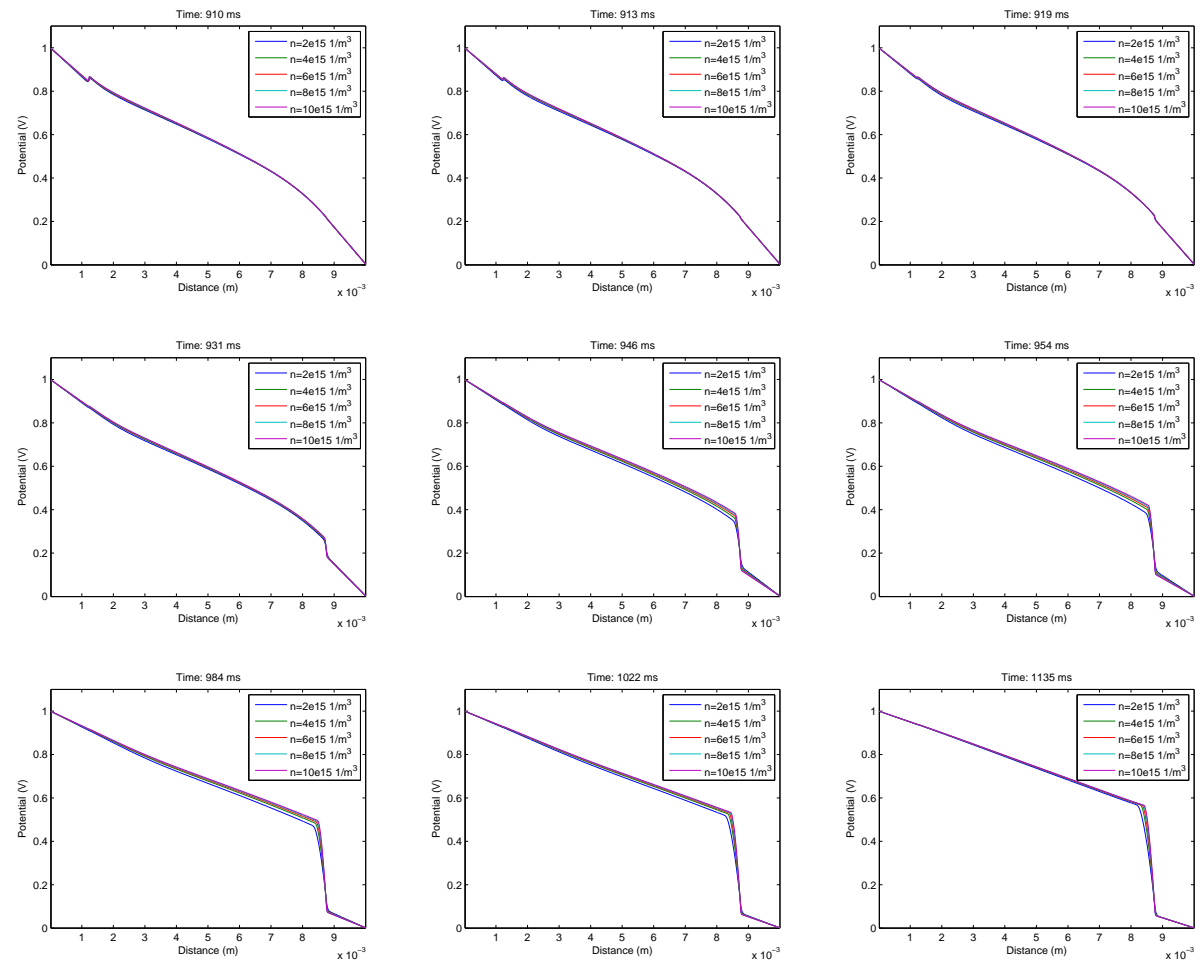
FIGURE 5.19
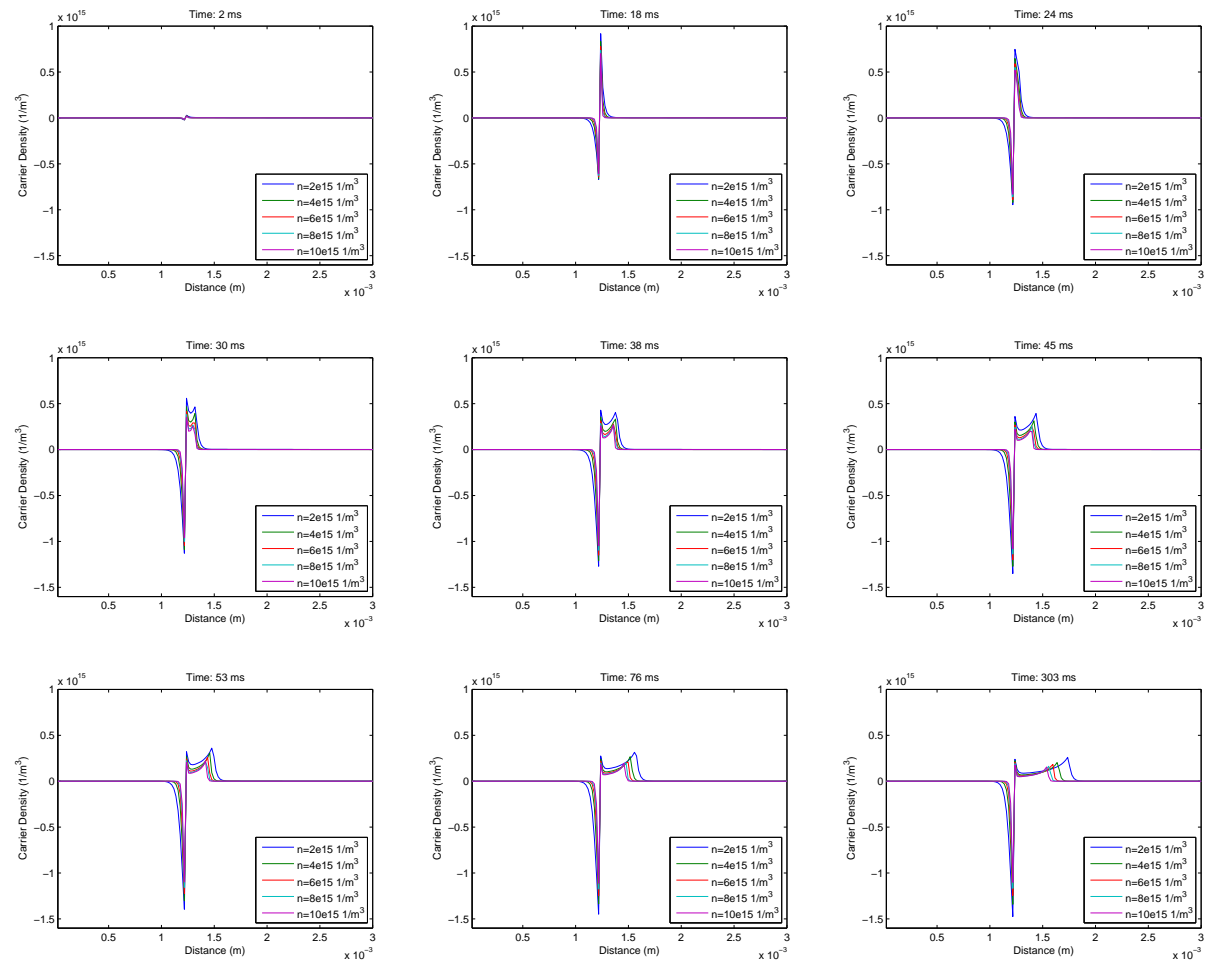
FIGURE 5.20
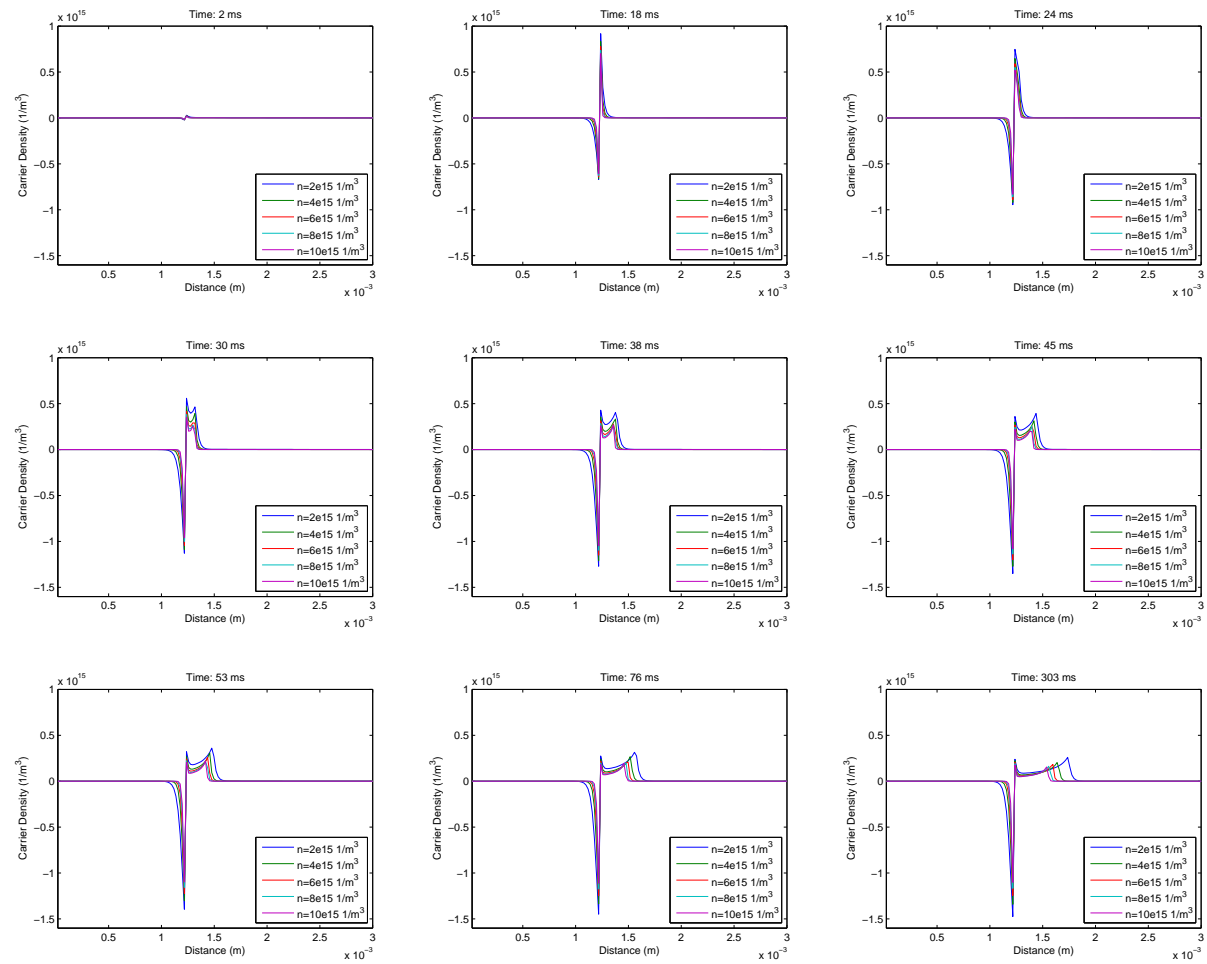
FIGURE 5.21
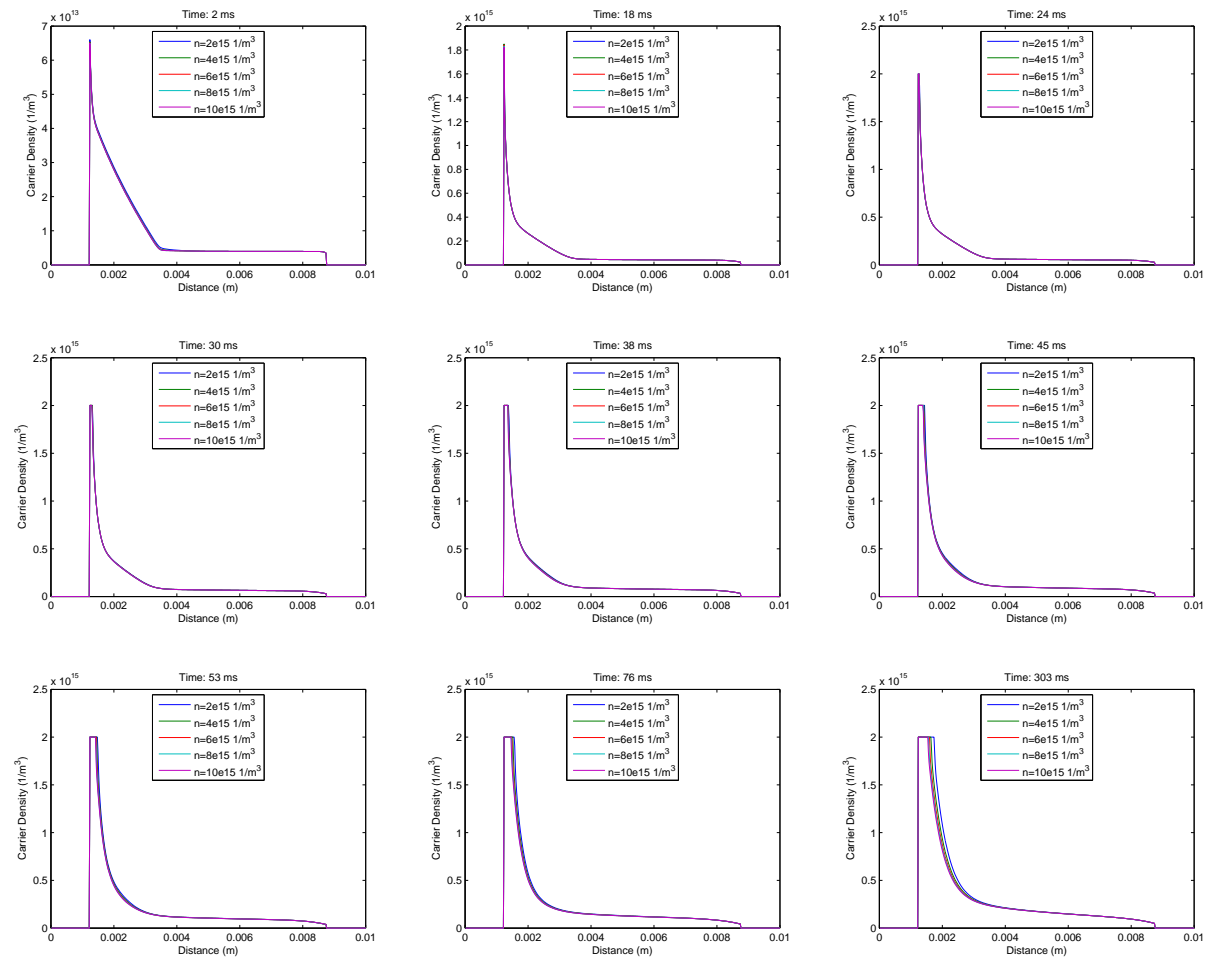
FIGURE 5.22
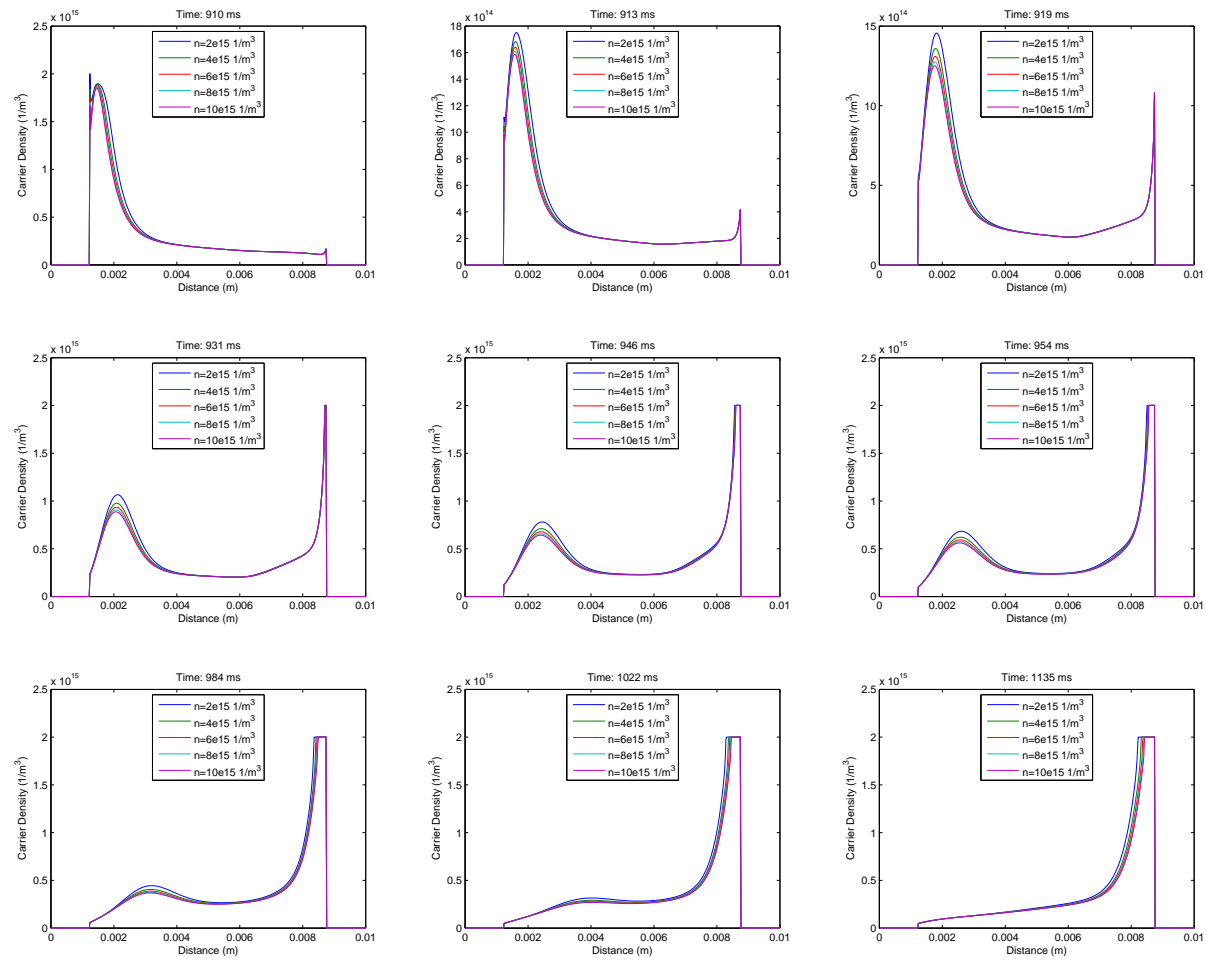
FIGURE 5.23
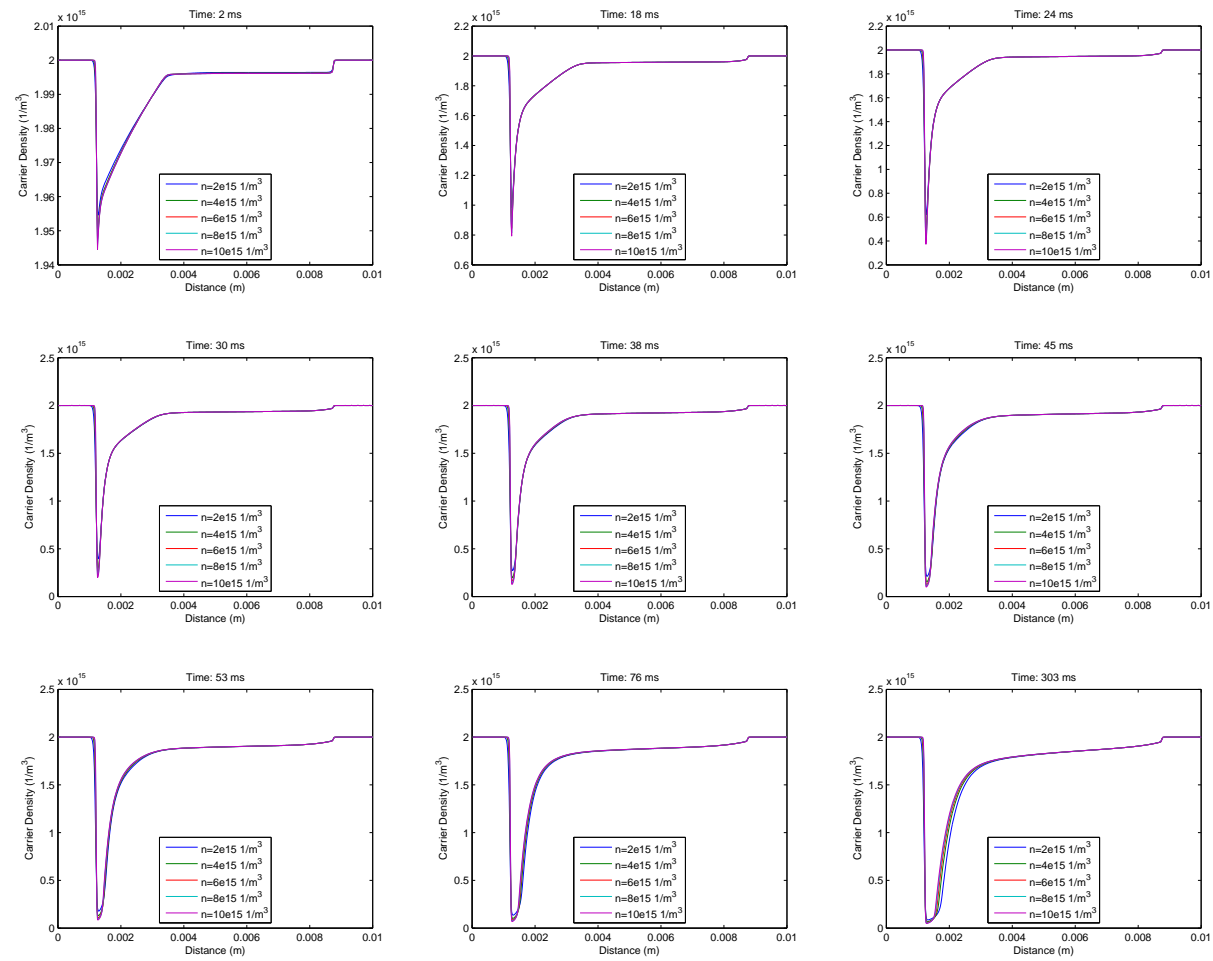
FIGURE 5.24
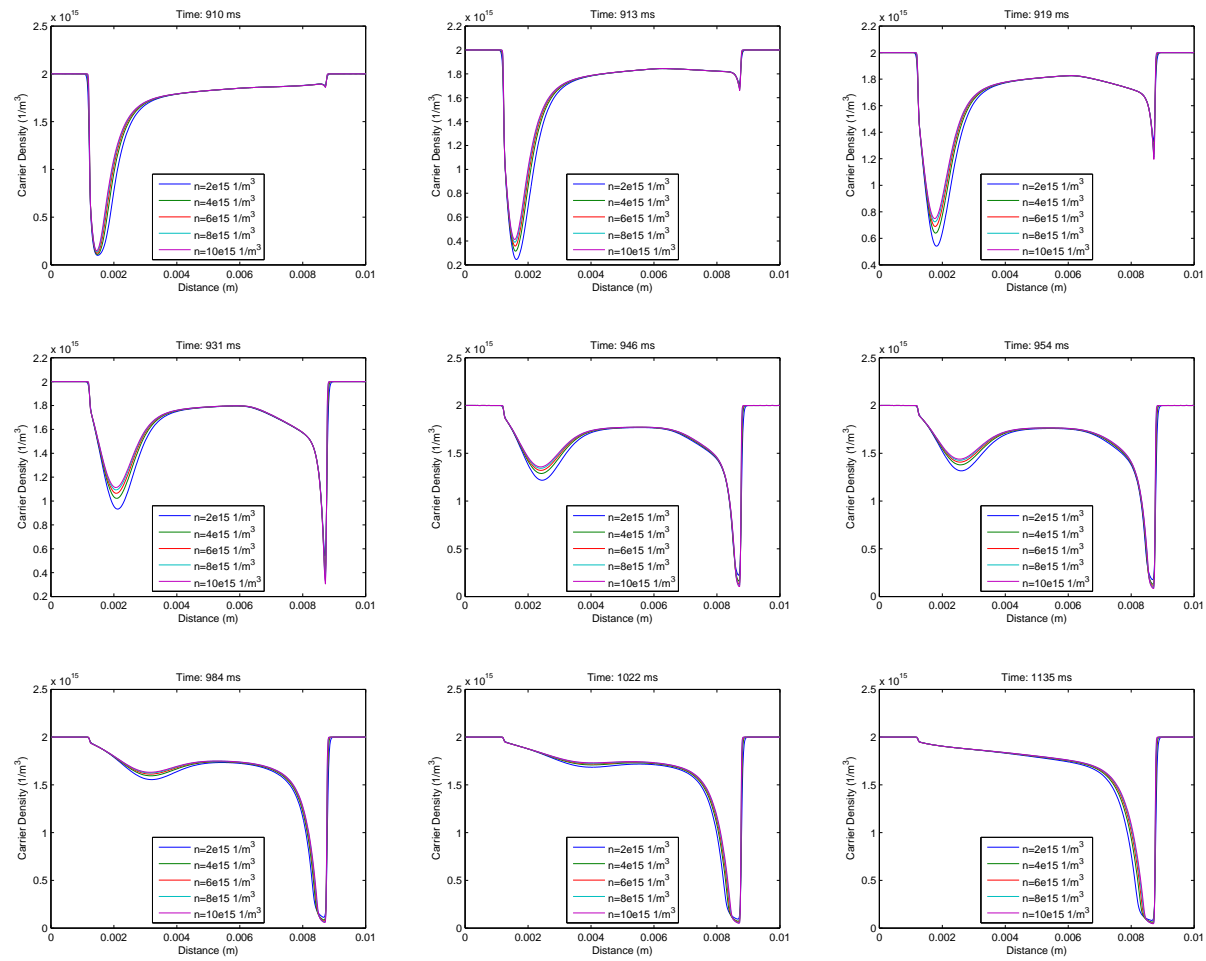
FIGURE 5.25
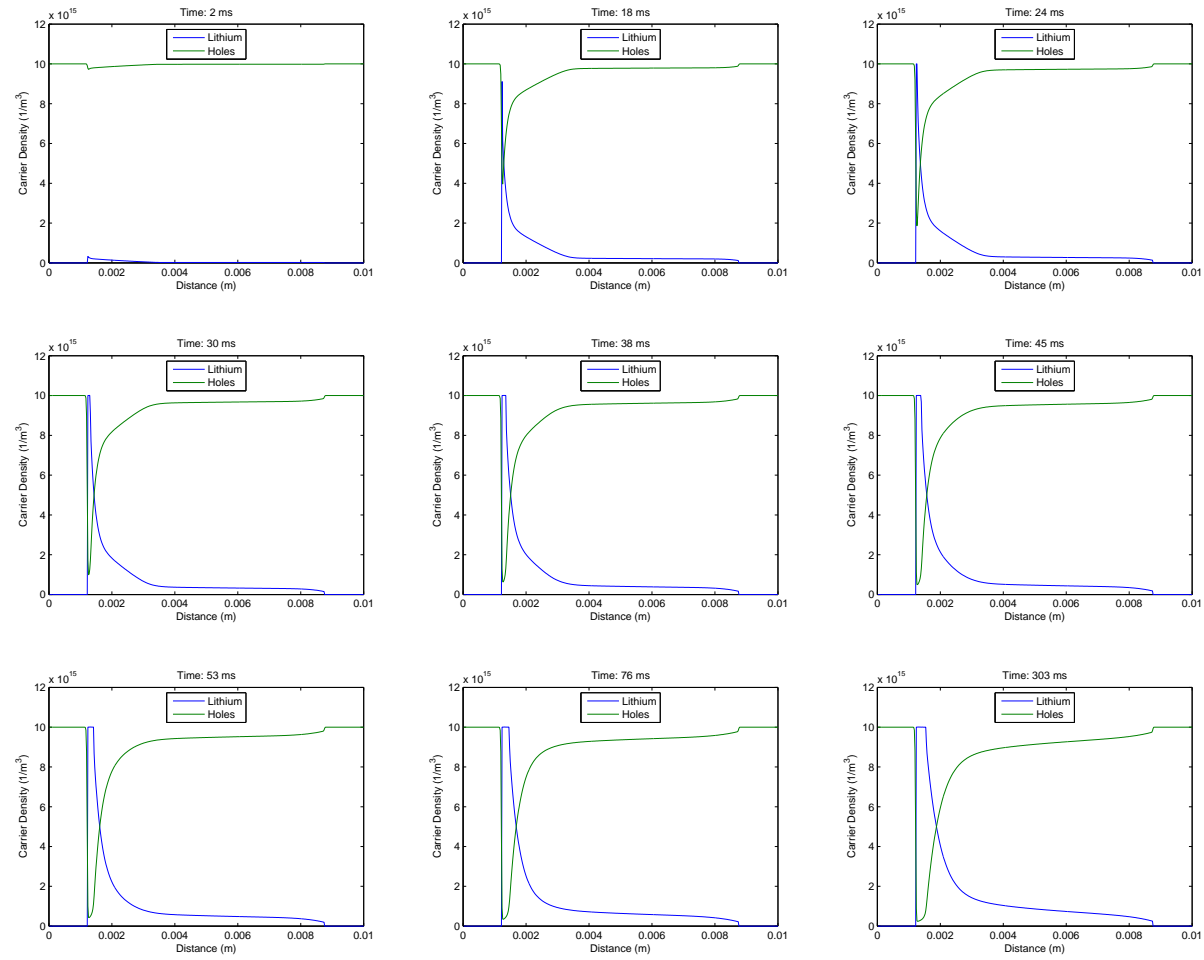
FIGURE 5.26
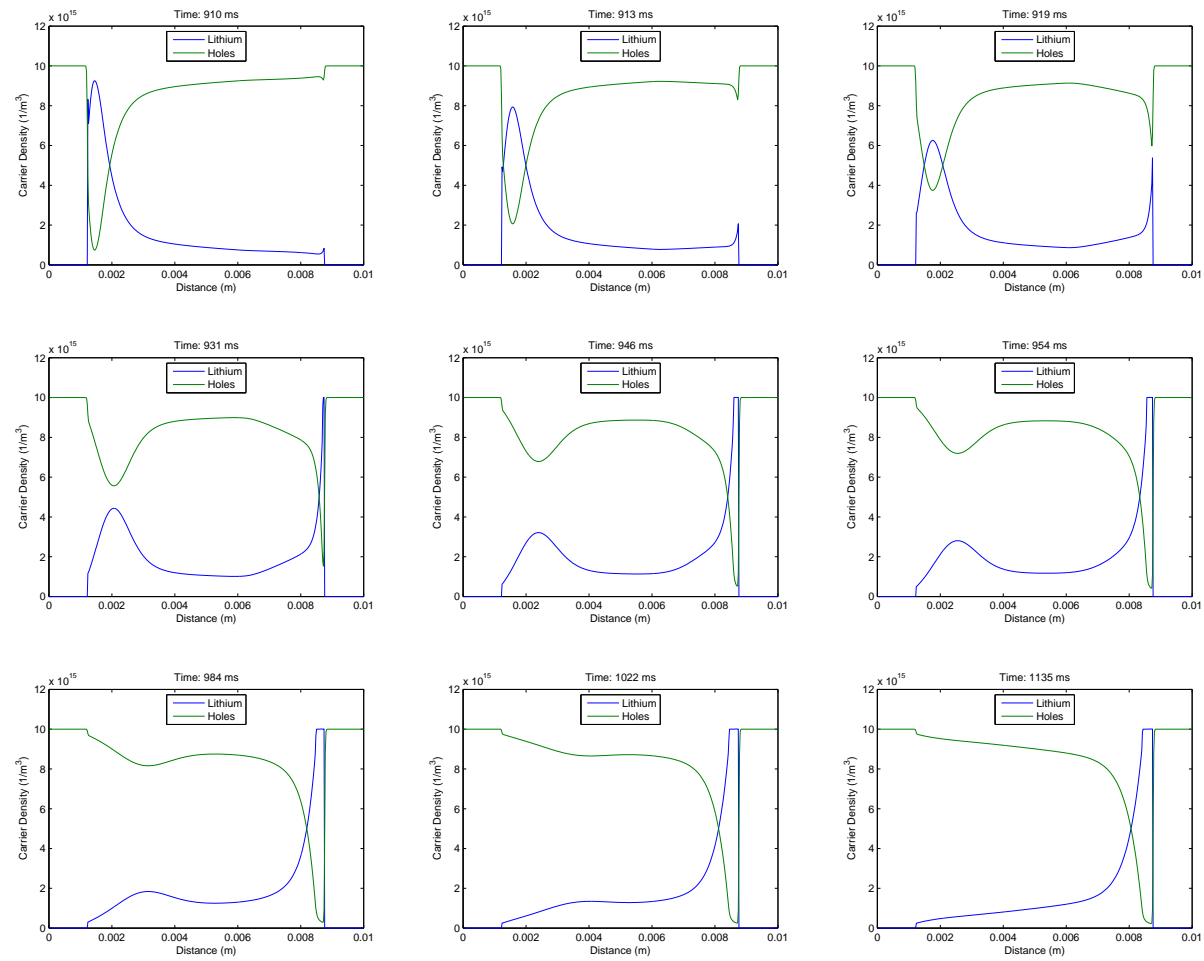
FIGURE 5.27
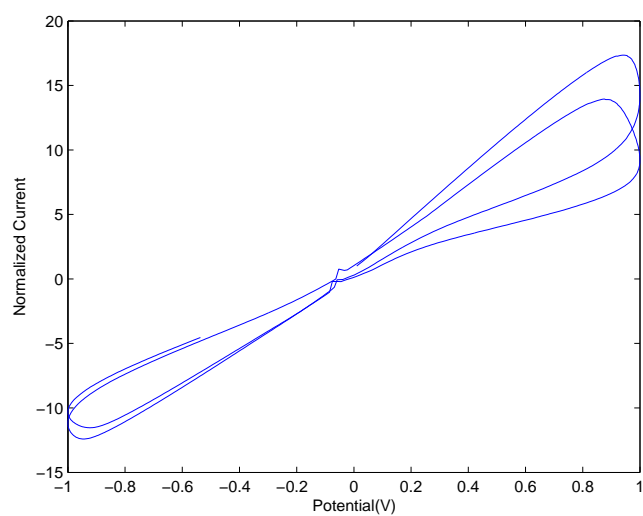
FIGURE 5.28

Chapter 6

Memristor Simulation

6.1   2-D Memristor Model

After creating a method to solve drift diffusion equations using finite difference in chapter
4 and testing it in chapter 5 we can now simulate an actual memristor. The most
basic memristor structure consists of a rectangular strip of PEDOT with metal/carbon
contacts on both sides. On top of the strip there is a drop of electrolyte solution. In order
to be able to simulate the memristor we first need to determine boundary conditions
and values, initial conditions and physical constans for this device.

We have two different materials and three charge carriers that are important for this
problem. The drop of electrolyte has lithium and perchlorate ions and PEDOT has
holes and electrons. All the carriers are not free to move everywhere. Due to PEDOT's
conduction mechanism the electrons are fixed in place and holes are mobile. Also because
of PEDOT's chemistry only lithium is allowed to move in so perchlorate ions always stay
in the electrolyte. When a lithium ion moves into the PEDOT, through drift or diffusion,
it replaces a hole. This replacement reduces the number of available holes in the PEDOT
and increases its resistance.

For the initial concentration of ions in the electrolyte we have assumed that there is no
net charge and everything is uniformly distributed. Similar to electrolyte PEDOT has
no net charge. All the electrons and holes are uniformly distributed and in equilibrium.
Boundary conditions for all species are no flow boundary conditions with the exception
of holes which can leave PEDOT through the contacts. On the contacts zero net charge
is always conserved through the movement of holes in and out of the device. Lithium
atoms can move between PEDOT and the electrolite but they cannot go through the
contacts. Also there is a limit on the amount of lithium PEDOT can accept. Once all
the holes have been replaced lithium ions cannot go into the PEDOT anymore.

The difference between the thickness of the PEDOT and electrolyte makes the simulation very difficult using uniform meshing. The thickness of the electrolyte was shortened by assuming that the amount of charge in the electrolyte is very large and more than enough to saturate PEDOT with lithium ions. Very thick electrolyte was replaced by a thinner one and the top part assumed to be an infinite source/drain for ions.

The contacts have constant potential so they have dirichlet boundary conditions. There were no constraints for the edges of the simulation domain so the potential was set to float using Neumann boundary condition.

Another important aspect of this device is the change in mobility between different materials. Lithium ions move very slowly when they get intercalated into the PEDOT. Also the regions of PEDOT that are in contact with the electrolite (wet region) has higher mobility for lithium compared to the regions that are not in contact (dry region).

6.1.1 Intercalation of Lithium Ions

The following series of simulations were done to study how adding various effects changes the intercalation of lithium ions into PEDOT. We have six different scenarios with increasing complexity. All the simulations start at same initial conditions shown in figure 6.1. The ions are all in the electrolyte and they are uniformly distributed. All the holes and electrons are in PEDOT and they are also uniformly distributed. All the positive charges in the system are balanced by negative charges. For the following six simulations the change of mobility between wet and dry regions are abrupt so lithium cannot move past the wet region of the PEDOT.
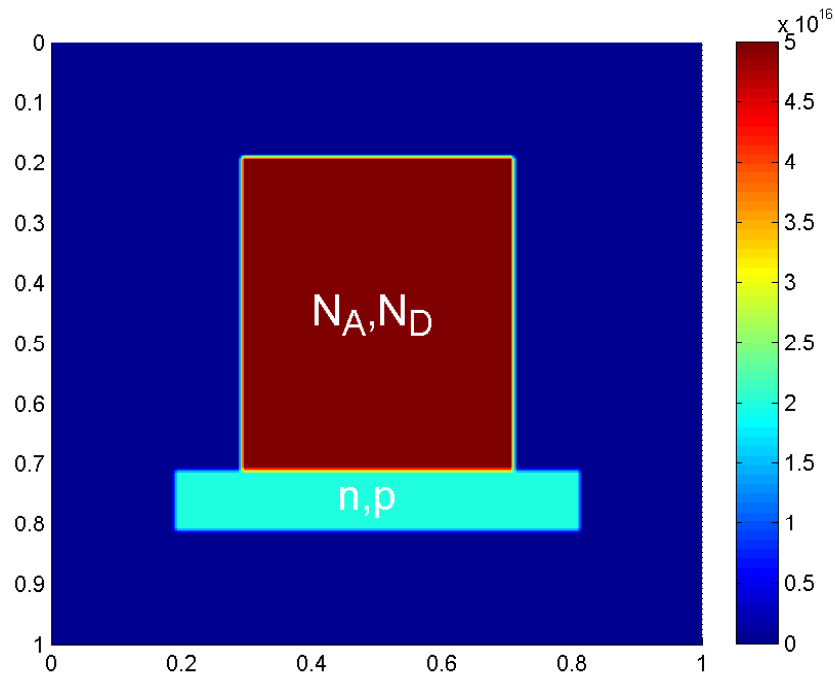
FIGURE 6.1: Initial distribution of holes, electrons, lithium and perchlorate

The result of the first simulation is shown in figure 6.2. In this case the equations are assumed to be decoupled and there is no applied potential at the contacts. This means that there is no electric field and the only force acting on the particles is diffusion. Perchlorate ions and holes have nowhere to diffuse into so their concentrations stay constant. However, lithium ions diffuse freely into the PEDOT until overall density is uniform since there is no limit on its density.

In this second example shown in figure 6.3 we kept all the conditions the same but applied a constant potential at the contacts. The electric field pulls lithium and perchlorate ions towards opposite sides. Lithium atoms drift and diffuse into the PEDOT and perchlorate
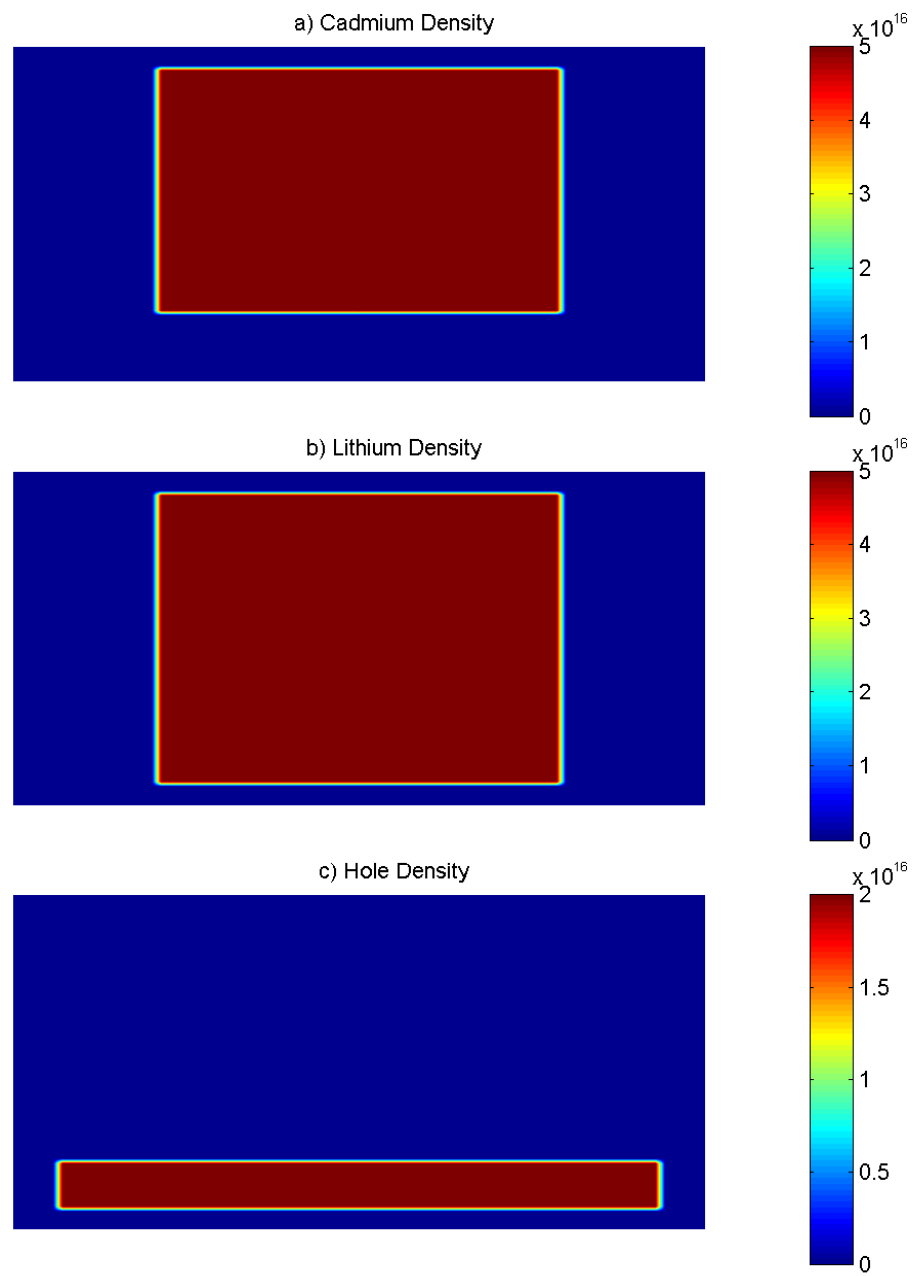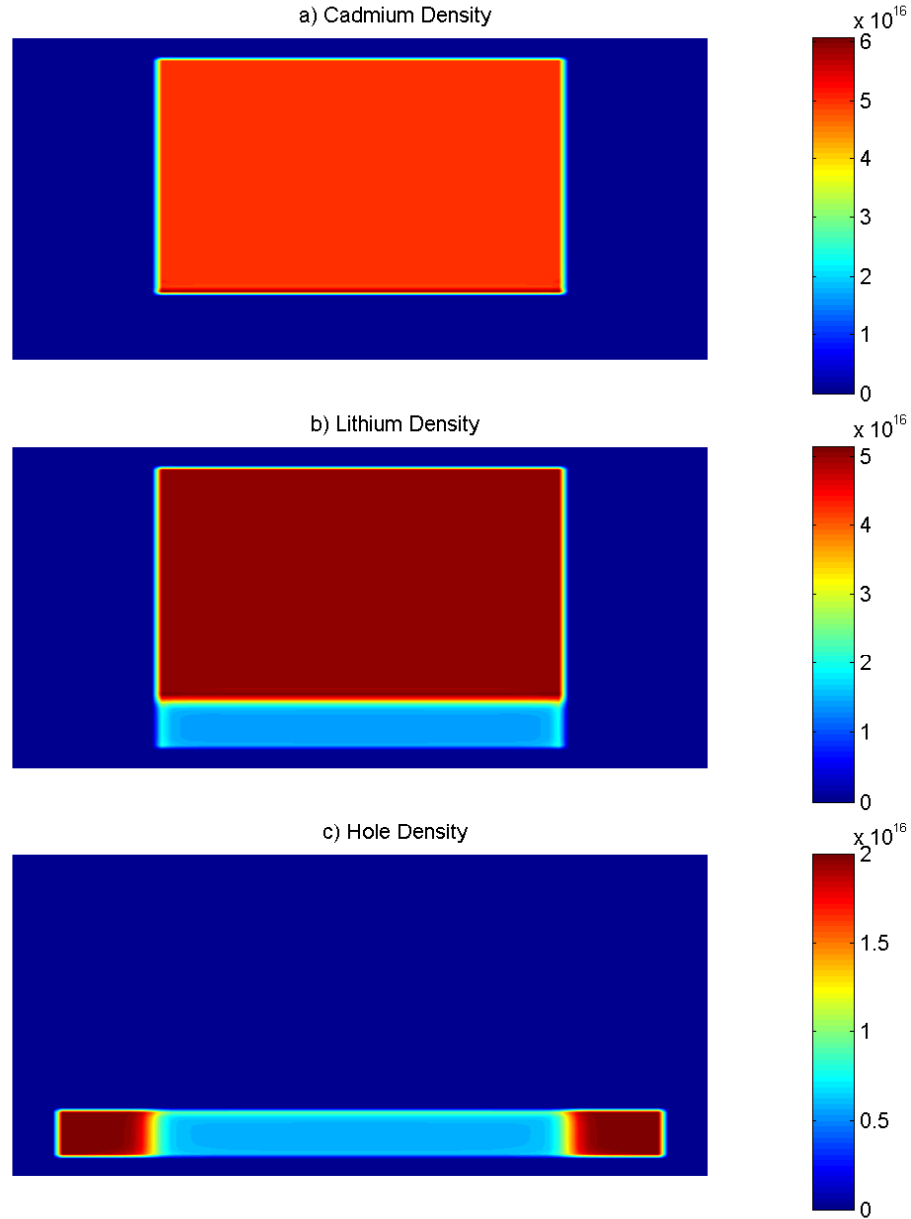
FIGURE 6.2: Particle distribution at steady state without any applied potential or density limit. Equations are decoupled

ions stay in the electrolyte as expected. PEDOT just behaves like a regular resistor and holes uniformly flow in and out of the device.
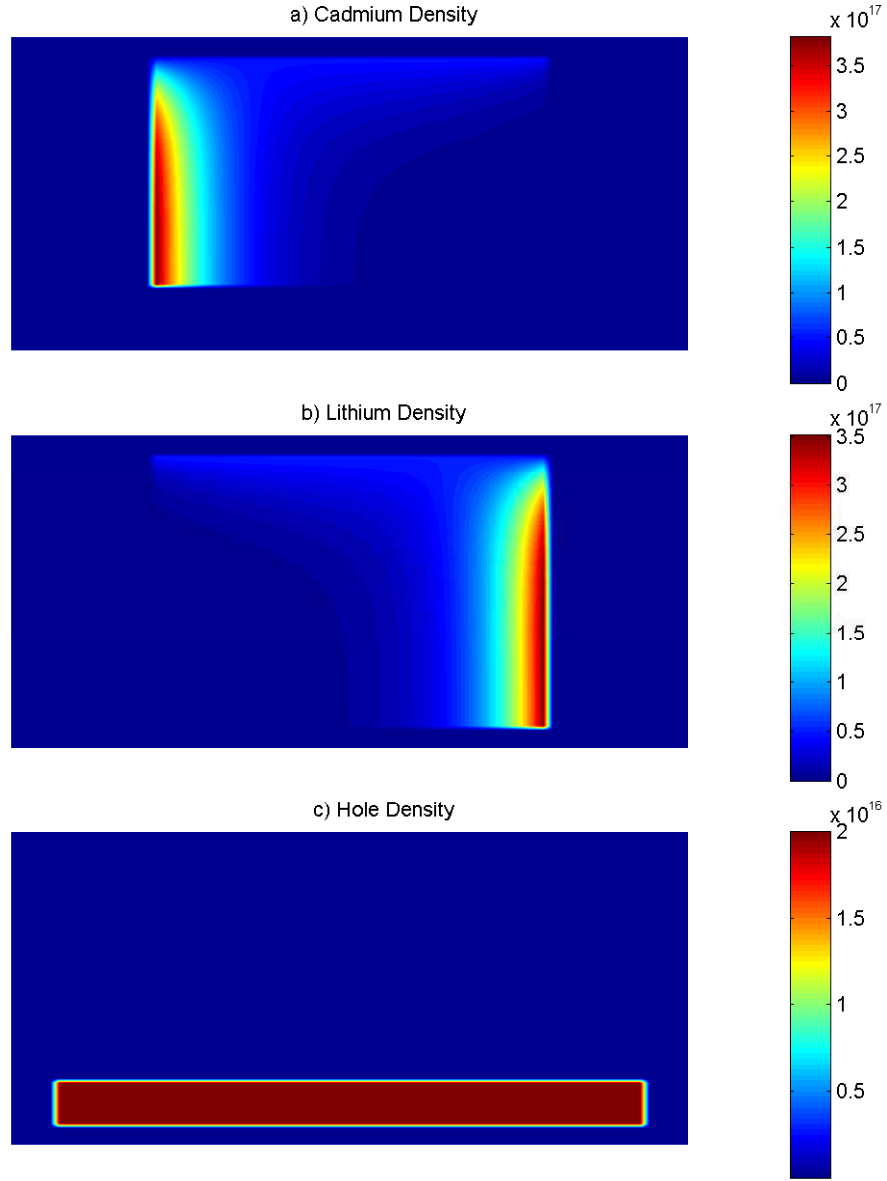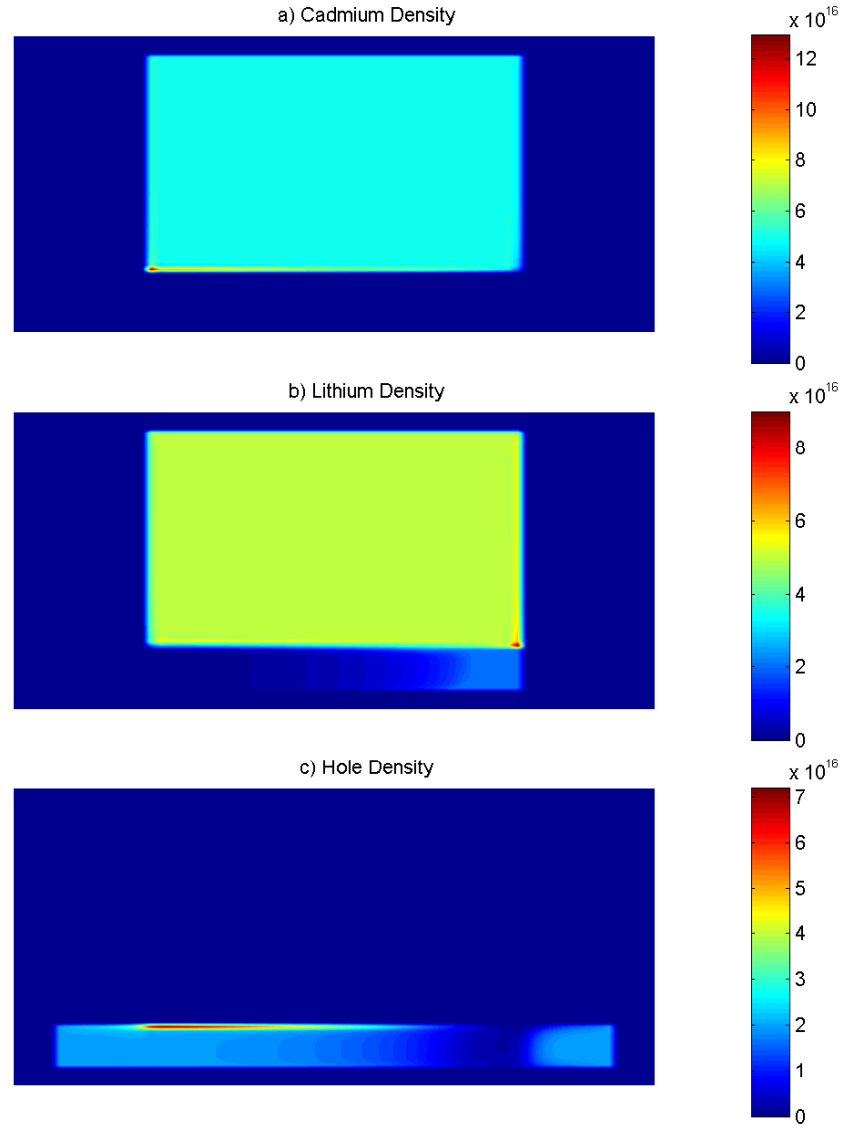

FIGURE 6.3: Particle distribution at steady state with applied potential and without density limit. Equations are decoupled

A limit for lithium was added for the last simulation without coupled equations. If we compare figure 6.3 and 6.4 we can clearly see the difference in lithium density in PEDOT as it gets uniformly distributed instead of exponentially collecting on one side. Lithium still has no effect on holes since the electric field due to charged particles are ignored.

For the last three examples we will be going over the same simulations by taking coupling into account. With the addition of coupling between Poisson's equation and drift

diffusion equations, the system of particles will always try to stay as charge neutral as possible.
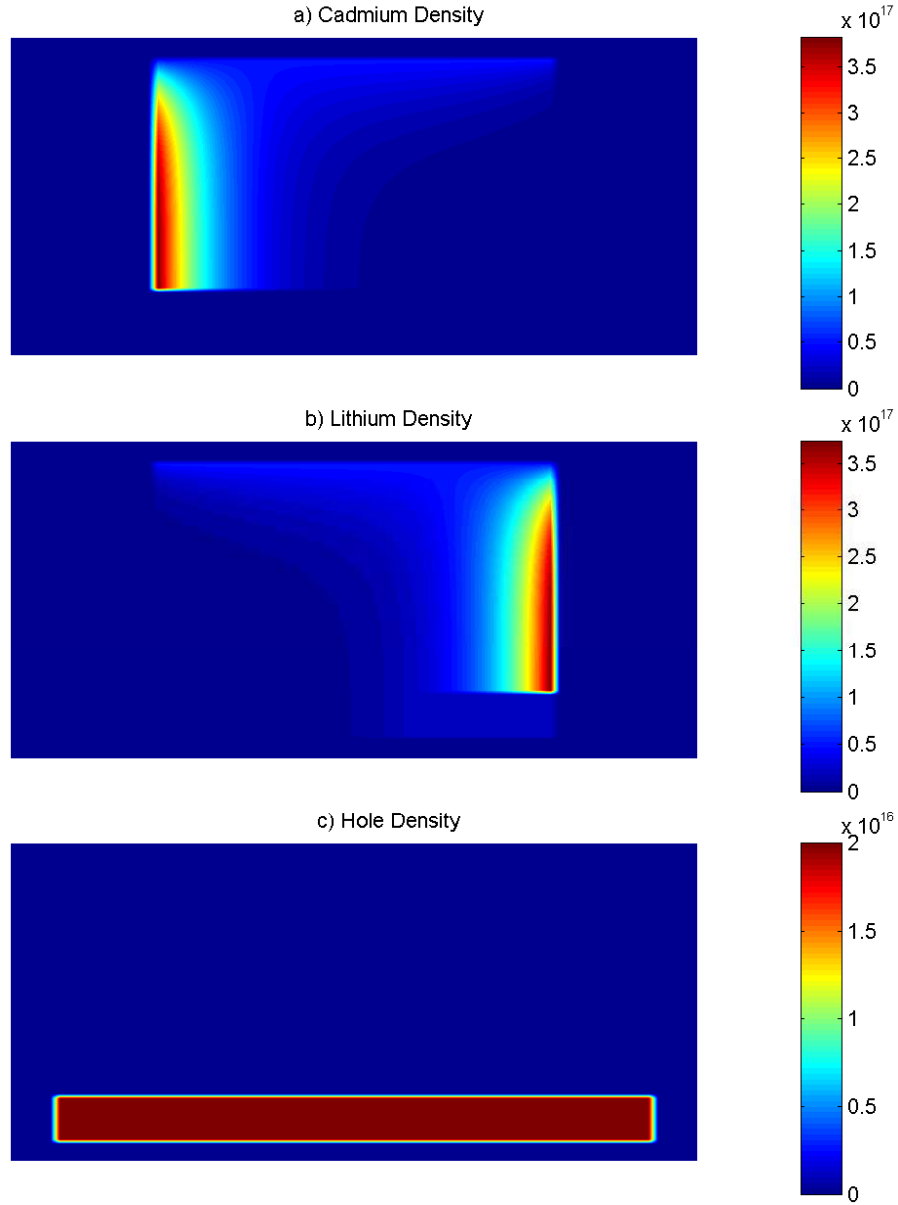
FIGURE 6.4: Particle distribution at steady state with applied potential and density limit. Equations are decoupled

Figure 6.5 is good example illustrating this effect since the only drift force pushing the particles are self generated. Lithium ions diffuse into PEDOT leaving a net negative charge near the interface which pulls them back into the electrolyte. Now since there is an accumulation of positive charge inside the PEDOT perchlorate ions move towards the interface. At the same time holes are being pushed out from PEDOT and they are

slowly getting replaced by lithium ions. Figure 6.5 clearly shows that there is a lack of holes where lithium ions have diffused in.

FIGURE 6.5: Particle distribution at steady state without any applied potential or density limit. Equations are coupled

As before adding a potential to the contacts separates positive and negative ions. This time hey will separate until the electric field is canceled out. In figure 6.6 we can see the negative charges in the electrolyte holding most lithium ions from moving into the PEDOT. Also as they move into the PEDOT the electric field gets weaker. So compared to the case without coupling (figure 6.3) there are less lithium ions in the PEDOT. On the right side of the PEDOT we can see a strip of missing holes due to the migration of

lithium. We can also see holes accumulating at the interface on the left side due to the increased amount of perchlorate ions right across the interface.
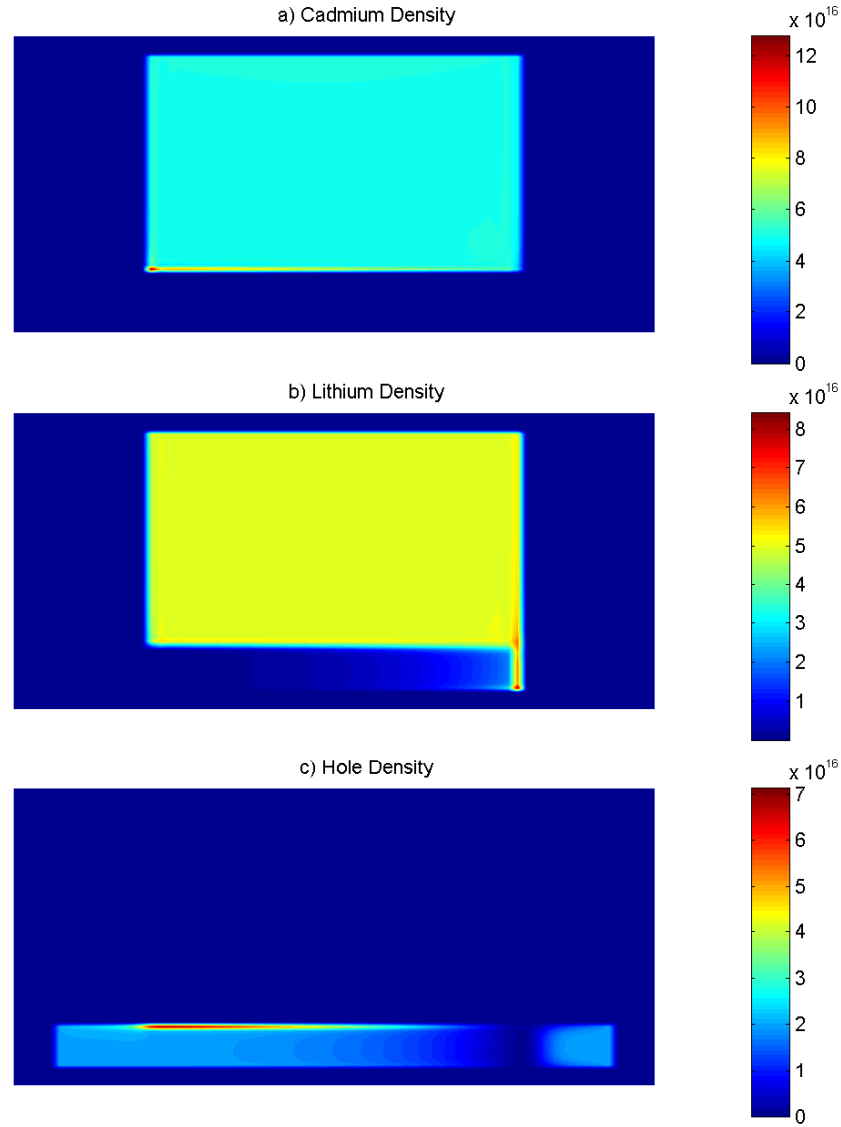
FIGURE 6.6: Particle distribution at steady state with applied potential and without density limit. Equations are coupled

In the last example (figure 6.7) the addition of the density limit flattens out the accumulation of lithium ions in the PEDOT. We can see that holes are getting replaced by lithium on a larger area since its accumulation is not as concentrated at the edge. The accumulation of holes due to perchlorate ions across the interface does not get affected by this change.

Finally we can look at how the electric field looks at steady state. We see an electric field in figure 6.8.a created by the excess of positive charge in the PEDOT due to the diffusion of lithium. Even though there is an electric field in this simulation, its magnitude is so

FIGURE 6.7: Particle distribution at steady state with applied potential and without density limit. Equations are decoupled

small that it does not have any impact on the movement of the charge carriers. In the last two figures at the top row (figure 6.8.b and 6.8.c) we can see the uniform electric field created by the potential applied at the contacts. Since the equations are decoupled the electric field does not get affected by the redistribution of charge. In figure 6.8.d most of the electric field is generated due to the diffusion of lithium into PEDOT. Net positive charge in the PEDOT, under the electrolyte, creates an outward electric field.

The effects of coupling in the potential can be easily seen by comparing figure 6.8.b and 6.8.e. In the electrolyte charges separate and cancel the electic field. In the PEDOT there is a very high electric field at the interface between wet and dry regions since lithium ions cannot travel into the dry region. The limitation of lithium density in the

PEDOT decreases the sharpness of the change in charge density therefore the electric field changes over a slightly longer distance.

a) Decoupled,No Lim, No V

b) Decoupled,No Lim, V

c) Decoupled,Lim, V

d) Coupled,No Lim, No V

e) Coupled,No Lim, V

f) Coupled,Lim, V
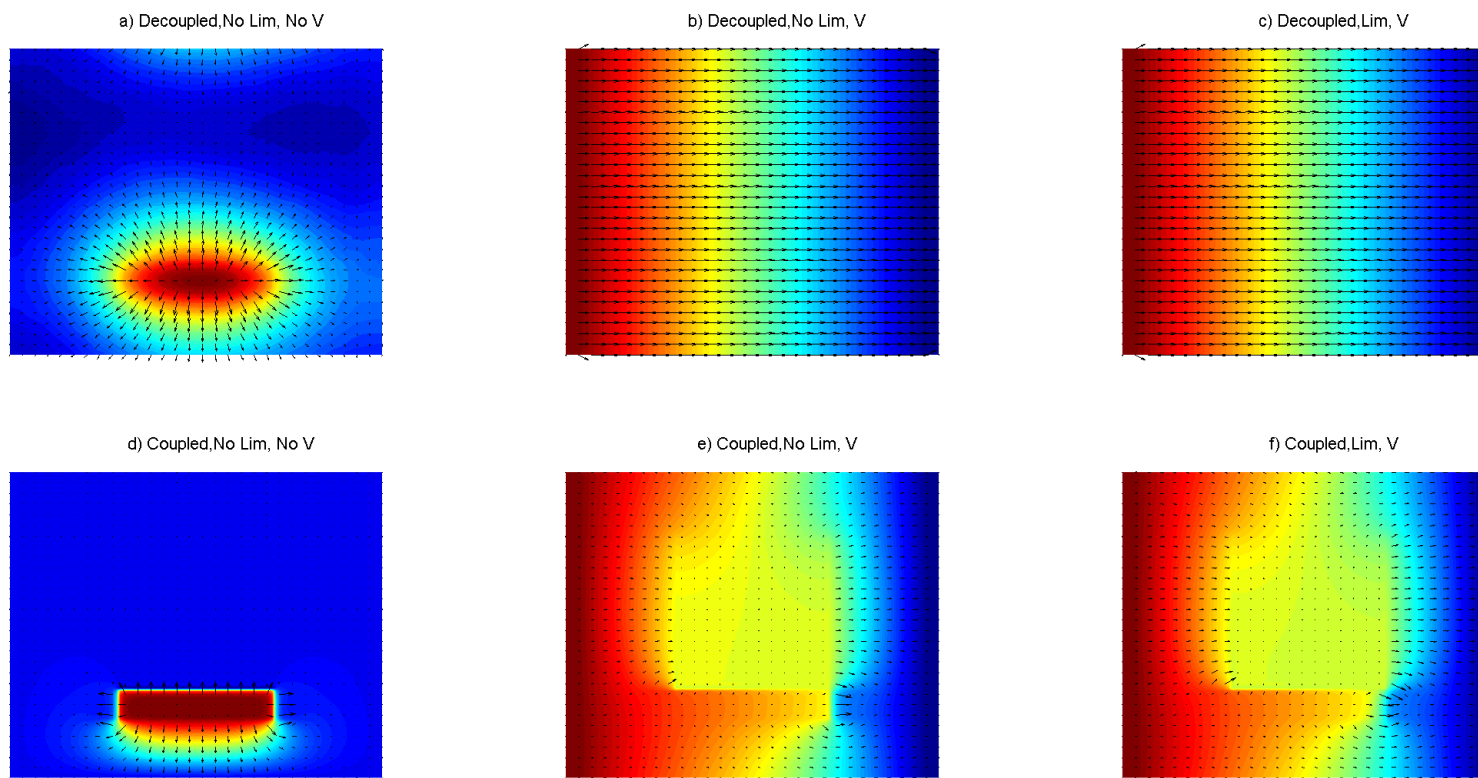
FIGURE 6.8: Potential and Electric Field in Steady State

6.2   Simulation vs. Experimental Results

6.2.1   Single Channel Memristor

In this section we will be looking into the transient simulation of a single channel memristor which is very similar to the last simulation of the previous section. Drift diffusion and Poisson's equations are coupled and lithium density is limited in PEDOT. In addition, the mobility of lithium is now gradually changing between wet and dry regions. This way lithium ions can penetrate the dry region but they cannot move too far. For transient simulation a constant potential has been applied until steady state. Once the memristor reached steady state the polarity of the potential has been switched and the simulation was run until it reached steady state.
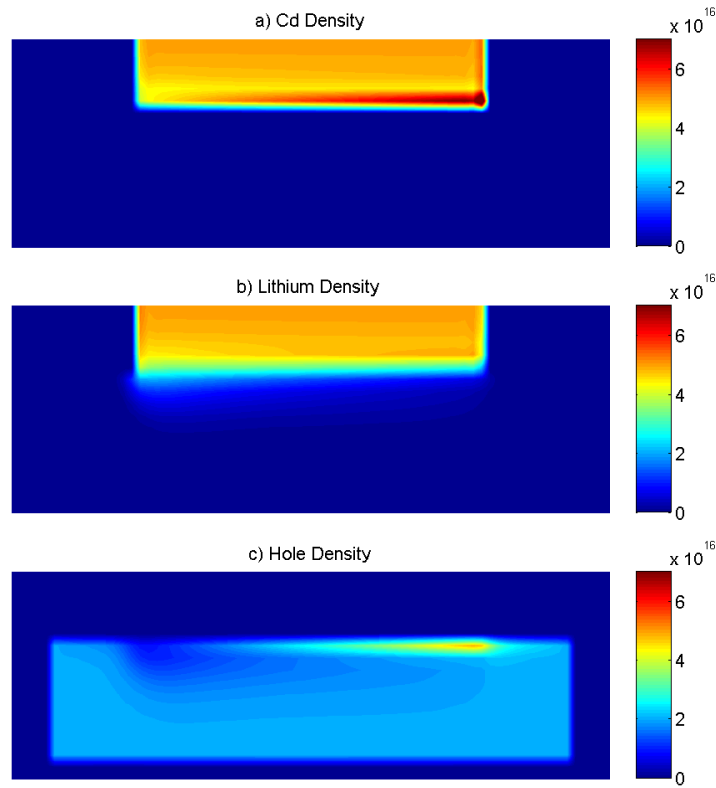
FIGURE 6.9: Particle distribution right after the simulation has started

Following graph (6.9) shows the distribution of charged particles right after the simulation has started using initial conditions described in figure 6.1. We can see that perchlorate ions quickly redistribute and pile up at the bottom right corner of the electrolyte. Lithium ions drift and diffuse into the PEDOT and move as far as they can towards the contact but they cannot reach it due to the decreased mobility in the dry

region. Holes accumulate right on the interface between PEDOT and electrolyte in response to perchlorate accumulation. We can also see holes being pushed out on the left side due to the migration of lithium into PEDOT.

At steady state we can see lithium accumulating on the left side of PEDOT and creating an area with very low hole density therefore high resistance (figure 6.10).
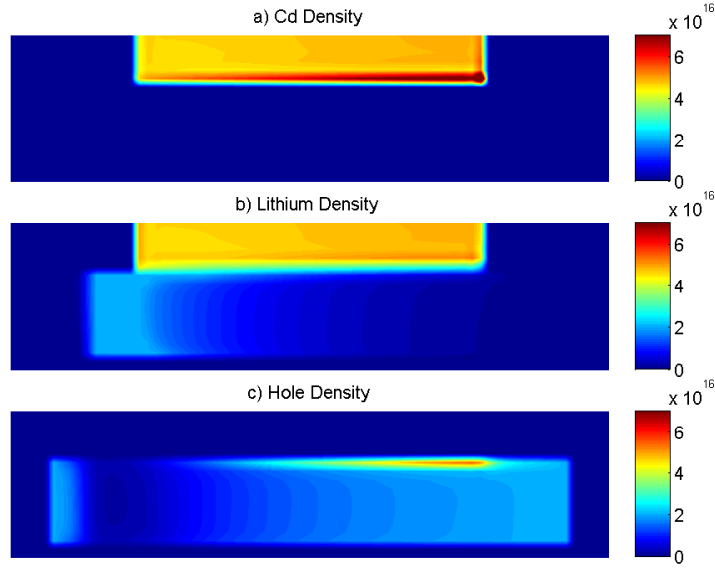
FIGURE 6.10: Particle distribution at steady state

After the potential has been flipped (figure 6.11) we can see that some lithium that got into the dry region of the PEDOT does not leave right away due to low mobility. Also, the change in potential forces lithium ions to accumulate on the right side of PEDOT.
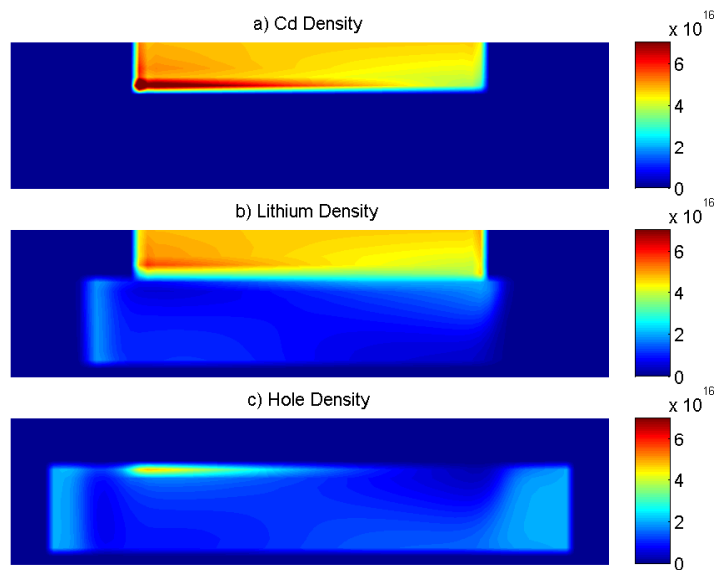
FIGURE 6.11: Particle distribution after the potential has been changed

Finally once everything reaches steady state again almost all of the lithium ions that ware stuck in the dry region of PEDOT moved away. The final distribution for all particles looks like a mirror image of the situation with opposite potential (figure 6.10). This is expected since the device is completely symmetrical.
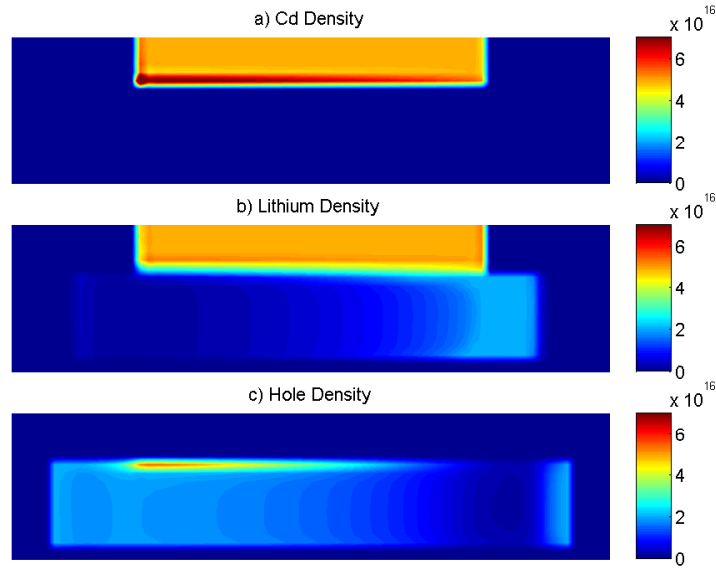
FIGURE 6.12: Particle distribution at steady state after the potential has been changed

The next five graphs show the evolution of the potential and the electric field over time. The snapshots were taken at the same time as the ones for charged particles. The first figure (6.13) shows the initial potential distribution. At te second figure (6.14) We can see the large electric field between the PEDOT and electrolyte created by the accumulation of holes and perchlorate on both sides. Additionally the electric field inside the electrolyte is getting canceled out due to separation of charge.
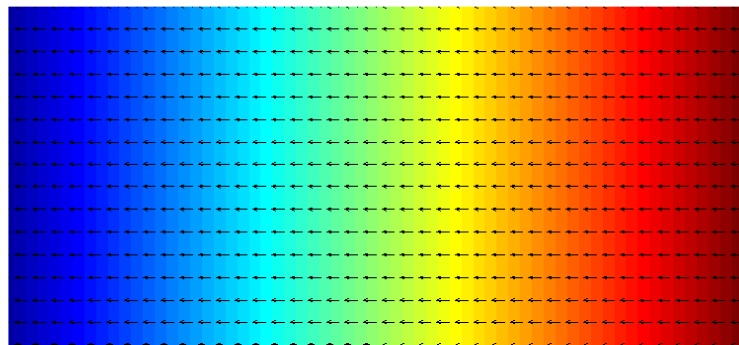
FIGURE 6.13: Electric field and potential distribution before any movement of charge

At steady state there is almost no electric field inside the electrolyte (figure 6.15). Most of the electric field inside PEDOT is also canceled out by the accumulation of lithium
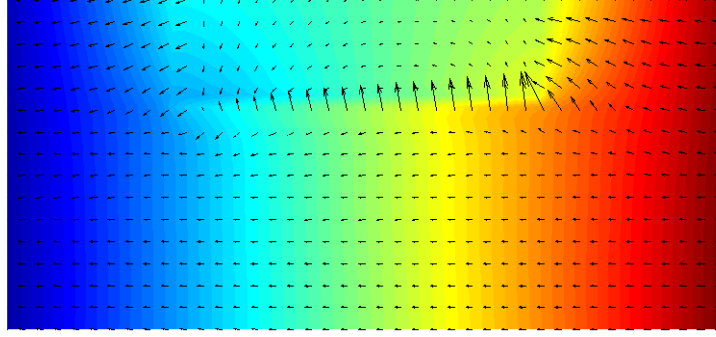
FIGURE 6.14: Electric field and potential distribution right after the simulation has started

on the left side. Almost all the electric field is concentrated around the region where lithium accumulates and forces holes out. Since the electrons are fixed in place, when holes move out they leave behind an exposed negative charge in the dry region. This strengthens the electric field even further.
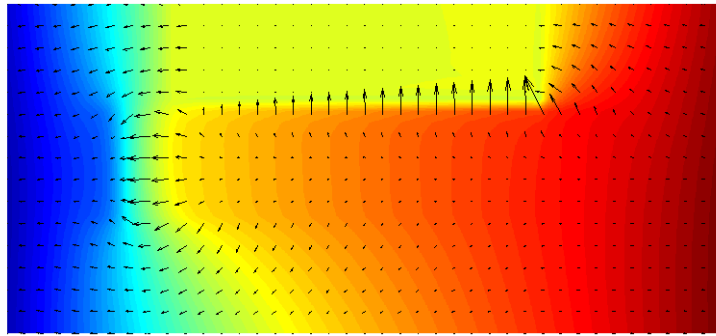
FIGURE 6.15: Electric field and potential distribution at steady state

As soon as the potential is switched we see a change in the electric field between PEDOT and electrolyte (figure 6.16). The electric field created by lithium on the left side of the PEDOT quickly disappears. The dark spot on the left side of PEDOT is due to lithium taking time to move towards the other side.

At steady state the potential distributions of 6.15 and 6.17 are mirror images of each other except the polarity of the applied potential at the contacts are opposite. This is not unexpected since charge particle distributions had the exact same behavior.

Figures 6.18 to 6.23 show the horizontal cross section of lithium around the wet dry/interface of PEDOT. The figures on the left side are simulation results and the figures on the right side are experimental results. Unfortunately we did not have any means of directly measuring the lithium density. The closest option to measuring lithium density in
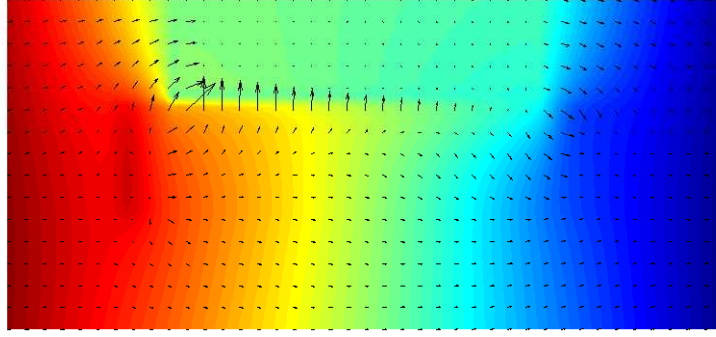
FIGURE 6.16: Electric field and potential distribution right after the applied potential has been changed
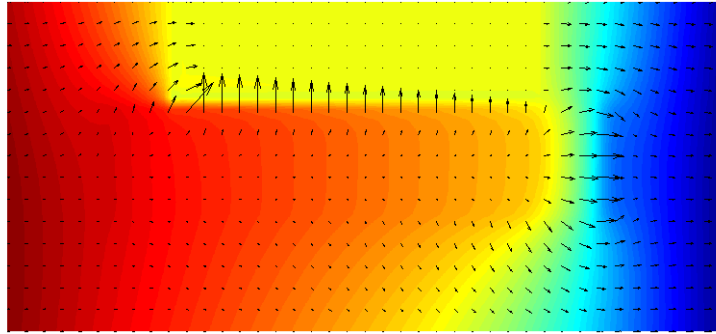
FIGURE 6.17: Electric field and potential distribution at steady state after the applied potential has been changed

PEDOT was to capture the blue coloration of PEDOT when it interacts with lithium. This was done by recording the video of the experiment as it goes through different stages. Afterwards, the images were filtered and processed to show high values for blue and low values for other colors.

The figure below shows the distribution of lithium right before the potential is flipped. We can see , from both simulation and experimental results, that as time progresses lithium moves towards the opposite side of the device and leaves behind a trail where mobility is very low.

Another phenomenon that was observed in the experiment was the change in lithium penetration into dry PEDOT due to increased applied potential. The last figure in this chapter (6.24) shows the maximum distance lithium travels into the dry region of PEDOT with increasing potential at the contacts. Both simulation and the experiment follow a similar trend but they deviate at higher voltages. There could be a few reasons for this discrepancy. First of all it is very hard to get an exact function for the change between wet and dry regions through experimentation so any function used to model this

gradual change had to be optimized by trial and error. Since the simulation for every data point takes a very long time to run, it is very difficult to find a general function that fits all the data points. Also the grid used to simulate this problem was quite coarse so there were only a few points to represent the change between two regions.
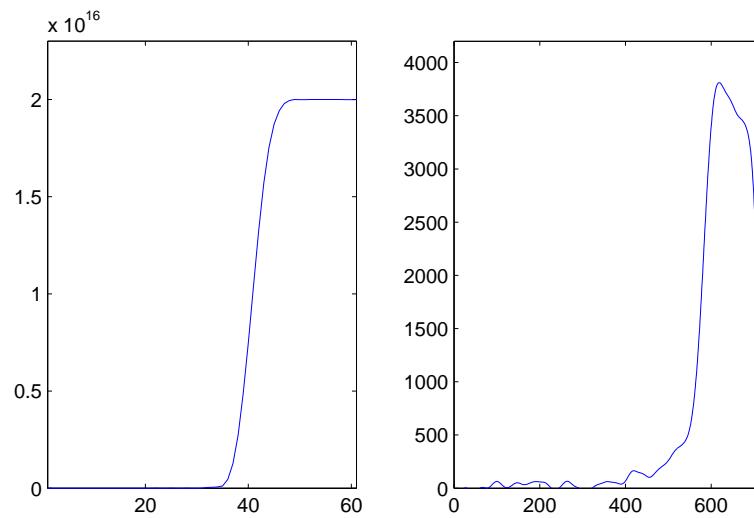
FIGURE 6.18: Lithium movement at wet/dry interface
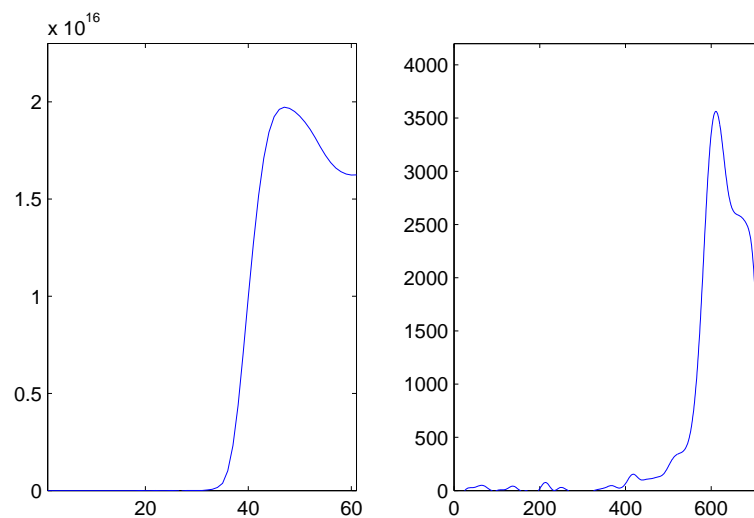
FIGURE 6.19: Lithium movement at wet/dry interface
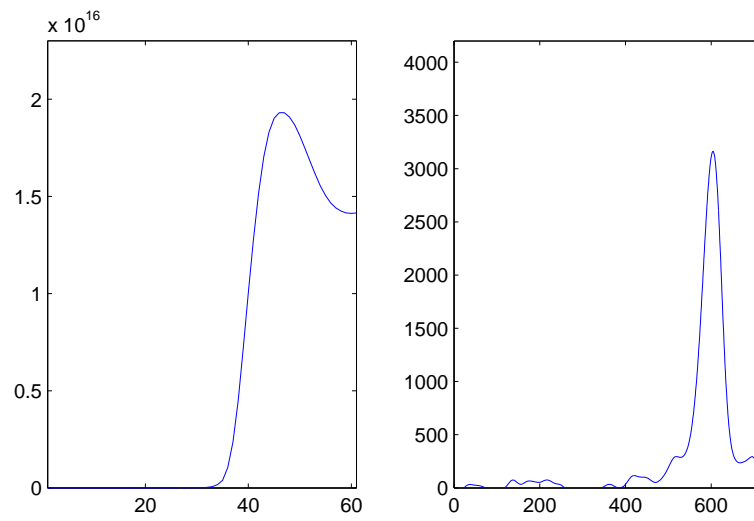
FIGURE 6.20: Lithium movement at wet/dry interface
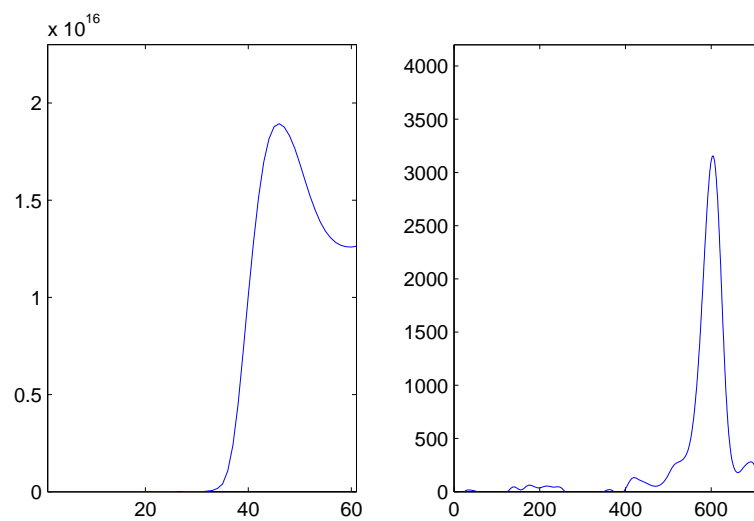
FIGURE 6.21: Lithium movement at wet/dry interface
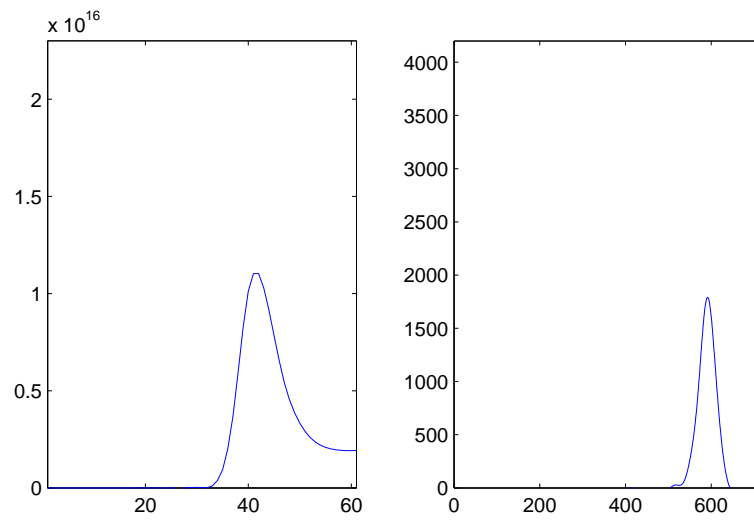
FIGURE 6.22: Lithium movement at wet/dry interface
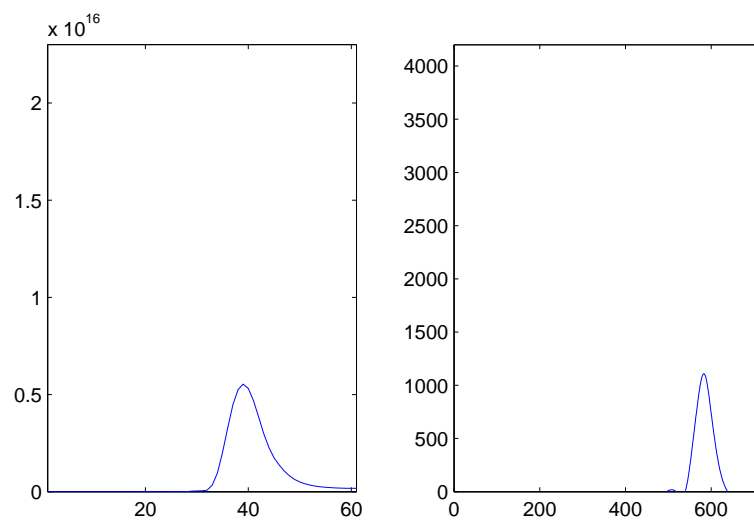
FIGURE 6.23: Lithium movement at wet/dry interface
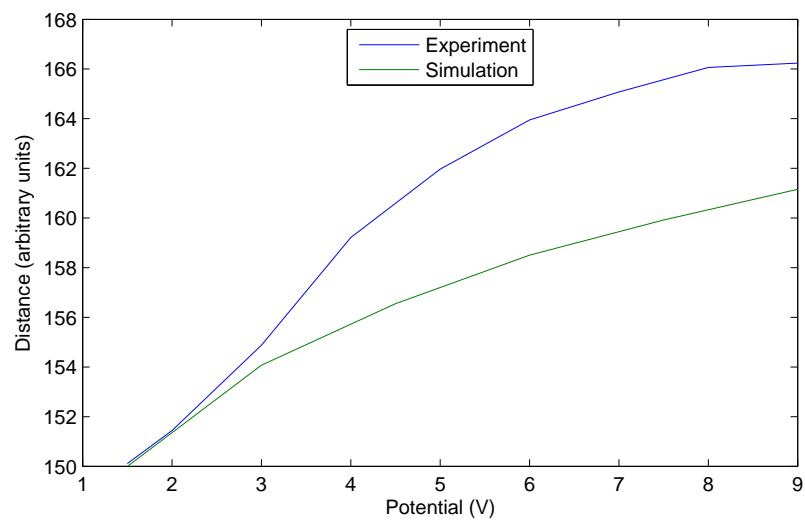
FIGURE 6.24: Penetration of lithium into dry PEDOT

6.2.2 Noteched PEDOT

In this section we will be looking at a structure which is very similar to the single channel memristor. All the boundary conditions and initial values are the same except this time there is a notch in the PEDOT (figure 6.25). So there is no hole current through the device and lithium cannot migrate into the notch. The device itself has very limited practical use but the experimental results are very suitable to test our numerical model.
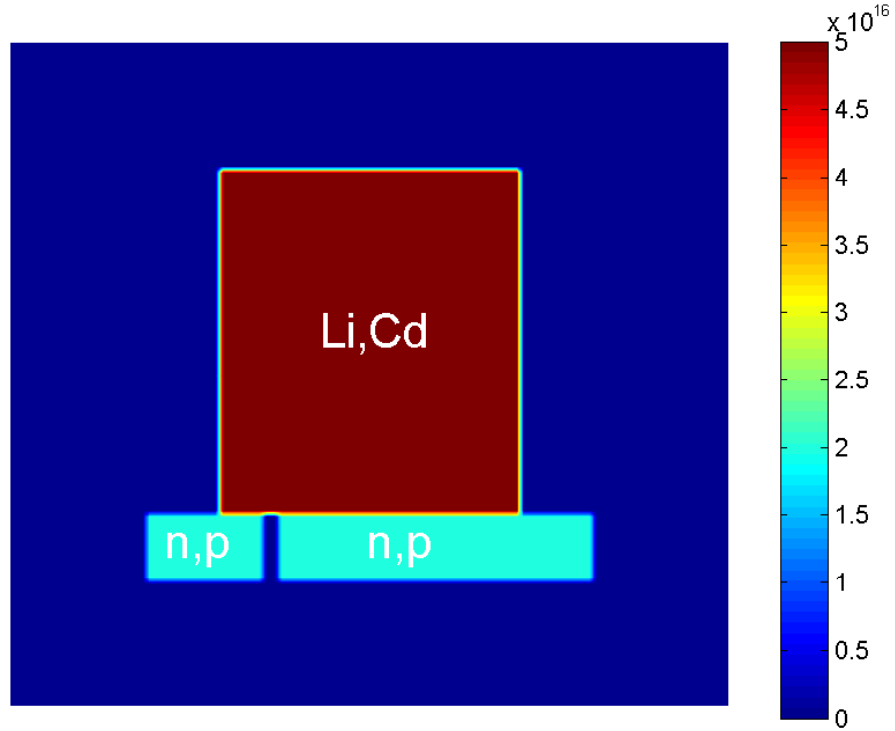
FIGURE 6.25: Initial hole, electron, perchlorate and lithium distribution for a notched memristor

The notch in the PEDOT is sandwiched between two conductive parts. This is analogous to having a simple circuit with two low and one high resistance in series. Based on this analogy we can see that almost all the potential drop is going to be on the notch. One side of the PEDOT will have a low potential and the other side will have a high potential. In figure 6.26 we can see lithium slowly moving towards the negative side of the PEDOT. At the same time perchlorate is starting to accumulate on the positive side. We can also see a significant hole accumulation inside PEDOT right before the notch.

As time goes by more lithium is pushed away from the positive side of the PEDOT and pulled into the negative side (figure 6.27). The here is a noticeable lack of lithium on the side with positive contact at the electrolyte/PEDOT interface. While lithium is pulled
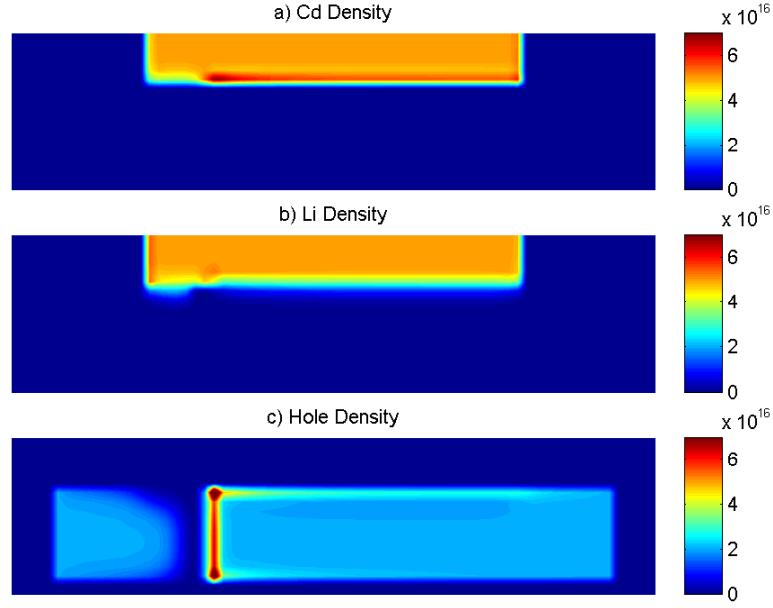
FIGURE 6.26: Particle distribution shortly after the simulation has started

into the PEDOT holes are being pushed away. Holes also accumulate at the surface of the PEDOT due to accumulation of perchlorate right across the interface.
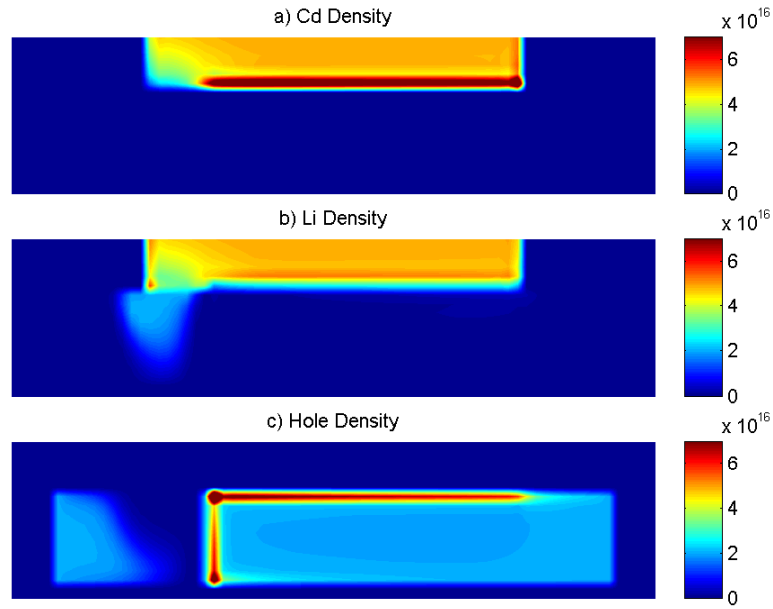
FIGURE 6.27: Particle distribution before steady state

At steady state we can see that lithium density in PEDOT is uniform and at its maximum value (6.28). At the same area we can see the lack of holes due to migration of lithium.

Once the potential is flipped everything starts to move in opposite direction (figures 6.29 and 6.30). Perchlorate moves towards the positive contact. Lithium ions start to leave
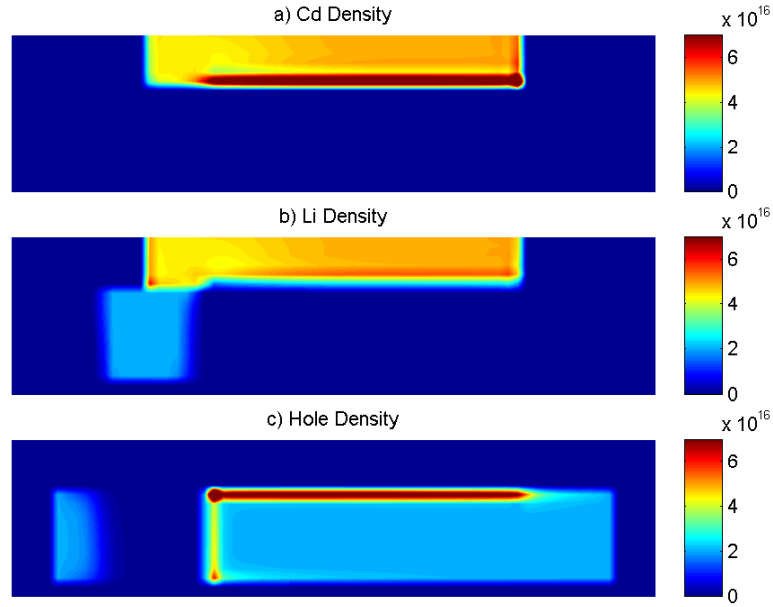
FIGURE 6.28: Particle distribution at steady state

the PEDOT on the left side of the notch and they get attracted towards the right side. Holes start to accumulate on the left side instead of the right side.

In figure 6.30 we can see that due to the strength of the electric field, holes and perchlorate ions gather on the left side of the PEDOT/electrolyte interface very quickly and leave behind a depleted region. Also as lithium settles in the right side of the PEDOT holes start to move away.
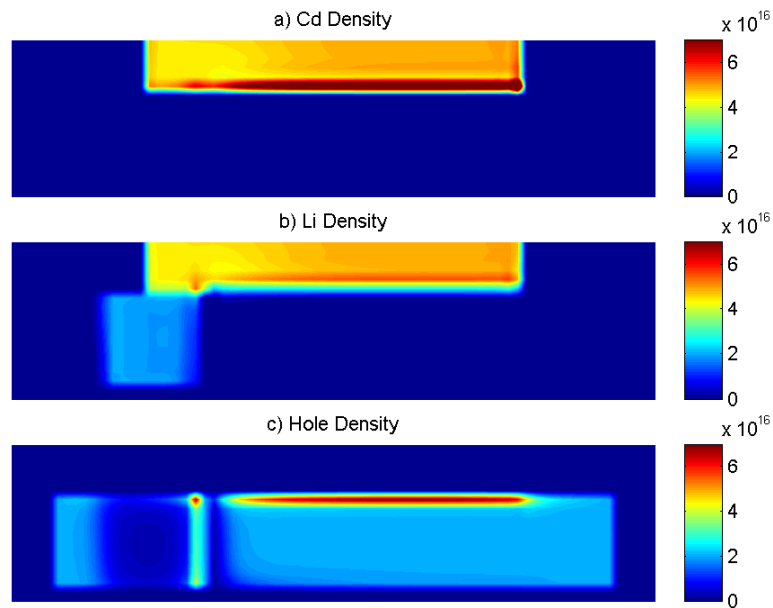
FIGURE 6.29: Particle distribution right after applied potential has been switched
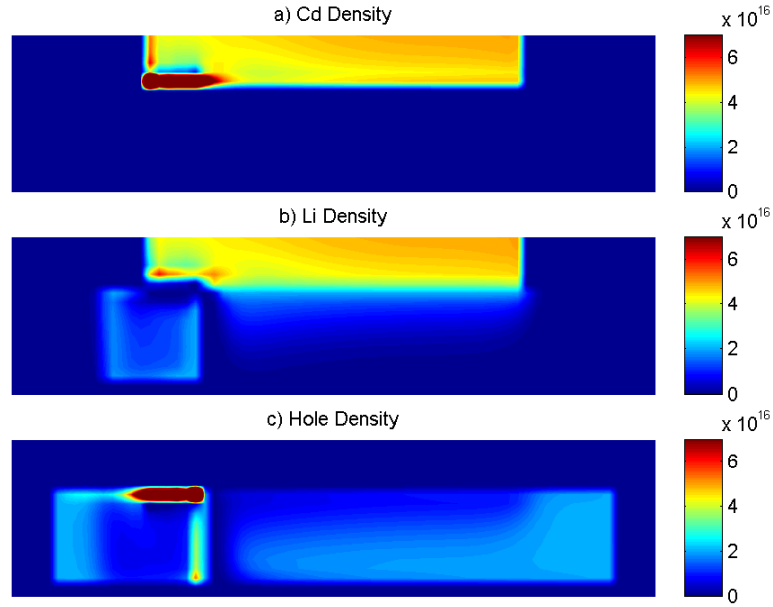
FIGURE 6.30: Particle distribution close to steady state after the potential has been switched

Steady state in figure 6.31 is the complete opposite of figure 6.28. The potential is flipped therefore everything else appears on the opposite side. In both cases lithium ions push out holes and perchlorate accumulates at the interface.
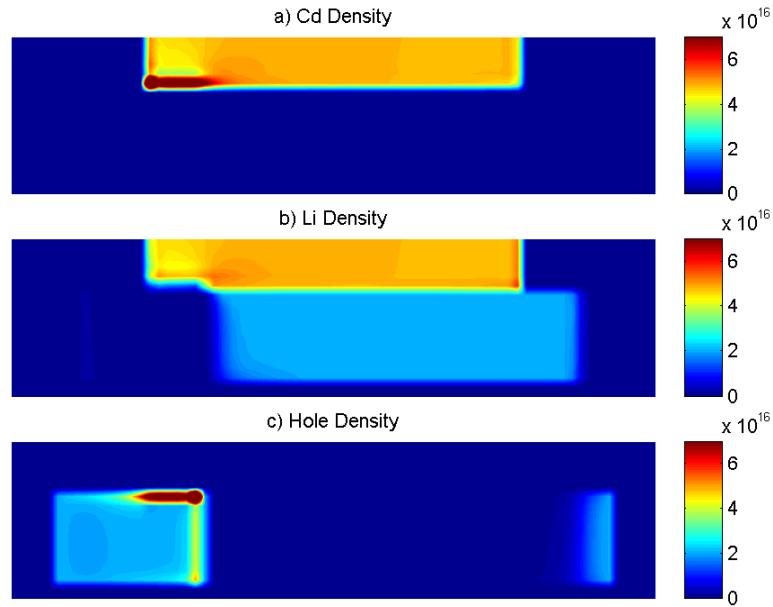
FIGURE 6.31: Particle distribution at steady state after the potential has been switched

Figures 6.32 to 6.38 show the evolution of electric field and potential over time. Right after the simulation has started we can see a large drop of potential and a large electric field at the gap (figure 6.33). There is also a large electric field forming at the

PEDOT/electrolyte interface as holes and perchlorate ions right across each other.
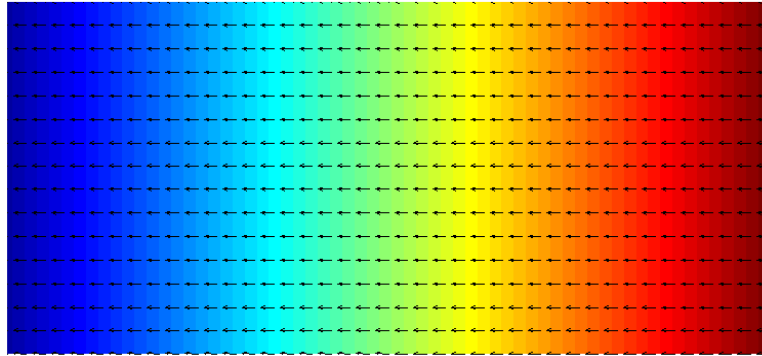
FIGURE 6.32: Electric field and potential distribution before redistribution of charge
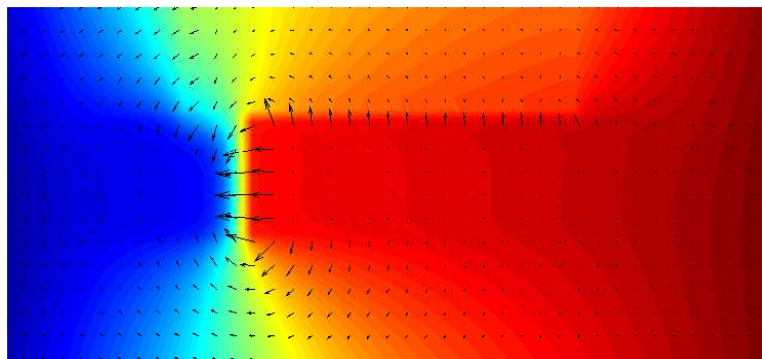
FIGURE 6.33: Electric field and potential distribution shortly after the simulation has started

In figure 6.34 we can see the cancellation of the electric field inside the electrolyte due to redistribution of charge. We can also see the effect of lithium ions moving in on the left corner of the notch.
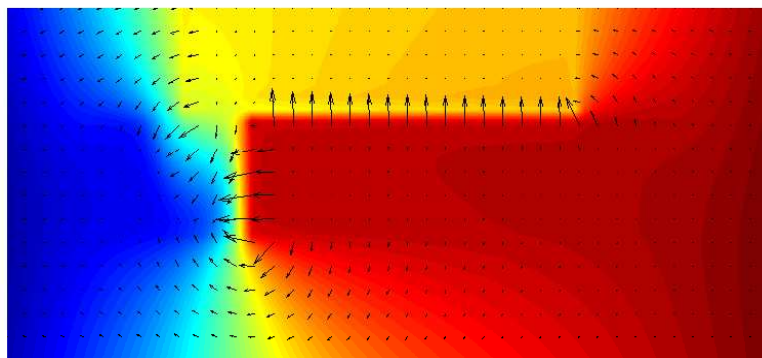
FIGURE 6.34: Electric field and potential distribution before steady state

At steady state we can see that the electric field on the right side of the notch was canceled but there is still an electric field on the left side (figure 6.35). This is due to the density limit of lithium. Holes cannot accumulate at the contact and lithium can only accumulate until a certain density so the electric field in that region does not get canceled out.
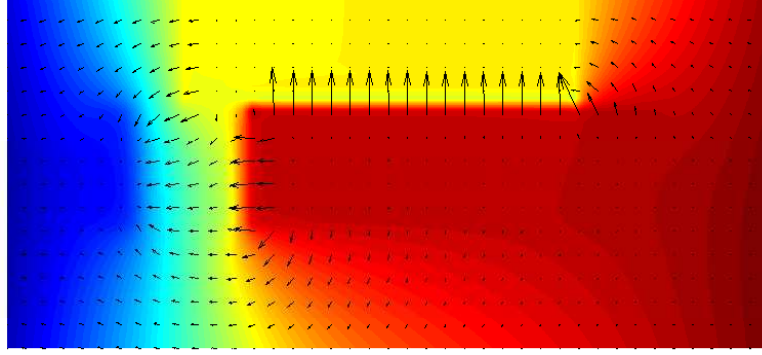
FIGURE 6.35: Electric field and potential distribution at steady state

The same process repeats itself after the applied potential has been switched (figures 6.36 to 6.38). Holes accumulate on the left side of the notch and cancel the electric field. Also there is a large electric field emerges due to the accumulation of perchlorate ions and holes at the boundaries on the left side (figure 6.38).
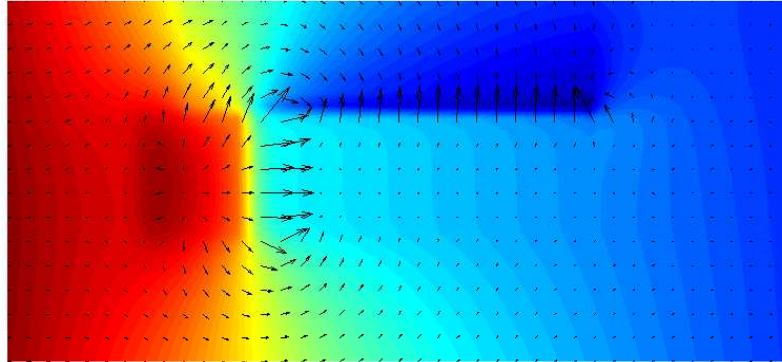
FIGURE 6.36: Electric field and potential distribution right after applied potential has been switched

The only experimental measurement directly showing the movement of lithium ions inside is the video showing the blue coloration of PEDOT. Figures 6.39 to 6.50 compare the simulation lithium movement with experimental results. Following figures show a horizontal cross section of PEDOT (only the side that is receiving lithium)near the electrolyte. The experimental results show the blue coloration of PEDOT after some
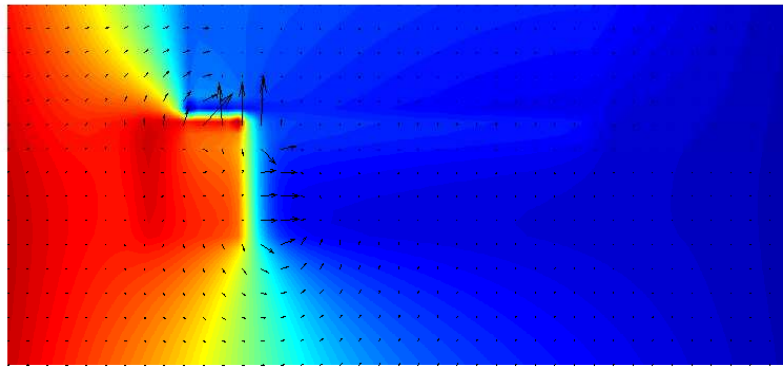
FIGURE 6.37: Electric field and potential distribution before steady state
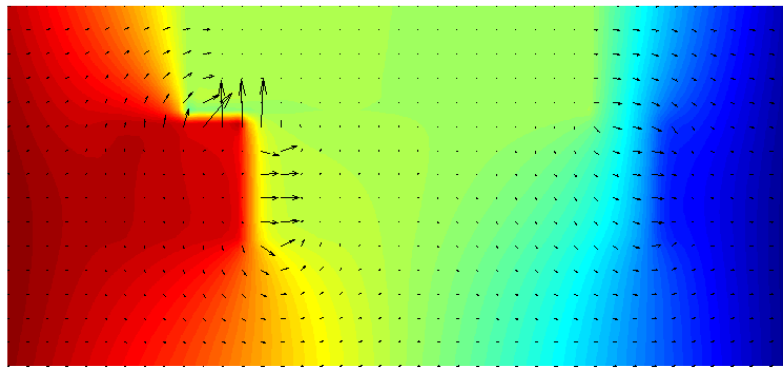
FIGURE 6.38: Electric field and potential distribution at steady state

filtering and image processing. High values in the y axis of signify blue coloration and low values are other colors.

In both experiment and simulation lithium ions start to move in from the notched side. As time progresses lithium ions move toward the contact. There are two effects contributing to this behavior. The electric field is at its highest right around the notch. So this is where the most amount of lithium is pulled into PEDOT. As lithium ions move in vertically, they drift horizontally through PEDOT due to electric field created by the contacts.

When ion movement approaches steady state, in the experiment, we can see that coloration becomes more uniform and stops changing. In the simulation lithium reaches its maximum density and PEDOT stops receiving any additional ions. Overall the behavior seen in this simulation matches the experimental observations quite well.
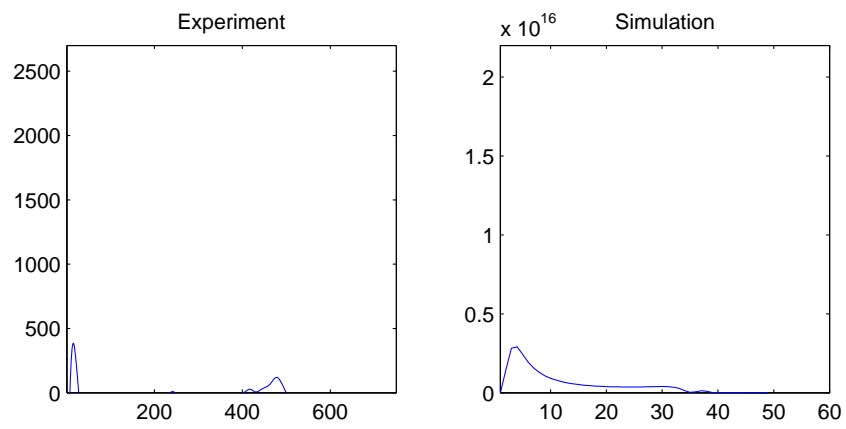
FIGURE 6.39: Movement of lithium ions into PEDOT
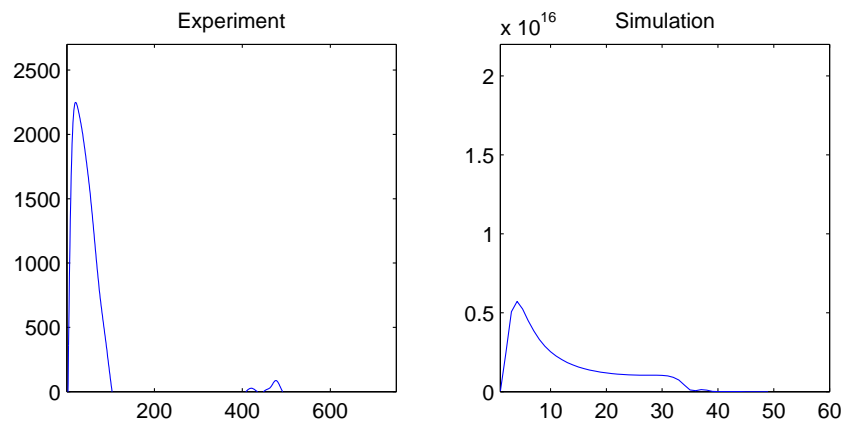
FIGURE 6.40: Movement of lithium ions into PEDOT
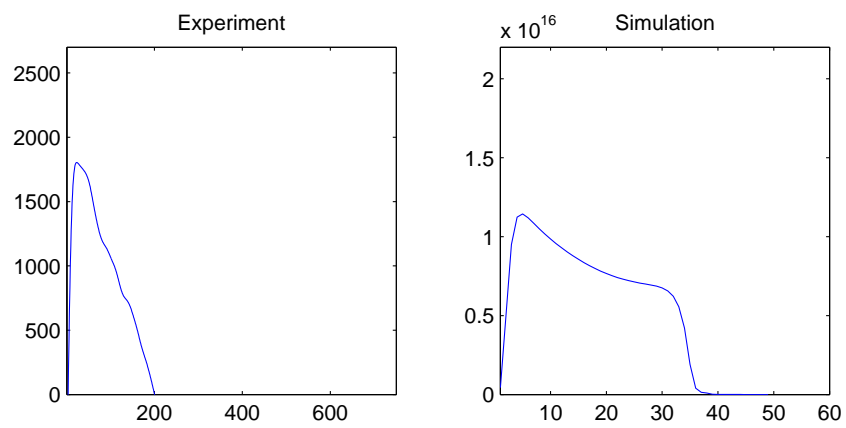
FIGURE 6.41: Movement of lithium ions into PEDOT
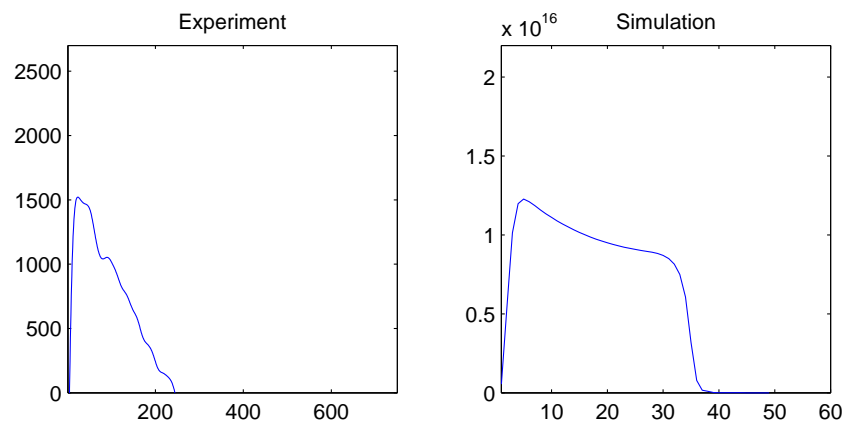
FIGURE 6.42: Movement of lithium ions into PEDOT
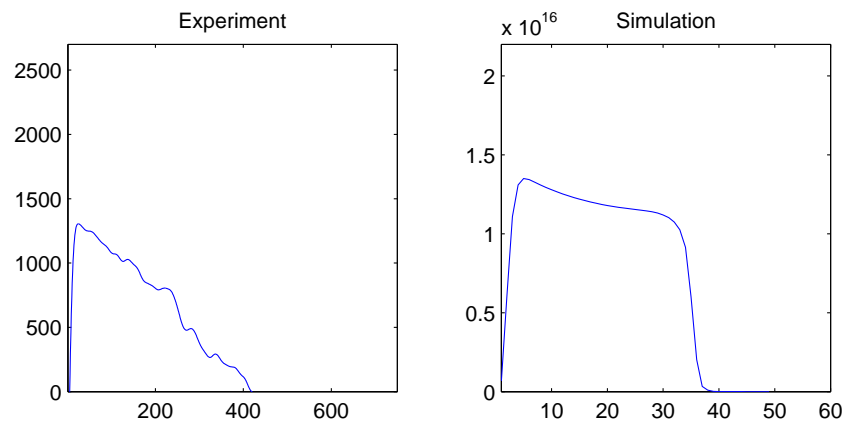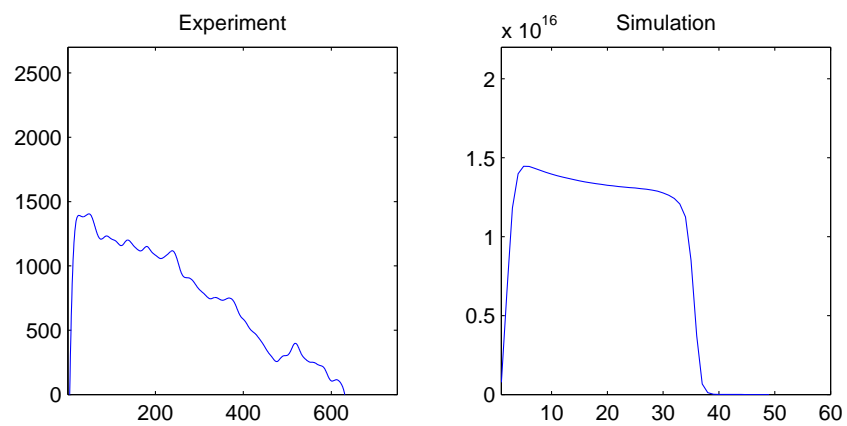

FIGURE 6.43: Movement of lithium ions into PEDOT

FIGURE 6.44: Movement of lithium ions into PEDOT
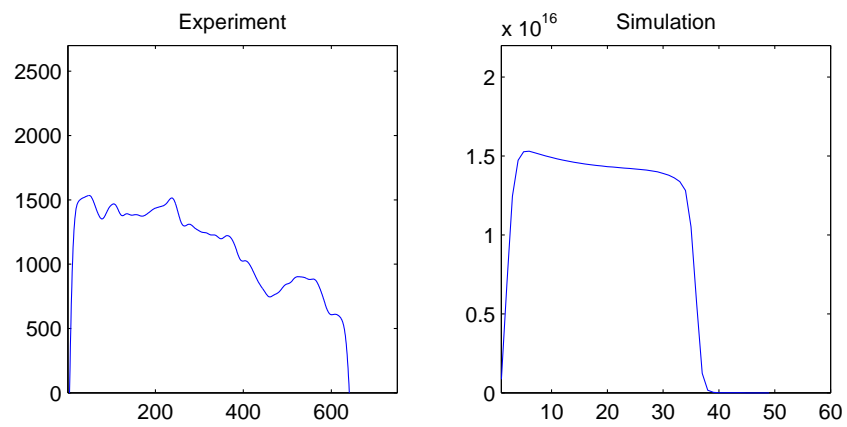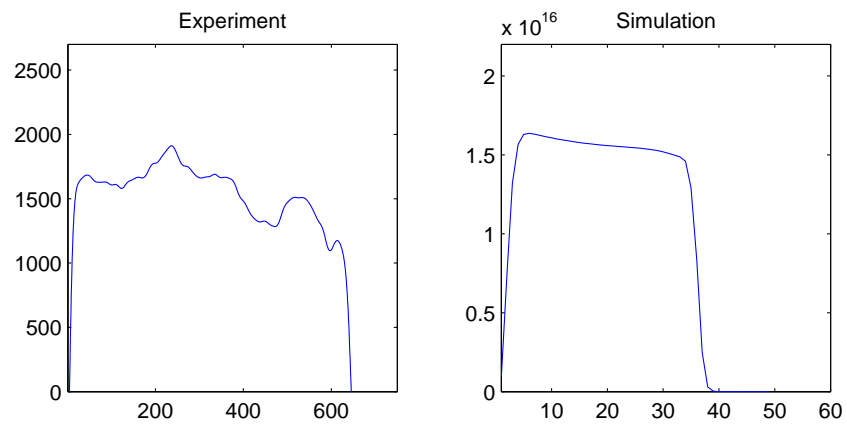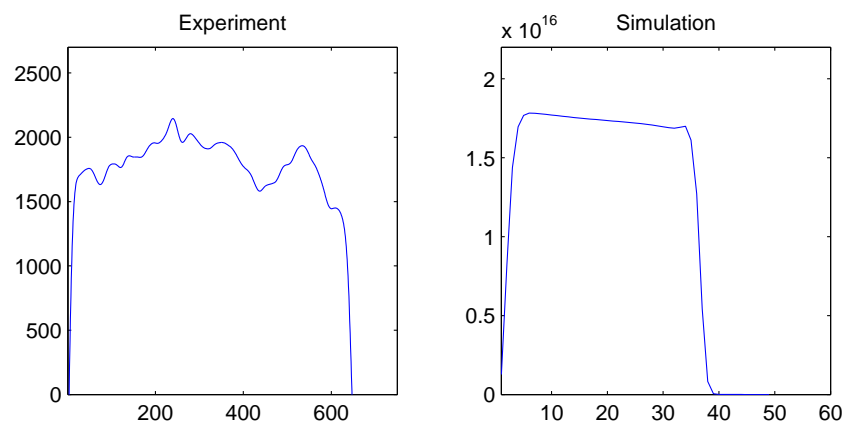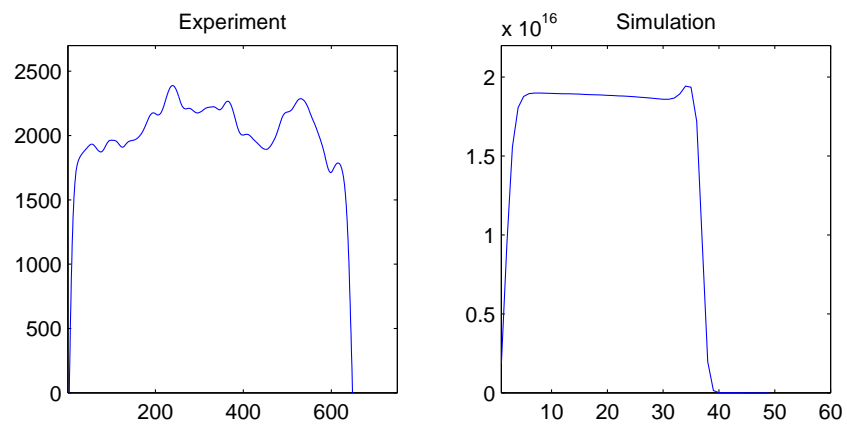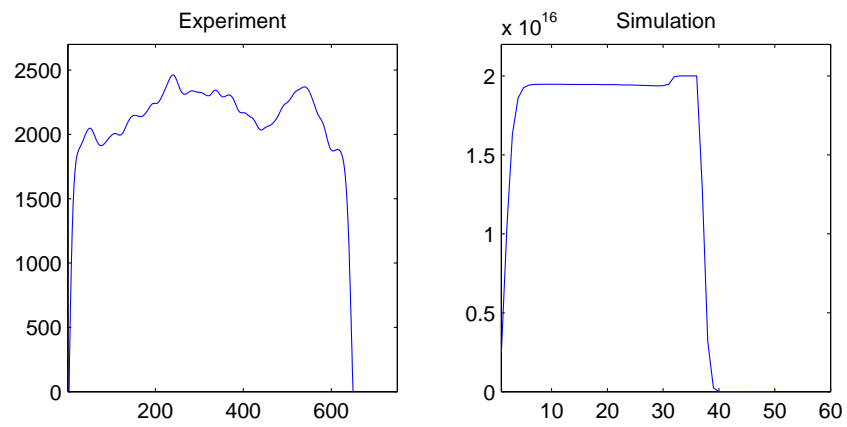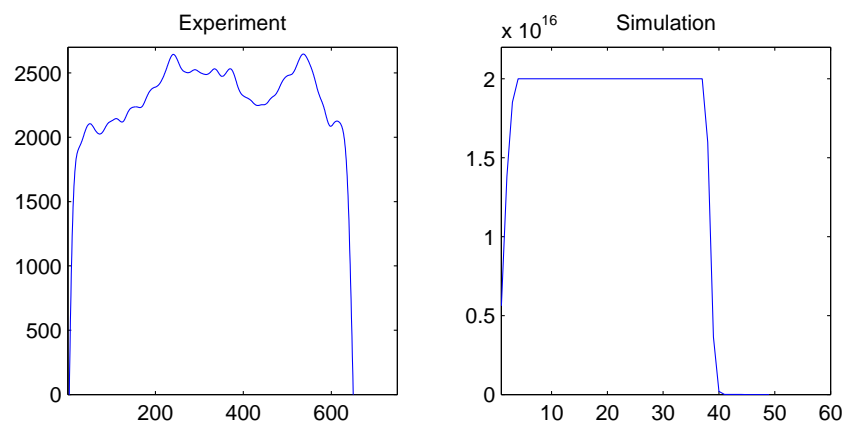
FIGURE 6.45: Movement of lithium ions into PEDOT

FIGURE 6.46: Movement of lithium ions into PEDOT

FIGURE 6.47: Movement of lithium ions into PEDOT

FIGURE 6.48: Movement of lithium ions into PEDOT

FIGURE 6.49: Movement of lithium ions into PEDOT

FIGURE 6.50: Movement of lithium ions into PEDOT

Chapter 7

Conclusion

The purpose of this thesis was to create a memristor model for computer simulation. We were able to model the change in conductivity through the movement of lithium and undoping of PEDOT. The transient simulation results match experimental data visually for both single channel and notched memristor. Although our simulation matched with the experimental data this model requires more work and can be improved through better numerical schemes, physical models and thorough experimentation. There are also few limitations of this model due to its size and physical features.

In terms of numerical methods there are a few down sides of using finite difference. The simulation for this device was done in 2-D instead of 3-D. This did not cause a lot of problems in our case since the structures we used were quite simple and produced reasonable results in 2-D. Unfortunately getting a transient response for devices using finite difference is computationally expensive. Even though we had a 100x100 grid, which is quite coarse, the simulation time was not less than 3 hours on a computer with multiple cores. Addition of another 100 points for a third dimension will make this simulation at least a 100 times longer. This makes 3-D simulations impractically long and very hard to test and optimize.

Another fundamental issue with this simulation arises from debye length. Maximum grid size in finite difference depends on the debye length, which is at least 5 or 6 orders of magnitude smaller than the device size. This means that we need at least 10^5 points in each direction in order to simulate this device. At this point the simulation becomes impossibly long so we had to compromise by either reducing the device size or carrier density.

The model we have developed is quite open for improvements on carrier transport models. A constant bulk mobility was used for holes in this model which is not the case in

an actual device. Holes move from site to site via hopping. Addition of lithium into PEDOT not only reduces the number of available holes but also decreases the number of possible sites through holes can move. A variable range hopping mechanism and thermal effects can be added into this model for a more complete simulation. Also PEDOT:PSS is a disordered material and the way it was deposited on a substrate can make a big difference on hole movement. Anisotropic hole mobilty can be implemented in order to account for this issue.

Overall we have showed that it is possible to simulate a memristor using a simple finite difference method which can be very useful model in understanding the way ions and holes move in PEDOT. Our results show a very promising start for a vast research and development opportunities on memristor and polymer conductors.

Appendix A

Lithium Intercalation

a) Decoupled,No Lim, No V b) Decoupled,No Lim, V c) Decoupled,Lim, V

d) Coupled,No Lim, No V e) Coupled,No Lim, V f) Coupled,Lim, V
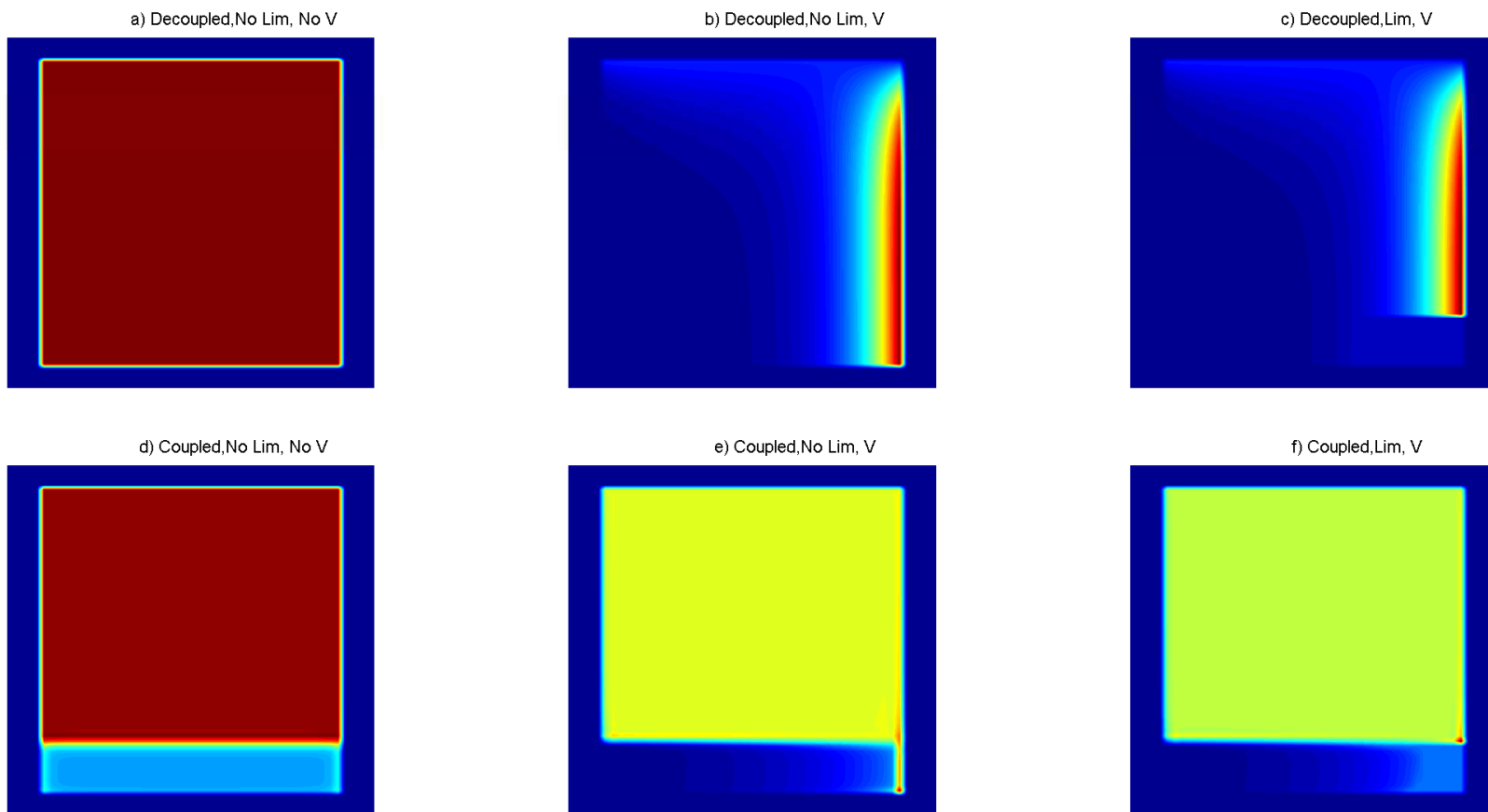
FIGURE A.1: Lithium Density in Steady State

a) Decoupled,No Lim, No V   b) Decoupled,No Lim, V   c) Decoupled,Lim, V

d) Coupled,No Lim, No V   e) Coupled,No Lim, V   f) Coupled,Lim, V
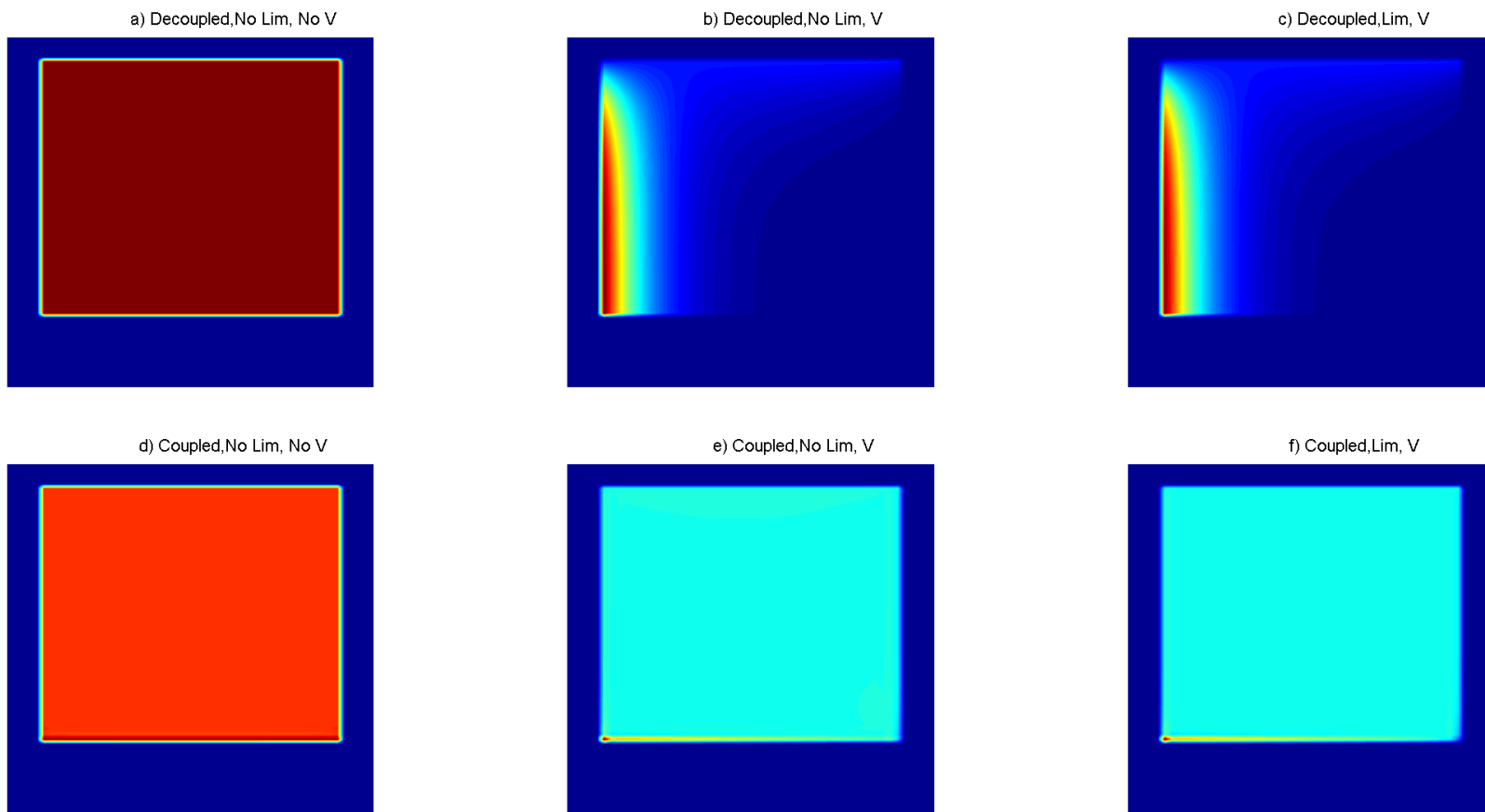
FIGURE A.2: Cadmium Density in Steady State

a) Decoupled,No Lim, No V

b) Decoupled,No Lim, V

c) Decoupled,Lim, V

d) Coupled,No Lim, No V

e) Coupled,No Lim, V

f) Coupled,Lim, V
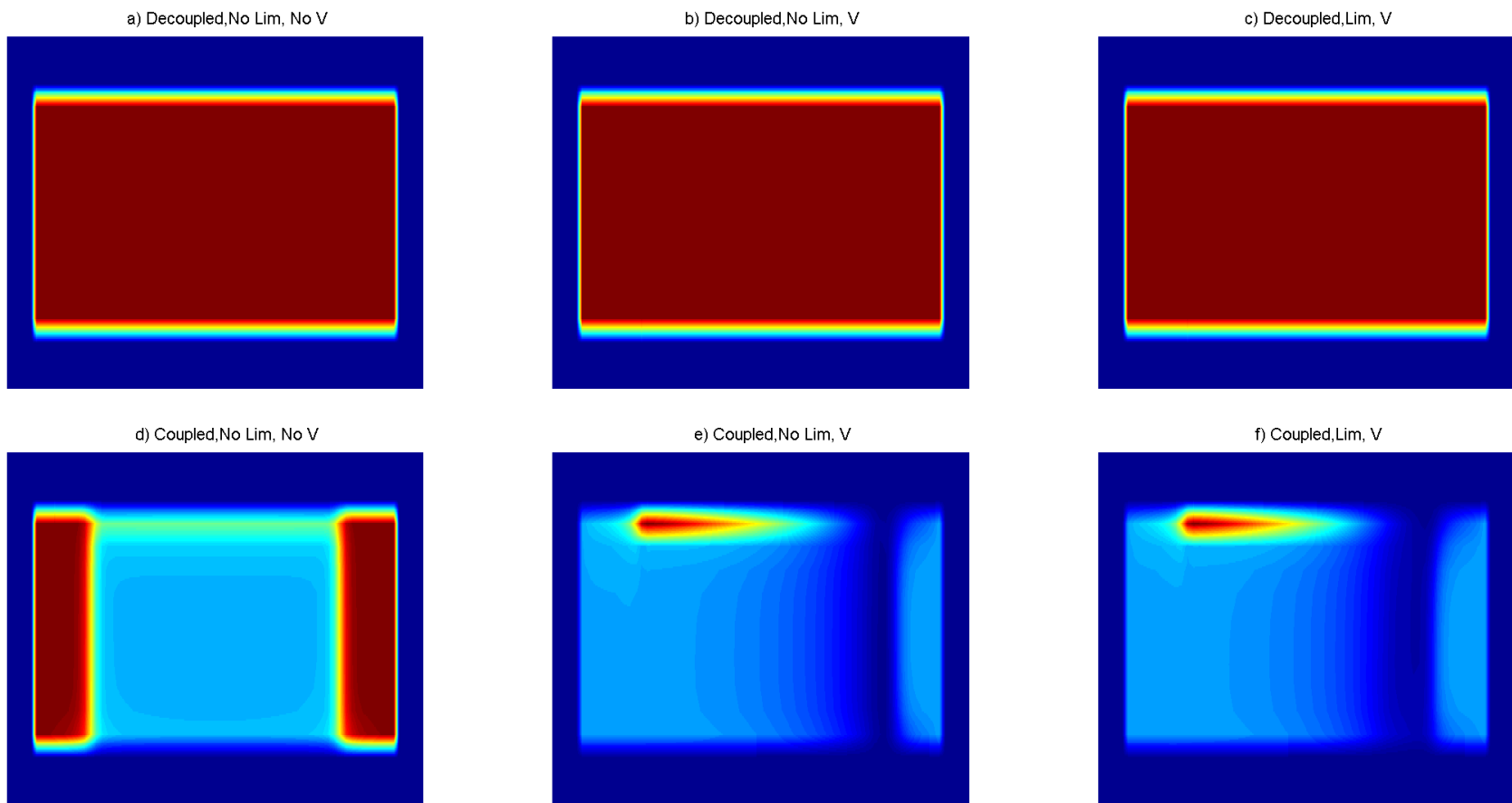
FIGURE A.3: Hole Density in Steady State

a) Decoupled,No Lim, No V   b) Decoupled,No Lim, V   c) Decoupled,Lim, V

d) Coupled,No Lim, No V   e) Coupled,No Lim, V   f) Coupled,Lim, V
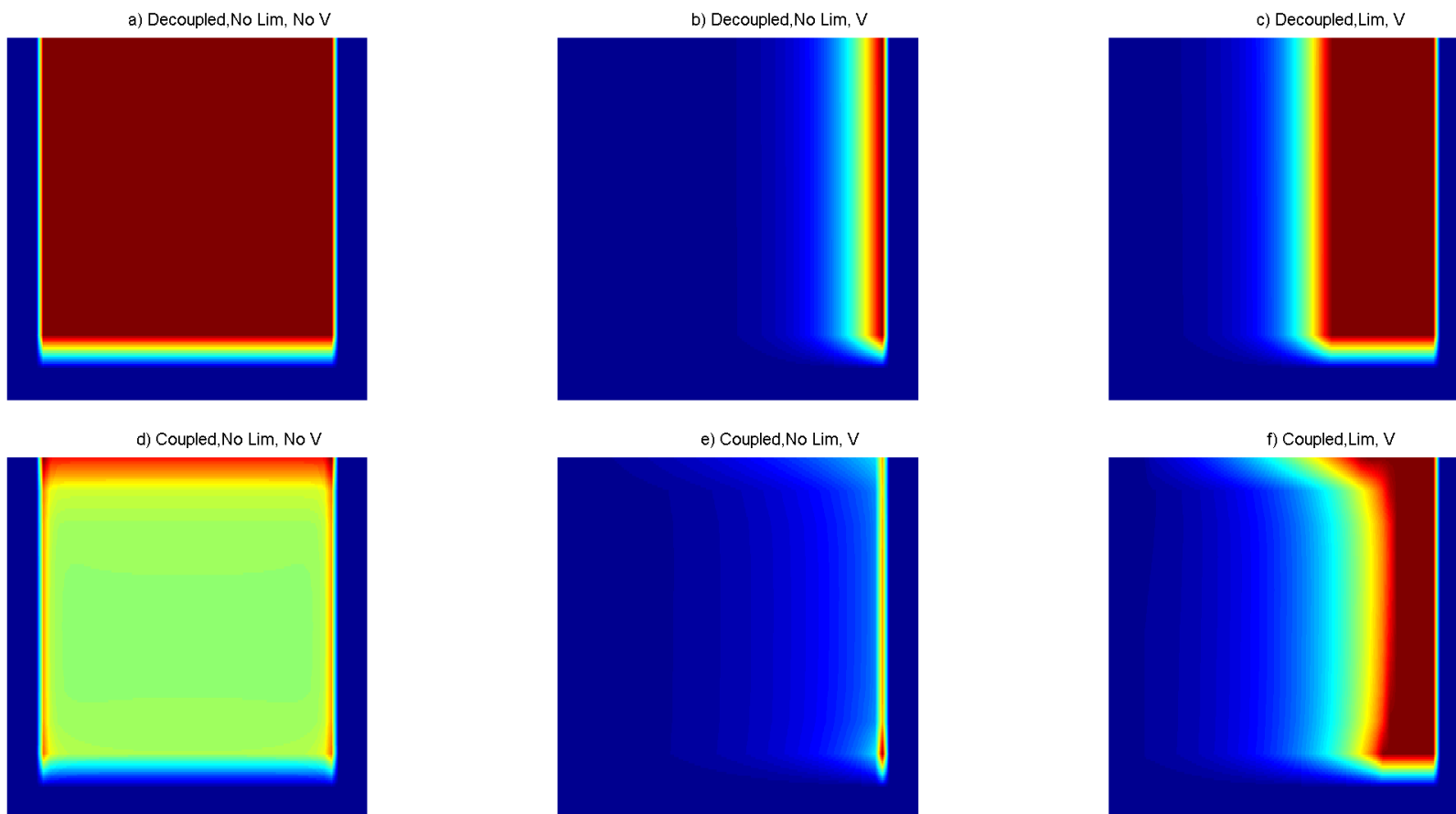
FIGURE A.4: 2d Lithium Steady State PEDOT
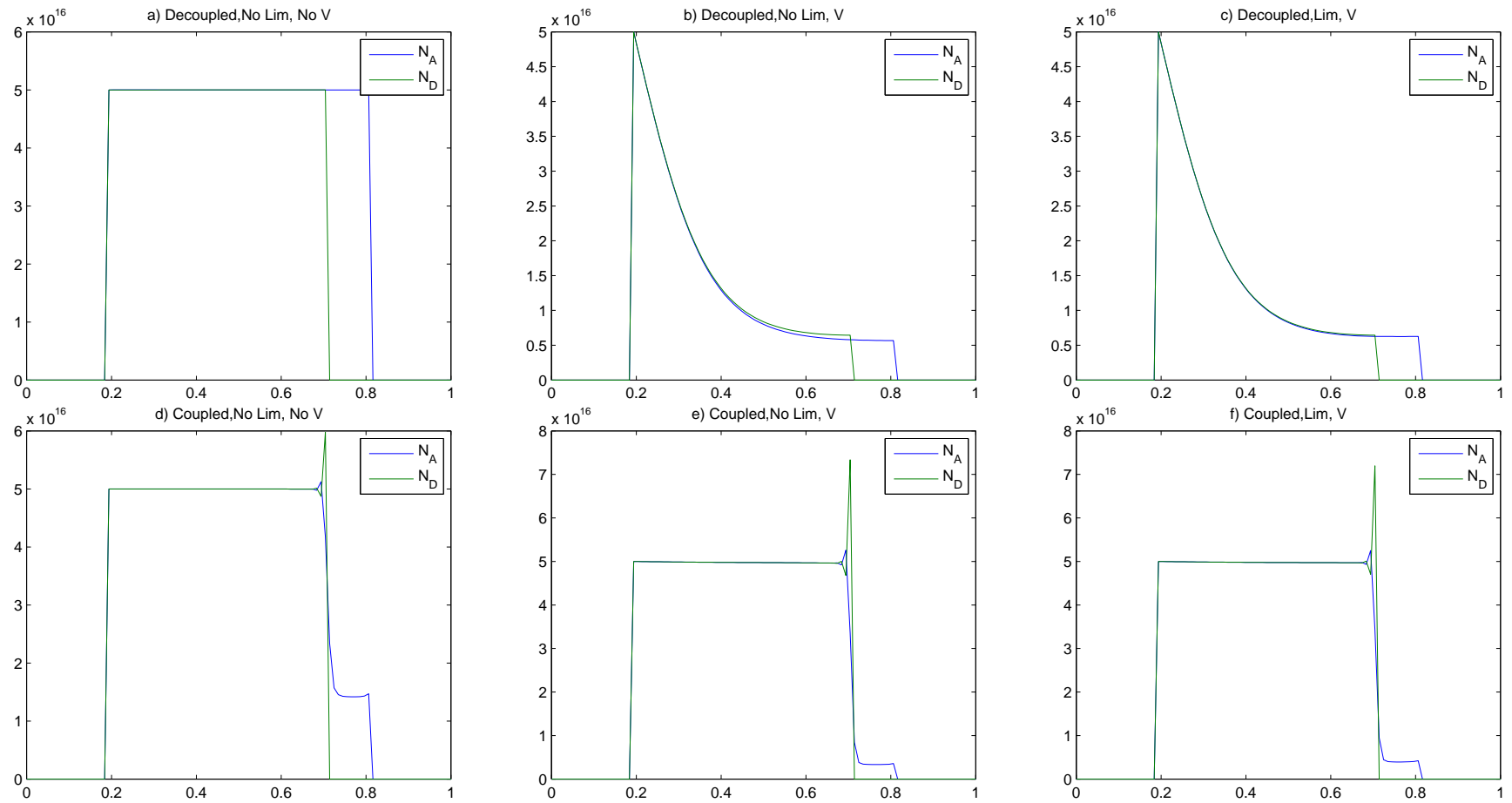
FIGURE A.5: 1D Nn Lithium Vertical
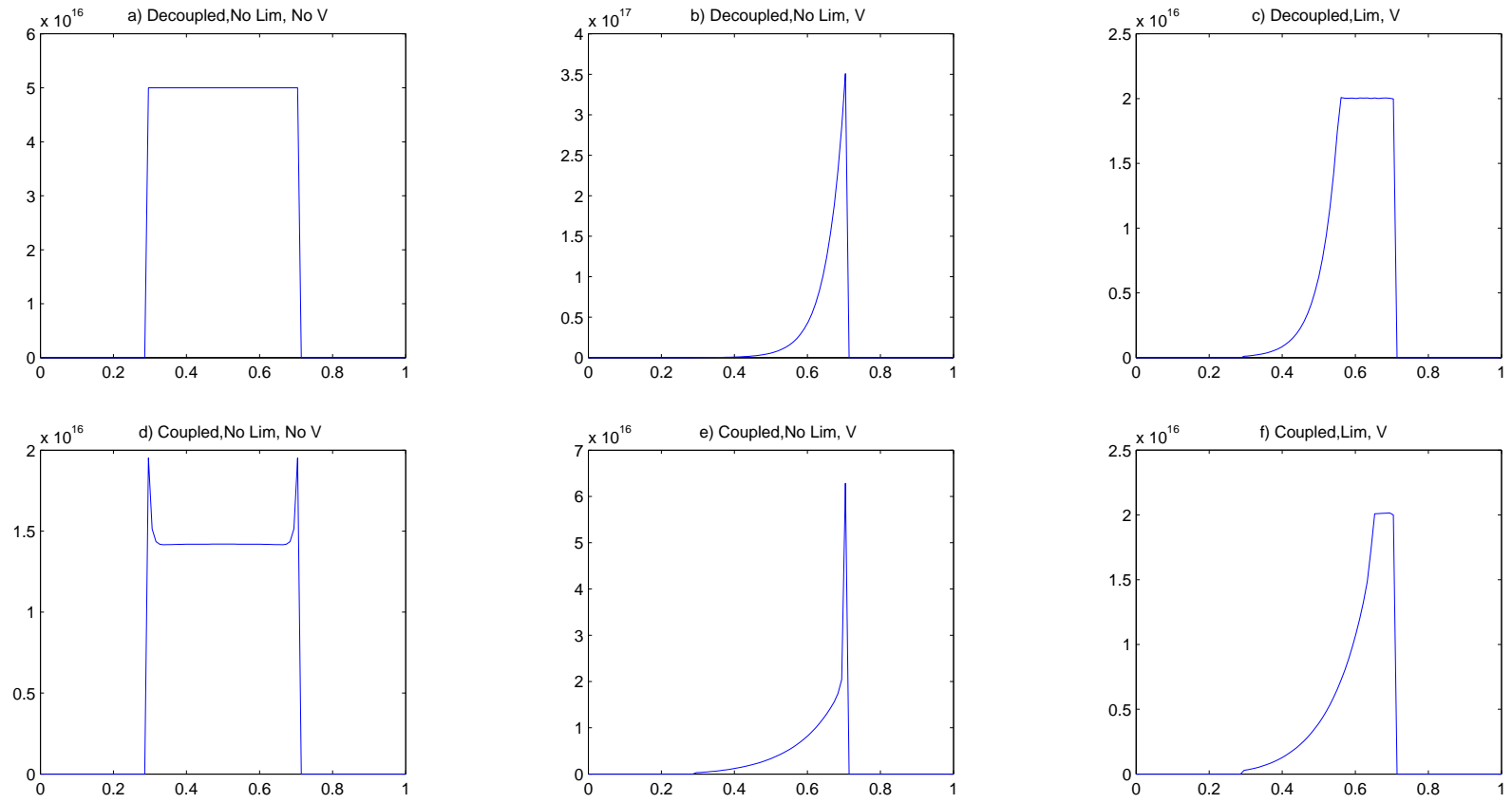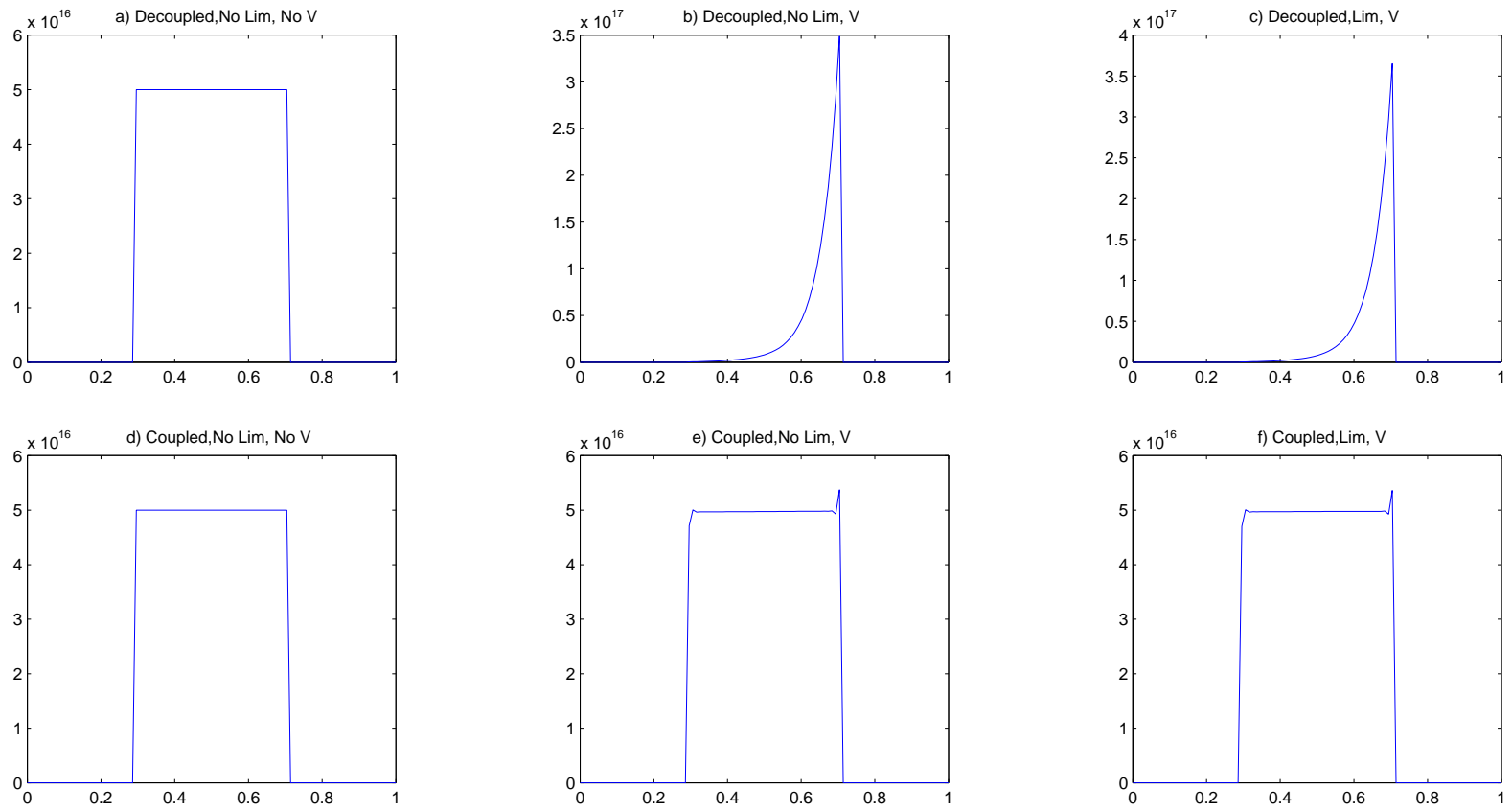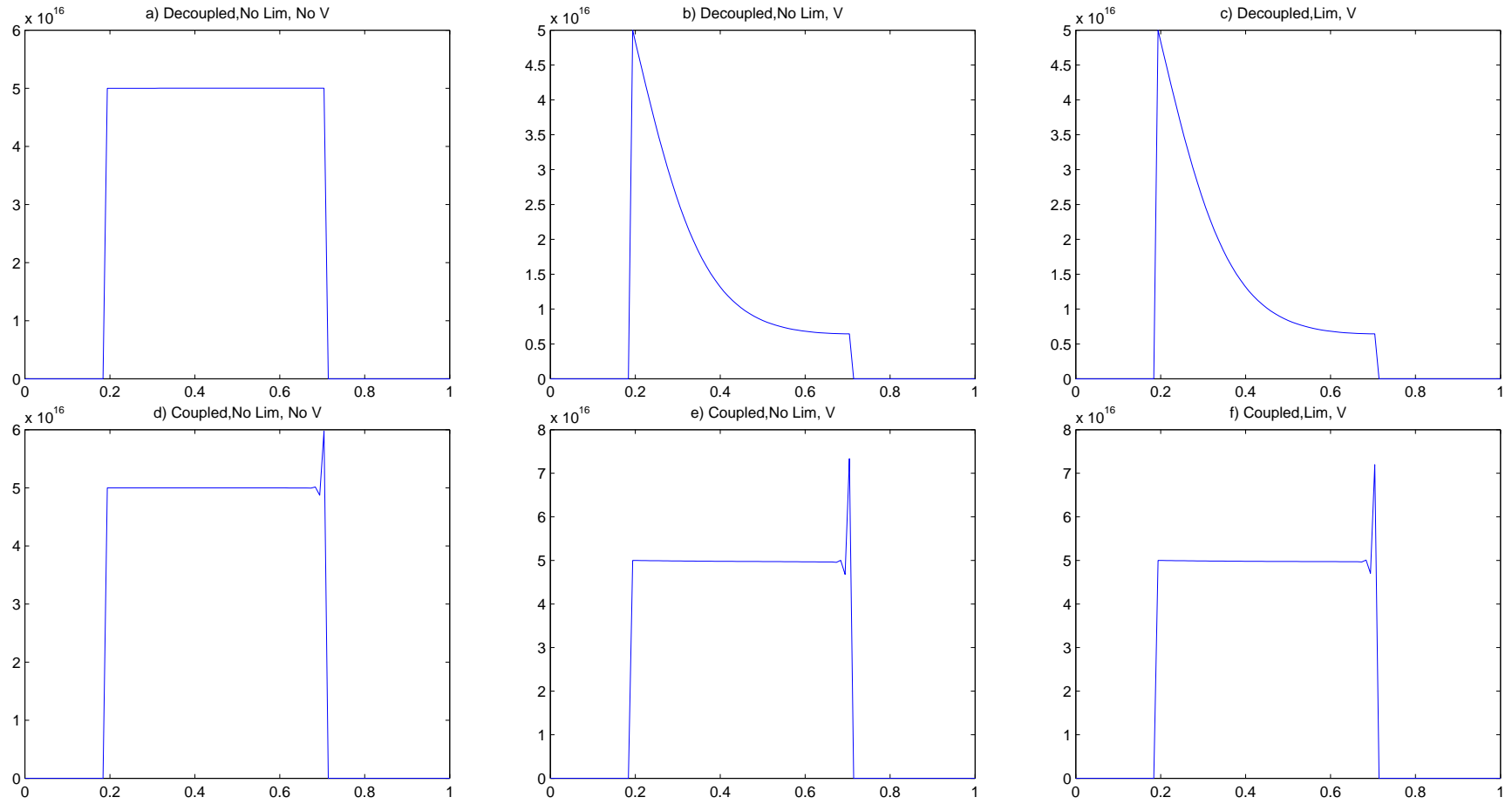
FIGURE A.6: 1d Lithium Horizontal
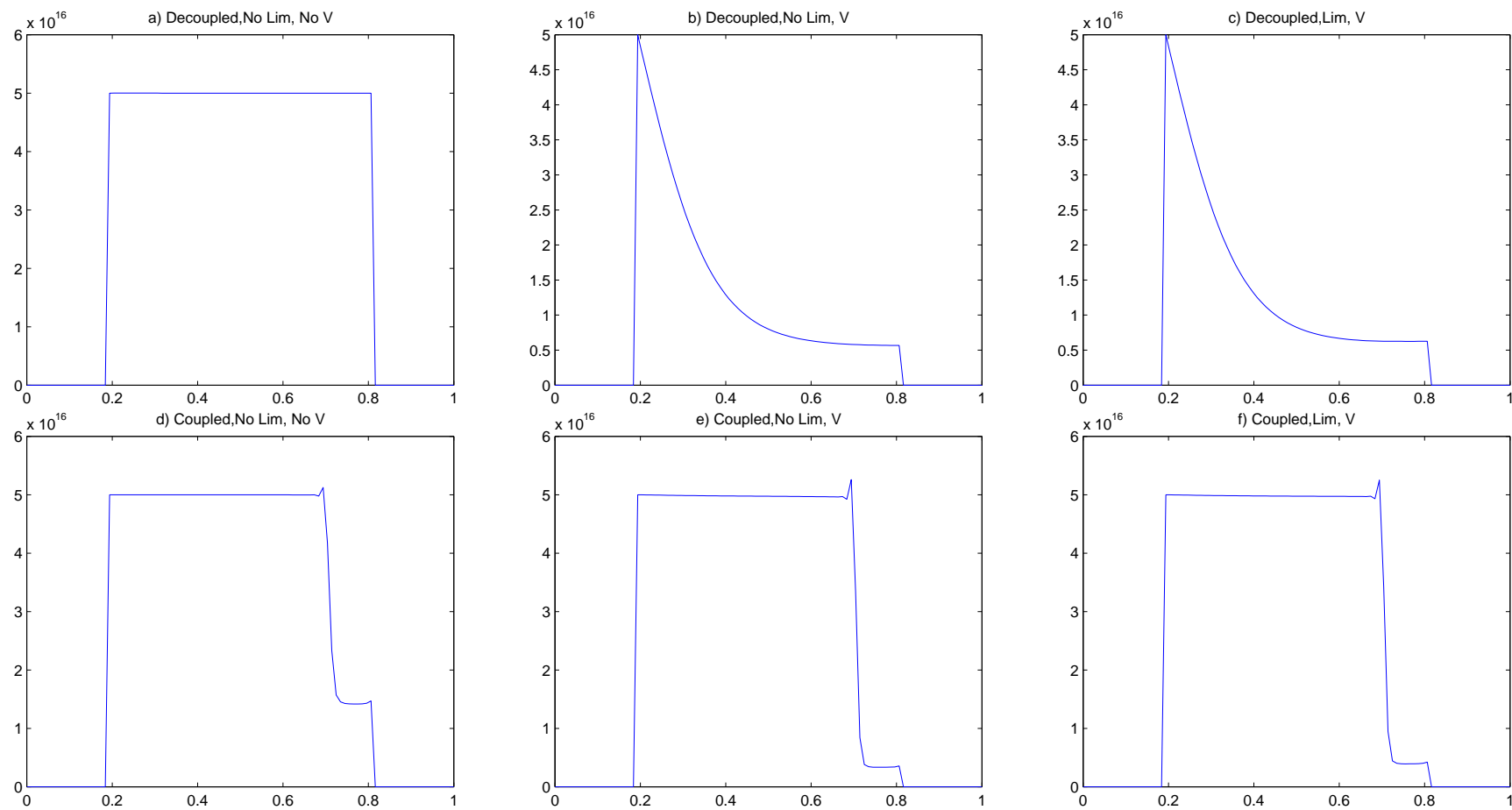
FIGURE A.7: 1d Lithium Vertical

FIGURE A.8: 1D Nn Horizontal
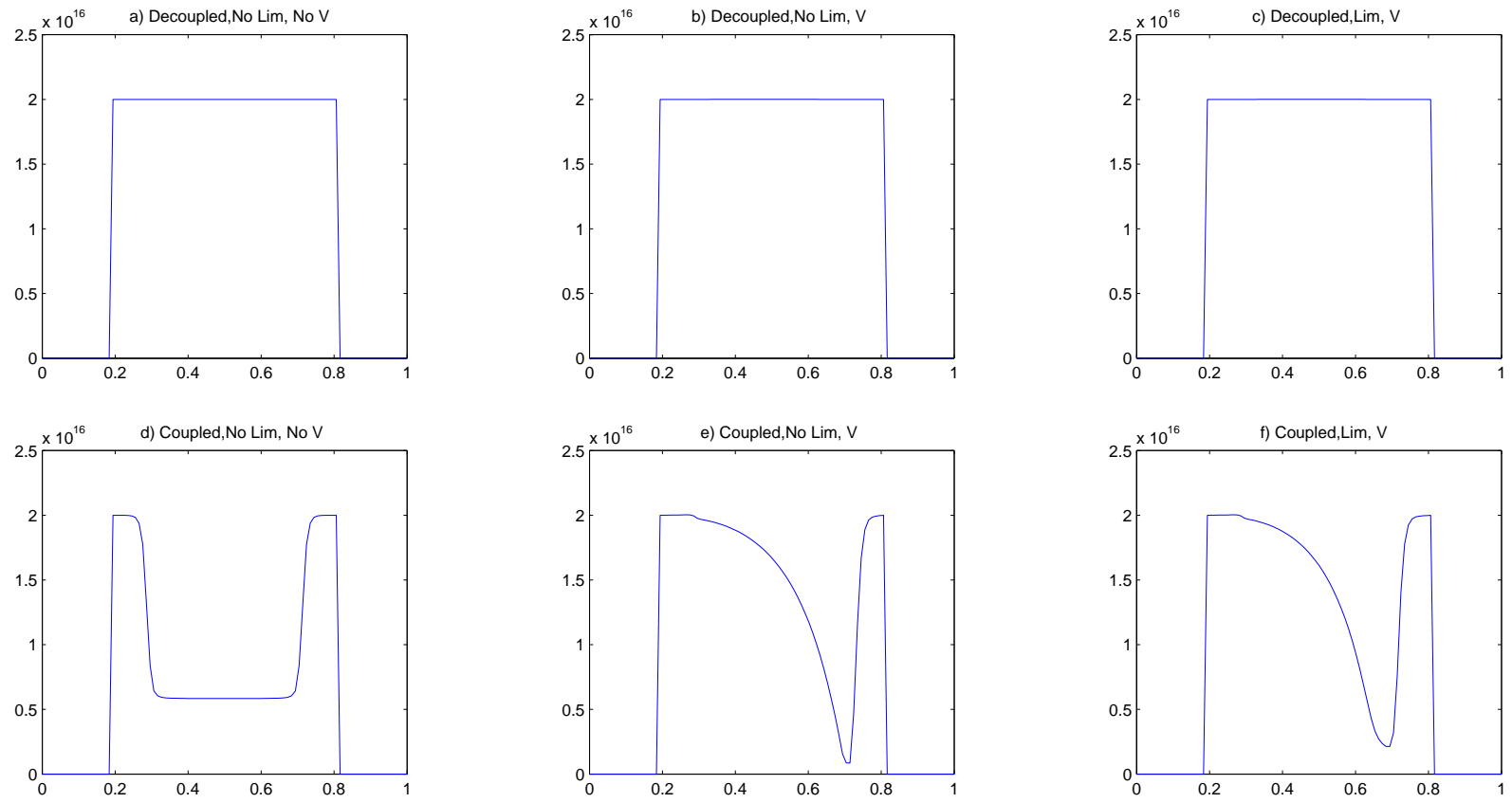
FIGURE A.9: 1D Nn Vertical

FIGURE A.10: 1-D Holes Vertical
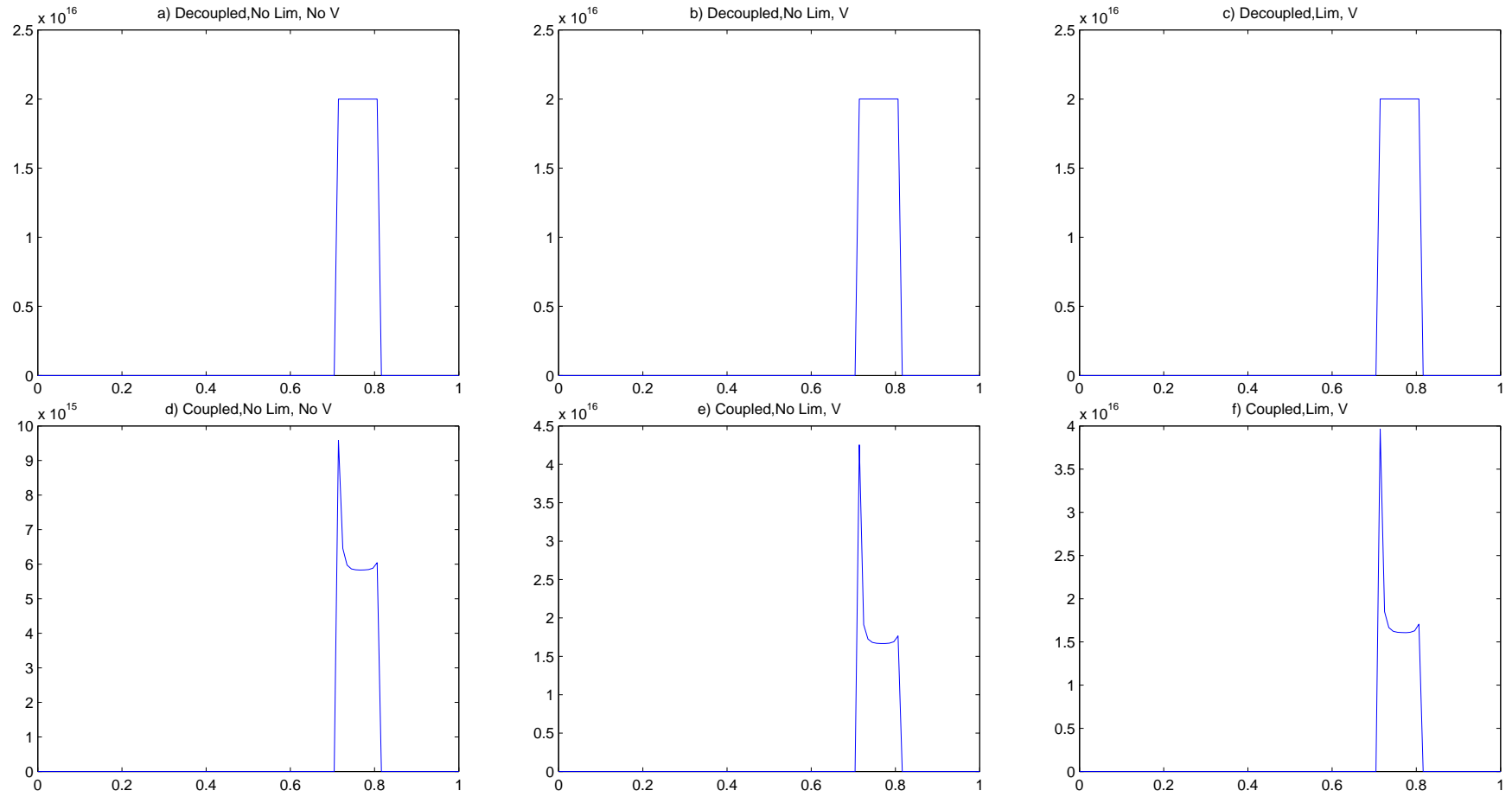
FIGURE A.11: 1 D Holes Horizontal

Appendix B
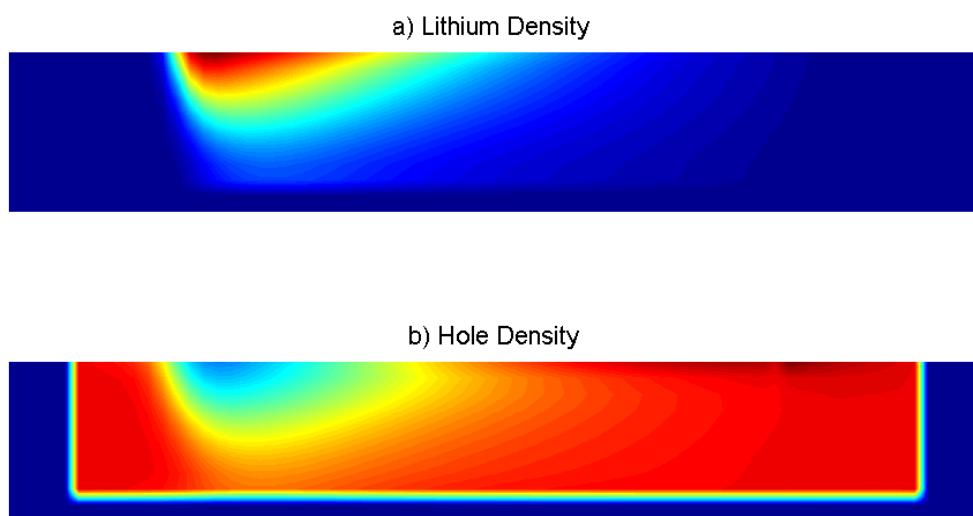
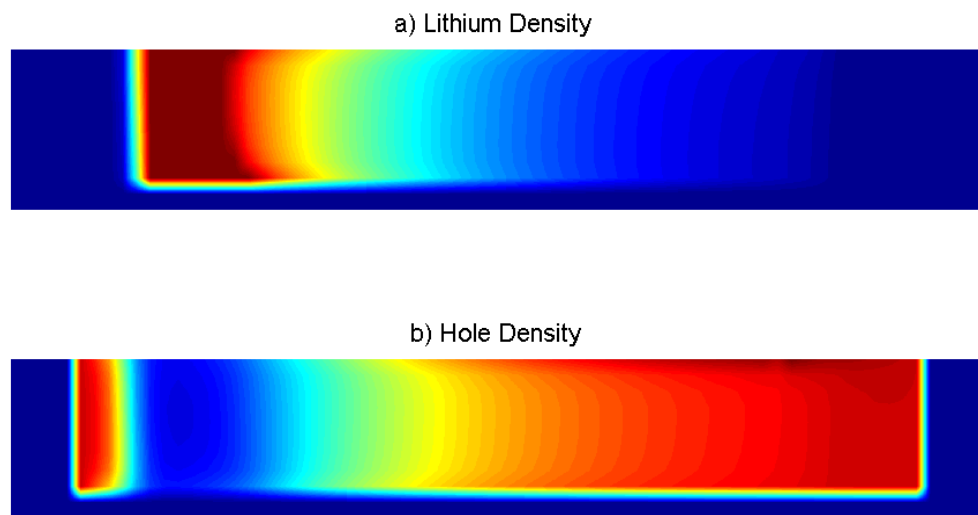# Single Channel PEDOT Lithium and Hole Density

FIGURE B.1

a) Lithium Density

b) Hole Density

FIGURE B.2

a) Lithium Density

b) Hole Density

FIGURE B.3

a) Lithium Density

b) Hole Density
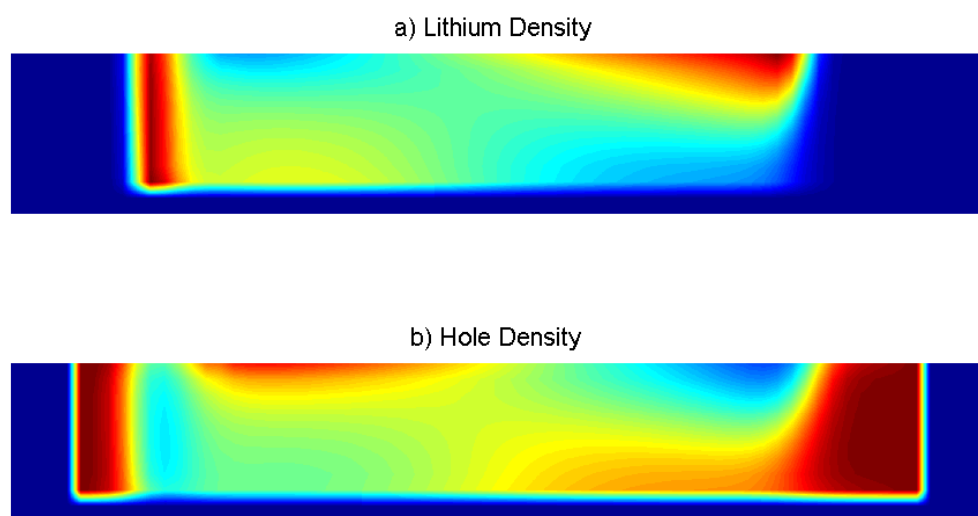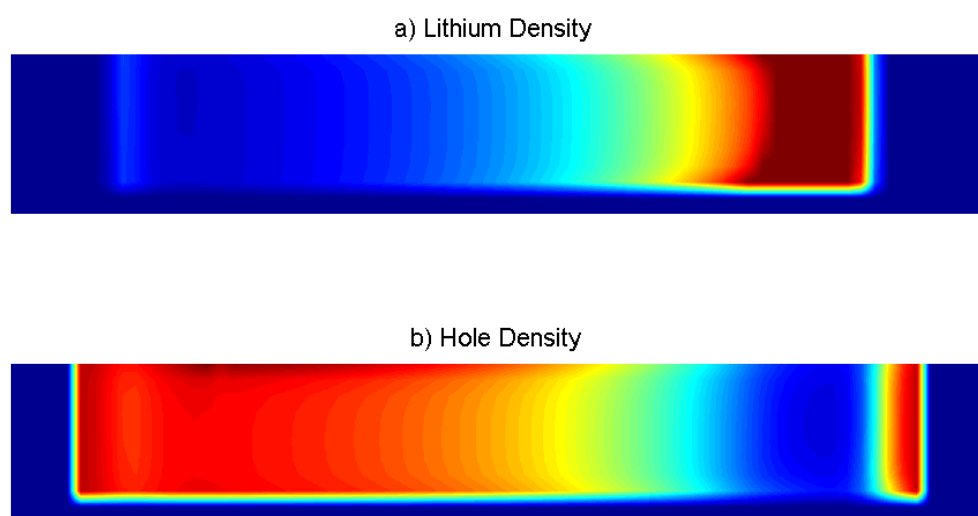
Figure B.4

Appendix C

Title 3

Bibliography

[1] L.O. Chua. Memristor-the missing circuit element. *Circuit Theory, IEEE Transactions on*, 18(5):507–519, 1971. ISSN 0018-9324.

[2] Stephen M. Goodnick D. Vasileska. *Computational Electronics*. Morgan and Claypool, Arizona,United States, 2006.

[3] D.L. Scharfetter and H.K. Gummel. Large-signal analysis of a silicon read diode oscillator. *Electron Devices, IEEE Transactions on*, 16(1):64–77, 1969. ISSN 0018-9383.

[4] Mark H. Holmes. *Introduction to Numerical Methods in Differential Equations*. Springer Science,Business Media,, New York,United States, 2007. ISBN 978-0387-30891-3.

[5] Duncan R. Stewart R. Stanley Williams Dmitri B. Strukov, Gregory S. Snider. Missing memristor found. *Nature*, 453:80–83, 2008. ISSN 0028-0836.

[6] H. U. Schwarzenbach E. Knapp, R. Husermann and B. Ruhstaller. Numerical simulation of charge transport in disordered organic semiconductor devices. *J. Appl. Phys*, 108, 2010. ISSN 1089-7550.

[7] W. Lvenich U. Merker K. Reuter A. Elschner, S. Kirchmeyer. *Introduction to Numerical Methods in Differential Equations*. Taylor and Francis Group,, Florida,United States, 2011. ISBN 978-1-4200-6911-2.

[8] Snowden C.M. *Semiconductor Device Modelling*. Peter Peregrinus Ltd., London,United Kingdom, 1988.

[9] A.M. Nardes. *On the conductivity of PEDOT:PSS thin films*. PhD thesis, Technische Universiteit Eindhoven, Eindhoven, 2007.